

VOLUME 24

AUGUST, 1936

NUMBER 8

PROCEEDINGS  
*of*  
The Institute of Radio  
Engineers



Application Blank for Associate Membership on Page XI



---

# Institute of Radio Engineers Forthcoming Meetings

---

CLEVELAND SECTION  
September 24, 1936

---

DETROIT SECTION  
September 18, 1936

---

LOS ANGELES SECTION  
September 15, 1936

---

NEW YORK MEETING  
October 7, 1936

---

PHILADELPHIA SECTION  
September 3, 1936

---

WASHINGTON SECTION  
September 14, 1936

---



## INSTITUTE NEWS AND RADIO NOTES

### Institute Meetings

#### ATLANTA SECTION

The Atlanta Section met on April 16 at the Atlanta Athletic Club with I. H. Gerks, chairman, presiding. There were eighteen members and guests present and eight attended the informal dinner which preceded the meeting.

A paper on "A Discussion of High Fidelity Broadcast Transmission Equipment" was presented by D. A. Reesor, district manager of transmitter sales, RCA Manufacturing Company. The development of sound and transmitter equipment was outlined historically. Greater fidelity in transmission, higher modulation capability, new tubes and circuits, and mercury-vapor rectifier tubes were briefly discussed. Recent trends in broadcast transmitters and possible future improvements in tubes and microphones were outlined. The major mechanical and electrical characteristics of various types of transmitters were illustrated. The paper was concluded with a brief review of police and aircraft transmitters.

#### BOSTON SECTION

The Boston Section met on April 24 at Harvard University. E. L. Bowles, chairman, presided and there were fifty members and guests present. Twenty attended the dinner which preceded the meeting.

A paper on "Experiments with Directivity Steering for Fading Reduction" was presented by Edmond Bruce of the Bell Telephone Laboratories. In it he pointed out that short-wave fading is due largely to phase interference between multiple path signals of varying path length. Stable angular differences usually exist at the point of reception. Antenna directivity which is "steerable" and sufficiently sharp to accept only one of the several paths may be used to reduce this fading. The use of such an antenna for the reception of transoceanic short-wave signals was described. The paper was discussed by Dr. Barrow and Professor Bowles.

The May meeting of the Boston Section was held on the 22nd at Massachusetts Institute of Technology and was presided over by H. R. Mimno, vice chairman. There were 100 present and fifteen at the dinner which preceded the meeting.

W. L. Barrow of the Electrical Engineering Department of Massachusetts Institute of Technology, presented a paper on "Transmis-

sion of Electromagnetic Waves in Hollow Tubes of Metal." Dr. Barrow pointed out that electromagnetic energy may be transmitted through the inside of hollow tubes of metal provided the frequency is greater than a critical value which is inversely proportional to the tube radius and to the dielectric coefficient to the tube interior. Calculations and measurements have been made to disclose the conditions for minimum attenuation. Terminal devices for connecting a hollow pipe system to a pipe conductor system and others in the form of horns for directly radiating radio waves have been developed. These electromagnetic horns may also be fed from ordinary coaxial lines. Certain types of terminals act as sharply resonant hollow tube elements. Several independent communication channels may be established within a single pipe line by utilizing distinct types of waves for each channel in a unique kind of multiplex operation. A section of hollow tube may be used as a high-pass filter. Although presupposing adequate technique for the generation and utilization of the shortest radio waves, this system possesses several advantages among which are a minimum dielectric loss, substantially perfect shielding, and a simplicity of structure. The paper was discussed by Messrs. Eastham, Frank, Hunt, Karplus, and Mimno.

#### CINCINNATI SECTION

The May 19 meeting of the Cincinnati Section was held at Caproni's Restaurant and was presided over by C. D. Barbulesco, chairman. Forty-seven members and guests were present and there were forty-one at the dinner which preceded the meeting.

A paper on "The Hammond Organ" was presented by Armand Knoblauch, engineer for the Baldwin Piano Company. Dr. Knoblauch described the Hammond organ and showed how the tempered scale, although it reduced the number of organ keys, had a disturbing effect on harmonic relations. The organ thus omitted the seventh harmonic because it was too much in error to be harmonious. The combination of fundamental tones with various harmonics to simulate other musical instruments was demonstrated on the organ and two musical selections played. The paper was discussed by Messrs. Rockwell and Silver.

The second paper on "A Novel Receiver for Phase or Frequency Modulated Signals" was presented by C. F. Wolcott, engineer in charge of radio, Noblitt-Sparks Industries. He described several systems of reception of phone modulated signals. One of these made use of a local oscillator with a large "flywheel" effect which locked in with the received signal carrier thereby producing a species of demodulation. The paper was discussed by Messrs. Felix, Platts and Tyzzer.



## DETROIT SECTION

The Detroit Section met on June 19 at the Detroit Edison Boat Club. Forty attended the meeting which was presided over by R. L. Davis, vice chairman, and there were fourteen at the dinner which preceded it.

"A Regenerative Timing-Axis Oscillator for Cathode-Ray Tubes" was the subject of a paper by J. A. Morton of the University of Michigan. He reviewed briefly the existent types of sweep circuits and outlined the fundamental requirements which must be met by timing oscillators. A relatively new method of obtaining a linear rise in voltage across the condenser was described. By adjusting the feed-back attenuation equal to the gain of the amplifier alone, in a direct coupled regenerative amplifier, the voltage across the output resistor was shown to be linear with respect to time. A demonstration was also presented in which it was shown how the sweep wave shape could be controlled by varying the ratio, the desirable linear wave being easily obtained within the range of control. An outline of the performance and applications of the regenerative sweep circuit concluded the paper.

## EMPORIUM SECTION

A special two-day meeting was held by the Emporium Section on June 26 and 27. Among the twenty-five out-of-town guests were L. C. F. Horle, nominee for president of the Institute for 1937, and E. C. Woodruff, recently elected president of the American Radio Relay League. Friday morning and evening were devoted to inspection trips through the Hygrade Sylvania plant at Emporium and the Stackpole Carbon Company and Spear Carbon Company factories in St. Marys. Those who were interested in sports were accommodated.

On Friday evening ninety members and guests attended a meeting at Creighton Hall where two papers were presented. R. R. Hoffman, chairman of the section, welcomed the guests to the meeting and then introduced Mr. Horle who acted as honorary chairman for the technical papers.

The first paper on "Diode Coupling Transformers" was by F. H. Scheer, an engineer for the F. W. Sickles Company. The gain in a diode coupling network was expressed as a function of a product of five quantities, mutual conductance, angular frequency, mutual inductance in primary and secondary windings of the coupling transformer, and the  $Q$  values of the primary and secondary windings. Curves were shown for gain and selectivity as functions of coupling and as functions of the inductance of the transformer secondary. The amplification of the diode network was discussed and curves of direct current through

the diode load plotted against input voltage were shown. The paper was discussed by Messrs. Horle, Jones, and West.

The second paper on "Applications of Cathode-Ray Oscillographs" was presented by H. J. Schrader of the Victor Division of the RCA Manufacturing Company. Construction and operation of cathode-ray oscillograph tubes and associated circuits were first described. This was followed by descriptions of such uses of the device as the aligning of coupled electrical networks, determination of the charge on a condenser, identification of frequency ratios, determination of phase relationships of two currents, and the testing of automobile receiver vibrators. These electrical uses were followed by the adaptation of the device for the study of mechanical vibration in machinery which permits tortional and translatory vibrational studies. Its application to the study of combustion chamber pressures was described. The paper was discussed by Messrs. Bowie, Horle, Lazich, Place, Waltz, and West.

The Saturday morning technical session was attended by seventy members and guests. A paper by C. T. Wallis, engineer of the Delco Appliance Division of the General Motors Corporation, was on "Vibrator Power Supplies." Plate power supplies for automobile receivers were outlined and the vibrator type discussed in detail. The early use of the nonrectifying vibrating reed required the use of a rectifier tube. Later developments produced a self-rectifying vibrator. For automobile use, these devices must operate over a range from five and a half to nine volts. Noise suppression requires the enclosing of the unit which limits heat dissipation and the temperature may frequently rise to two hundred degrees Fahrenheit. Contact materials were then discussed and effects of improper values of inductance, capacitance, and resistance, as well as the timing of the vibrators with respect to the electrical circuits were pointed out.

C. J. Franks of the Ferris Instrument Corporation presented a paper on "Extending the Upper Frequency Limit of Receiver Sensitivity Measurements." He discussed first the essentials of a signal generator and then outlined the problems in the design of one to cover the range from thirty megacycles to one hundred megacycles. The limitations of the resistive type of attenuator were pointed out. Difficulties in coupling the output of the generator to the input of the receiver were discussed and the use of a properly terminated concentric transmission line described.

The afternoon was devoted to final inspection trips and an outing at a near-by camp where supper was served.



## PHILADELPHIA SECTION

At the June 4 meeting of the Philadelphia Section which was held at the Engineers Club, Knox McIlwain, the retiring chairman, and Irving Wolff, chairman-elect, presented short addresses.

A paper on "Operating Characteristics of Power Tubes" was presented by E. L. Chaffee of the Research Laboratory of Physics, Harvard University. The method used for testing power tubes consists in impressing on the tube plate and grid direct voltages derived from generators and alternating voltages obtained from two power transformers operating from the sixty-cycle supply circuits. The transformer in the plate circuit of the tube simulates the resonant circuit load. Low-frequency watt meters and voltmeters can be used for direct measurements of input and output powers and grid and plate voltages. The alternating and direct voltages can be varied independently and the readings of the instruments give the power input or driving power, power output, grid loss, and plate loss. From these can be obtained the efficiency, plate load resistance, effective input resistance, and other important quantities.

The results were presented in contour diagrams and showed the most favorable conditions of operation either as class *B* or class *C* amplifiers or as an oscillator. The method may be extended to obtain the modulation characteristics of a power tube. A system of graphical harmonic analysis which is considerably simpler than the usual methods was described. With very little labor, one may calculate the plate operating characteristics of a power tube from its static characteristic curve. Messrs. Barton, Murray, Peterson, and Wolff entered into the discussion. The attendance was 220 and there were eighteen at the informal dinner which preceded the meeting.

## PITTSBURGH SECTION

The Pittsburgh Section met on April 21 at the Fort Pitt Hotel with Lee Sutherlin, chairman, presiding and there were twenty-one in attendance.

A paper on "Frequency Stability of Radio-Frequency Oscillators Using Multielectrode Tubes" was presented by R. T. Gabler of the Electrical Engineering Department of the Carnegie Institute of Technology. The speaker described a beat frequency oscillator employing a crystal oscillator for one frequency and a second vacuum tube oscillator the frequency of which could be varied and maintained for an indefinite period of time at any set frequency.

In this second oscillator, tubes such as the 6A7, 6D6, and 6C6 were

successfully used. Compensation was obtained by proper selection of inductances and capacitances as well as by a special compensating variable condenser operating by the deflection of a bimetallic structure caused by temperature variation. It was possible to obtain a frequency constant to within a few cycles in 1780 kilocycles. The paper was discussed by Messrs. Mouromtseff, Stark, and Sutherlin.

The annual meeting of the section was held on June 16 at Villa D'Este and Lee Sutherlin, chairman, presided. A report on the annual meeting of the Sections Committee in Cleveland was presented and discussed.

In the election of officers for next year, B. Lazich of the Union Switch and Signal Company was named chairman; R. T. Gabler, Carnegie Institute of Technology, vice chairman; and W. P. Place of the Union Switch and Signal Company, secretary-treasurer.

#### SAN FRANCISCO SECTION

The June meeting of the San Francisco Section was held on the third in the Auditorium Annex Room of the Telephone Building. It was presided over by V. J. Freiermuth, vice chairman, and attended by twenty-five, eight of whom were present at the dinner which preceded it.

The meeting was devoted to a discussion of three papers which had been published in the *Bell System Technical Journal*. The first was on "The Commander," by Mathes and Wright, and was reviewed by H. L. Kertz of Stanford University. The second paper was on "Hyper-frequency Wave Guides," by G. C. Southworth, and was reviewed by Earl Schoenfeld of Heintz and Kaufman. The third paper, "The Stabilized Feed-Back Amplifier," by H. S. Black, was reviewed by E. F. Kulikowski of Stanford University.

#### SEATTLE SECTION

A meeting of the Seattle Section was held at the University of Washington on June 19. E. D. Scott, chairman, presided and there were forty present. This was the annual student meeting of the section and three papers were presented by graduating students in electrical engineering from the University of Washington.

The first paper was on "Portable Radio Research," by N. Frost. He described a complete radiotelephone receiving set to be carried on the person of a policeman. The three-tube receiver built into a small aluminum can is fastened to the policeman's belt which supports also a canvas battery case. A loop antenna is built into the belt. The entire



equipment including the belt weighs five pounds. In tests, an eight-watt transmitter covered a radius of about one-third mile except when the receiver was located within a reinforced concrete building. The equipment was demonstrated.

The second paper by J. C. Campbell was entitled "Vacuum Tube Distortion Compensator." Distortion in an amplifier was defined as a condition in which the output voltage is something other than a constant times the input voltage. The compensator described a method by which a voltage can be fed back from the output to the input of the amplifier in such a way as to maintain closely the requirements for no distortion. The application and performance of the system were covered.

"A New Type of Mercury-Pool Rectifier" was the title of the third paper which was presented by T. M. Libby. A special type of mercury-pool rectifier tube designed to avoid the usual danger of flash back was described. It is built into a vertically mounted glass tube. An inner boiler tube within the lower half of the rectifier contains the mercury pool and a heating element. There is a deflector at the top of the boiler and the anode is mounted in the upper end of the main tube. A single stage Langmuir pump maintains a very low pressure in the upper part of the tube. A water jacket surrounding the main tube acts as a cooling agent and as a third electrode. In operation, the rectifier has been tested at voltages as high as 40,000 volts and extrapolation of its flash back voltage versus temperature curve, indicates it would withstand over one hundred kilovolts. At fifteen kilovolts it can handle one hundred and fifty kilowatts. By adjusting the phase of the voltage on the third electrode, complete control of the tube current is obtained. The tube was demonstrated at fifteen kilovolts with a lamp bank load. A cathode-ray oscilloscope permitted its operating characteristics to be observed.

A committee of judges awarded first prize to Mr. Campbell and second prize to Mr. Libby.

#### WASHINGTON SECTION

On April 13 a meeting of the Washington Section was held at the Potomac Electric Power Company Auditorium. C. L. Davis, chairman, presided and the attendance was fifty, fourteen of whom were present at the dinner which preceded the meeting.

A paper on "High Voltage Mercury-Pool Tube Rectifiers" was presented by C. B. Foos of the General Electric Company and appears in the July, 1936, issue of the PROCEEDINGS.



The April 30 meeting of the Washington Section was held jointly with the American Physical Society at the National Museum Auditorium and presided over by J. H. Dellinger, past president of the Institute. There were 550 present.

V. K. Zworykin of the RCA Manufacturing Company presented a paper on "Applied Electron Optics." This was followed by a second paper by G. C. Southworth of the Bell Telephone Laboratories on "Hyperfrequency Transmission through Wave Guides."

On May 1 a joint meeting of the American Section of the International Scientific Radio Union and the Washington Section of the Institute was held at the National Academy of Sciences. There were 250 present and Dr. Dellinger presided. The papers presented at this meeting are listed in the April, 1936, PROCEEDINGS.

The June meeting of the Washington Section was held on the eighth at the Potomac Electric Power Company Auditorium and was attended by 120, of whom twenty-six were present at the dinner which preceded the meeting.

E. H. Armstrong, Professor of Electrical Engineering at Columbia University, presented his paper on "A Method of Reducing Disturbances in Radio Signaling by a System of Frequency Modulation" which appears in the May, 1936, issue of the PROCEEDINGS.

---

### Personal Mention

Formerly with the U. S. Patent Office, R. W. Armstrong has joined the staff of Naval Research Laboratory at Anacostia, D.C.

D. C. Beard, Lieutenant U.S.N., has been transferred from the *USS Detroit* to the Naval Research Laboratories at Anacostia, D.C.

Previously with General Household Utilities Company, L. D. Boji has become factory superintendent for Fairbanks, Morse and Company of Indianapolis, Ind.

Michael Buckley, Jr., Captain U.S.A., has been transferred from West Lafayette, Ind., to Fort Leavenworth, Kansas.

J. A. Chambers, formerly with Crosley Radio Corporation, has entered a consulting engineering partnership under the name of McNary and Chambers in Washington, D.C.

L. R. Daspit, Lieutenant U.S.N., has been transferred from Annapolis, Md., to the University of California, Berkeley, Calif.

R. G. DeWardt, superintending engineer of the British Post Office Engineering Department has been transferred from Croydon to Manchester, England.



N. H. Edes, Captain, British Army, has been transferred from London to Cairo, Egypt.

Formerly with Audiola Radio Company, Mortimer Frankel has become assistant general manager of Fairbanks, Morse and Company of Indianapolis, Ind.

J. H. Foley, Lieutenant U.S.N., has been transferred from Boston, Mass., to the *USS Humphreys*, basing at New York City.

L. S. Hansen of the General Household Utilities Company has been transferred from Marion, Ind., to Chicago, Ill. and placed in charge of the automobile radio division.

J. C. Harrower has left the Fleet Air Base at Coco Solo, Canal Zone, to become affiliated with Marconi's Wireless Telegraph Company at Medellin, Colombia.

A. Herczeg has left Edge Radio, Ltd., to become a research engineer for E. K. Cole, Ltd., Southend-on-Sea, England.

C. F. Holden, Lieutenant Commander U.S.N., has been transferred from Hawaii to the *USS Idaho*, basing at San Francisco, Calif.

Previously with Turnbull and Jones, Ltd., F. J. Macedo is now a radio engineer for the RCA (New Zealand) Ltd., at Wellington, N.Z.

J. C. McGinley is now with Aladdin Radio Industries, Chicago, Ill., having formerly been with Meissner Manufacturing Company.

G. B. Myers, Lieutenant U.S.N., has been transferred from the *USS California* to the Navy Department, Washington, D.C.

L. E. Barton has joined the staff of Philco Radio and Television Corporation, having formerly been with the RCA Victor Company.

W. J. Howell is now placement interviewer in the Buffalo Office of the New York State Employment Service, having formerly been with the Emergency Employment Service of the Institute.

H. C. Humphrey, previously with Electrical Research Products, is now with the Western Electric Company, Ltd., of London, England.

J. F. Inman, formerly with the Illinois Testing Laboratories, is now with Associated Research, Inc., of Chicago, Ill.

Previously with the U.S. Department of Commerce, C. H. Jackson has joined the Airway Radio Laboratory of Chicago, Ill.

K. W. Jarvis is now with the Norwalk Engineering Corporation of South Norwalk, Conn., having formerly been with Meissner Manufacturing Company.

L. H. Larime, formerly with WJBK, is now technical supervisor for the West Coast for Jam Handy Picture Service.

V. C. MacNabb, chief radio engineer for Fairbanks, Morse and Company, has been transferred from Chicago, Ill., to Indianapolis, Ind.



P. D. Miles has become communication superintendent for Hearst Radio, Inc., at Redwood City, Calif., having formerly been with Mackay Radio and Telegraph Company.

C. F. Miller of Hygrade Sylvania Corporation has been transferred from Emporium, Pa., to Salem, Mass.

H. G. Moran, Lieutenant U.S.N., has been transferred from Lakehurst, N.J. to the *USS Ellis*, basing at New York City.

H. B. Morris, assistant superintendent of R.C.A. Communications, Inc., has been transferred from New York City to Manila, P.I.

J. H. Muller of R.C.A. Communications, Inc., has been transferred from Manila to New York City.

W. J. O'Brien, formerly with RCA Radiotron Company, is now with Modern Research Corporation of New York City.

J. V. Pareto of Cia Radio Internacional de Brasil at Rio de Janeiro, has been made technical director.

A. W. Peterson, Lieutenant U.S.N., has been transferred from Balboa to the *USS Argonne* basing at San Pedro, Calif.

J. J. Pierrepont, Lieutenant U.S.N., is now on the *USS Charleston*, basing at New York City, having previously been at the Navy Yard, Charleston, S.C.

J. R. Ruhsenberger, Lieutenant U.S.N., has been transferred from San Diego, Calif., to the Naval Air Station at Norfolk, Va.

C. M. Ryan, Lieutenant U.S.N., has been transferred to the U.S. Naval Academy, Annapolis, Md., from the *USS Oklahoma*.

B. A. Schwarz is now chief engineer of the radio division of General Motors at Detroit, having formerly been with Zenith Radio Corporation.

G. H. Sparhawk, Captain U.S.A., has been transferred from Hawaii to Maxwell Field, Montgomery, Ala.

H. E. Thomas has left United American Bosch Corporation to join the staff of Philco Radio and Television Corporation at Philadelphia, Pa.

R. R. Welsh has left RCA Victor Company at Camden, N.J., to become chief engineer for RCA Victor Company, Ltd., of Canada at Montreal.

L. J. Wolf, formerly with the Westinghouse X-Ray Company, has joined the Engineering Department of the RCA Manufacturing Company at Camden, N.J.



TECHNICAL PAPERS

DESIGN AND EQUIPMENT OF A FIFTY-KILOWATT  
BROADCAST STATION FOR WOR\*

By

J. R. POPPELE,

(The Bamberger Broadcasting Service, Newark, New Jersey)

F. W. CUNNINGHAM, AND A. W. KISHPAUGH

(Bell Telephone Laboratories, Inc., New York City)

**Summary**—*With its novel directional antenna, WOR produces a maximum field strength toward both New York and Philadelphia while limiting radiation in the direction of the ocean and sparsely populated areas. Radiation distribution measurements are given.*

*The layout of the station and the unique arrangements for lighting, heating, and ventilation of the building are described.*

*A serious attempt has been made to design and operate the equipment for a performance consistent with advanced ideas of high fidelity. Measurements from microphone to antenna of distortion, noise, and frequency response are presented.*

THE widespread interest in the unusual features of the new WOR fifty-kilowatt station has prompted the authors to describe its design and performance in some detail with the thought that their experience might prove of benefit to engineers planning the installation of transmitters of high power.

The Bamberger Broadcasting Service began the consideration of plans for a high power transmitter several years ago. The selection of a suitable site in the New York area is probably more difficult than in almost any other section of the country. The peculiar distribution of population to be served, combined with the unusual topographical conditions including hills, rivers, and grouping of tall buildings, complicates the problem. The site of WOR's five-kilowatt transmitter at Kearny was one of the most effective in the area for a station of that power. The use of this particular site was deemed inadvisable for the location of a fifty-kilowatt station in view of the high population density within the first few miles from the site.

An extended study of the problem led to the tentative selection of a site in the vicinity of Tremley, New Jersey, about sixteen miles southwest of New York City. A field intensity survey indicated that this

\* Decimal classification: R612.1. Original manuscript received by the Institute, October 4, 1935; revised manuscript received by the Institute, May 19, 1936. Presented before Tenth Annual Convention, Detroit, Michigan, July 1, 1935.



site was satisfactory, but it was found that an antenna structure would affect the reception at a near-by receiving station of a high-frequency radio service transmitted from South America. A site about a mile distant from Tremley, near Carteret, on the banks of the Rahway River, was finally selected and checked by a field intensity survey. Fortunately, this site proved to be equally advantageous from practically every standpoint and was sufficiently removed to avoid interference with the South American service.

The Carteret site is on fairly level ground, part of which is marshy, in a region of particularly low density of population. The path between Carteret and New York City consists largely of water and swampy ground with no high ground or structures in the direct line. The distance to Columbus Circle, which is regarded as the center of the population of the New York area, is 16.6 miles. The Lincoln highway runs close to the station property. Power facilities from two separate distributing points in opposite directions from the station are available at the highway. An objection to this site was its proximity to established airways which imposed a restriction on the height of the antenna structure.

The Carteret site is comparatively close to the Atlantic Ocean, which is a few miles to the southeast. To the northwest is found the sparsely populated mountainous terrain of northern New Jersey and northeastern Pennsylvania. At right angles to these directions lie the cities of New York, Philadelphia, Trenton, and Newark, approximately in line. This fact, together with the limitation upon antenna height, at once indicated the desirability of a directional antenna which would provide maximum signal intensity in the northeast-southwest direction.

A distribution pattern resembling an hourglass in shape with major axis along the line from New York to Philadelphia appeared most suitable. This pattern can be obtained from several different types of antenna array. The one chosen, after considerations of flexibility, control of high angle radiation, and economy of structure, consisted of three quarter-wave antennas approximately one-quarter of a wave length apart, driven in phase with substantially equal currents. These antennas are located on a line at right angles to the major axis of the pattern.

Fig. 1 is a general view of the station and the antenna structure. The end antennas of the array are 350-foot, self-supporting steel towers, sixty feet square at the base, mounted on, and insulated from individual structural steel bases thirty-five feet in height. This construction reduces dielectric losses at the base and provides a more desirable dis-

tribution of current along the tower. The center antenna of the array is a copper cable suspended vertically from a steel messenger cable supported by the towers. The electrical effect of the messenger cable is minimized by the insertion of insulators at frequent intervals. The towers are spaced 790 feet apart (approximately one-half wave length), and each is designed for a horizontal working load of 4000 pounds at the top. If it becomes desirable in the future to change the shape of the radiation pattern of the array, this can be accomplished by changing the distribution of the power to the individual elements, the relative



Fig. 1—Transmitter building and directional antenna.

phasing, or both. In the extreme case, the center antenna alone can be fed, with an approximately circular pattern as a result. It can be seen that except for the additional transmission lines, coupling units, and ground system the cost of the array is no greater than that of a conventional antenna.

The provisions for the promotion of safety of aviation are thorough and up to date. The towers are painted for day visibility and furnished with powerful fixed and flashing lights, according to the standards prescribed by the Bureau of Aeronautics, Department of Commerce. A red-beam rotating searchlight is mounted on the roof deck of the building. The operation of the lights is controlled by photoelectric means which are entirely automatic. When any warning light fails an indication appears on a control panel in view of the operator.

A beacon transmitter is employed to warn aircraft directed by the Newark Airport range beacon of the presence of the WOR antenna



towers. This transmitter is of Western Electric manufacture with an output of thirty watts. Its carrier frequency, 1200 cycles higher than that of the Newark beacon, is maintained by crystal control. The oscillator is followed by a buffer stage and a modulating amplifier where the signal, consisting of five-dash, 120-cycle tone, is supplied to the suppressor grid. (In emergencies speech may be substituted for the motor-coded tone.) The power amplifier which follows utilizes a fifty-watt vacuum tube. The transmitter with its power supply rectifiers is mounted as a unit on a wall panel. Meters and signal lamps indicate the functioning of the equipment and warn the operator upon the occurrence of any unsatisfactory condition, including failure of the antenna.

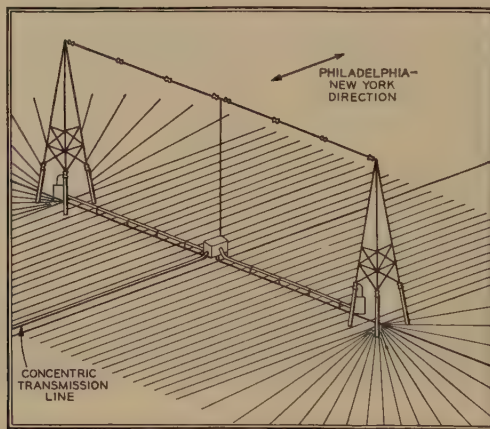


Fig. 2—Antenna and ground system.

The ground system, shown on Fig. 2, consists of a grid formed of No. 10 copper wires, each 600 feet long, spaced at intervals of three feet, centered on and laid at right angles to a line joining the towers. The wires were buried at a depth of twelve to fourteen inches by means of a special plow, which carries a heavy blade designed to lay in the wire without turning a furrow. A copper strip one-thirty-second of an inch by six inches was laid in a trench between the towers and brazed to each wire. From the ends of this ground strip, wires of the same size and buried in a similar manner with a six-degree spacing were extended outward to a distance of 300 feet. About 169,000 feet of wire were required for the ground system.

Coaxial lines are used to connect the transmitter to the center of the array and to supply power from that point to the end antennas. The outer conductor of the line is a two and five-eighths-inch outside

diameter copper water tubing with an eighty-mil wall. The inner conductor is tubular with an outside diameter of 0.7 inch and a forty-two-mil wall. Glazed ceramic insulators, having a long leakage path with a minimum mass of dielectric, are spaced at intervals of thirty inches throughout the line. The insulators are secured to the inner conductor by means of spring clips.

The main transmission line from the transmitter building to the coupling equipment at the center of the array is 660 feet long. This line is buried at a minimum depth of four and one-half feet in order to minimize temperature changes which would result in changes of the over-all length of the line and probable mechanical creepage between the inner and outer conductors. Calculations show the expected over-all expansion of the buried line to be less than one inch. The ten-foot vertical section at the center coupling house flexes to allow for this expansion. From the coupling equipment at the center of the array, branch lines of the same dimensions and construction run horizontally to the bases of the towers and then vertically to coupling units mounted on platforms at the top of the tower subbases. The latter lines could not be buried due to the marshy condition of the soil, and consequently are supported by brackets and cables from the railing of the elevated catwalk between the towers. They were covered with magnesia steam-pipe insulation protected from the weather by painted canvas jacketing. This insulation minimizes the relative change of length between the inner and outer conductors which would result from sudden changes in temperature. Over-all expansion, a maximum of four and one-fourth inches for each branch line, is taken care of by flexure of its twenty-two-foot vertical portion.

In order to prevent the entrance of water or water vapor, the lines are filled with dry nitrogen gas and equipped with a pressure gauge for inspection purposes. The lines are so constructed that the presence of gas is not required for insulation; however, it does tend to increase the factor of safety. Special insulating end seals and gas-tight coupling boxes were developed for this installation and tested at 110 pounds pressure. Before the lines were sealed and given a final test at sixty pounds pressure, they were blown out with dry nitrogen to remove any moisture condensed in the lines during construction.

A schematic diagram of the array coupling circuit is given on Fig. 3. Each antenna is provided with an antenna coupling unit. That for each of the end antennas matches the impedance of the branch transmission line to that of the antenna. These units also contain special choke coils through which the tower lighting system is fed. The coupling unit for the center antenna matches the impedance of the latter



to that of a phase correcting network used to compensate for the phase displacement at the end antennas due to the length of the branch transmission lines. The branch transmission lines connect, as does the phase correcting network, to a line-branching network located at the center of the array. The line-branching network or transformer provides for the adjustment of relative current amplitudes in each antenna and matches the impedance of the three branch circuits to the main transmission line from the transmitter.

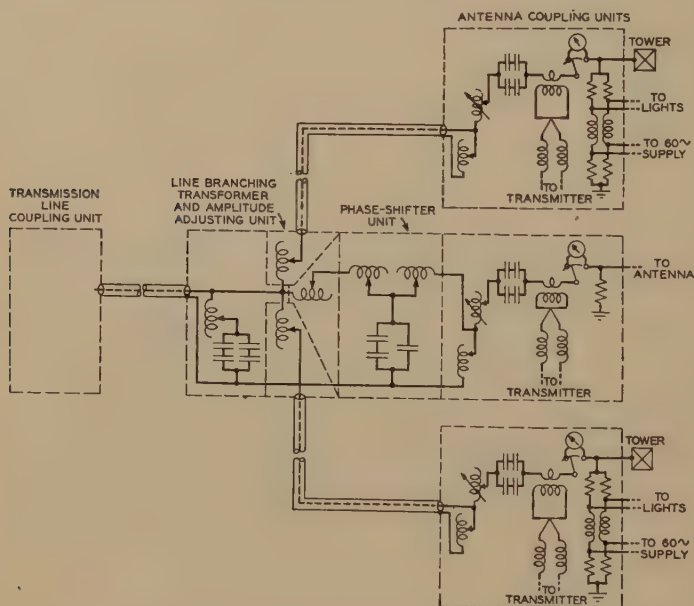


Fig. 3—Antenna array coupling circuits.

The design of the station building for WOR is unique in general and in detail. The building houses the fifty-kilowatt transmitter, a five-kilowatt transmitter (formerly operated at Kearny) for emergency use as auxiliary, and the aircraft warning beacon transmitter. In addition, space is provided for a short-wave transmitter to be installed in the future. All of these equipments are arranged to face on a central transmitter room as shown by the floor plan, Fig. 4. The structure of the building is also centered on this room. The building is sixty by sixty-six feet, exclusive of the five-car garage, and consists of a main story having a ceiling height of fourteen feet and a basement twelve feet in height, of which about ten feet are below grade. The construction is of reinforced concrete and brick with a steel-truss roof supported entirely by the walls. The transmitter floor is of reinforced con-

crete, supported by six columns having a special capping which provides a flat basement ceiling surface, free from the usual bulky column shoulders. This type of construction facilitates the installation of ceiling mounted ducts and conduits.

The architects have produced a modern design in which no purely decorative features are necessary. The appearance of the interior has been harmonized to that of the transmitters it contains. The transmitter room is semioctagonal in shape with a control desk in the center

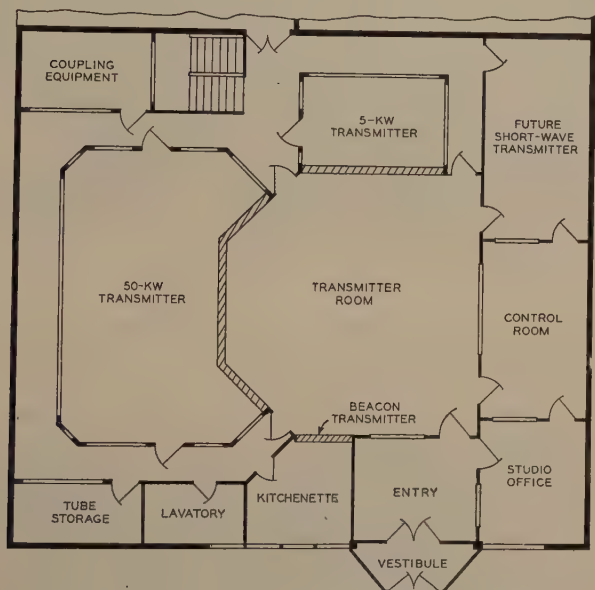


Fig. 4—Main floor plan of transmitter building.

directly underneath a large indirect lighting unit. The eight panels of the fifty-kilowatt transmitter, shown on Fig. 5, form the lower part of the walls on three sides facing the operator, who thus has a clear view of all the meters, indicating lamps, and most of the tubes. To the operator's left is the beacon transmitter, and to his right are the panels of the five-kilowatt transmitter. The panels of these transmitters also are set in the walls. Certain of the more important controls and indicating lamps are extended to the two control units on the operator's desk where they can be under his more immediate supervision. The control room containing the speech input equipment and the control operator's desk is immediately behind the transmitter operator. As Fig. 6 shows, the control operator can view the entire transmitter room through a large plate glass window from his position at the control desk.



There are three associated features of this building which are especially noteworthy; namely, the arrangements for lighting, ventilating, and heating. So much of the wall space of the transmitter room is



Fig. 5—View of transmitter room.

taken up with equipment that some artificial lighting would be required during the brightest part of the day. A mixture of artificial light



Fig. 6—Control operator's position.

and sunlight is unsatisfactory for rapid and accurate observation of meters. The building is almost windowless; only five outside windows are used, and these are in the rooms adjacent to the glassed-in entry.

The transmission of heat and the admission of dust through windows is thus avoided. The ventilating system supplies a filtered mixture of fresh and recirculated air to the rooms. When it is desirable to heat the air it is passed through four multiplied copper radiators in the main supply duct of the ventilating system. The distilled water, which has absorbed the waste heat in the power tubes of the fifty-kilowatt transmitter, is passed through these radiators before it is further cooled in the intercooler and returned to the pumps. This utilization of waste heat has been found very satisfactory during the past winter. In the early morning periods when the transmitter is shut down, two thirty-five-kilowatt electric heaters in the duct, supplied at off-peak rates, will provide any necessary heating. In the summer the duct radiators are by-passed, and all of the heat from the transmitter is dissipated through the intercooler by the spray pond located in the front of the transmitter building.

The spray pond has been made one of the features of the landscaping of the grounds. It has been constructed in two sections, either of which will provide more than the necessary dissipation for the fifty-kilowatt transmitter. The section not in use is available to facilitate cleaning without shutting down the transmitter. A novel feature of this pond is an arrangement which makes unnecessary the use of the sprays in cold weather, merely circulating the cooling water in contact with the ice instead. Another feature is the extension of the five-kilowatt distilled water system to include a single turn of copper water tubing around the bottom of the pond thus avoiding the use of radiators.

The history of the two most available power supply circuits, one from Carteret and the other from Rahway, was examined and found remarkably good. Over a long period, one circuit has never suffered an interruption. The other has been out only once in several years, and in that case only a few minutes were lost. On this basis, manual change-over of the main circuit was decided upon with automatic change-over for a low power emergency circuit which provides at least one light in every room and supplies the crystal heater circuits and the indicating lamp system of the transmitter.

The two 4150-volt supplies enter the basement of the building through several hundred feet of underground cable, which reduces radio-frequency pickup. These circuits are switched and metered in the switching vault and passed to the adjacent transformer vault where the supply voltage is stepped down by means of separate banks of transformers to 480 volts for the fifty-kilowatt transmitter, 220 volts for the five-kilowatt transmitter, and 220-110 volts for lighting



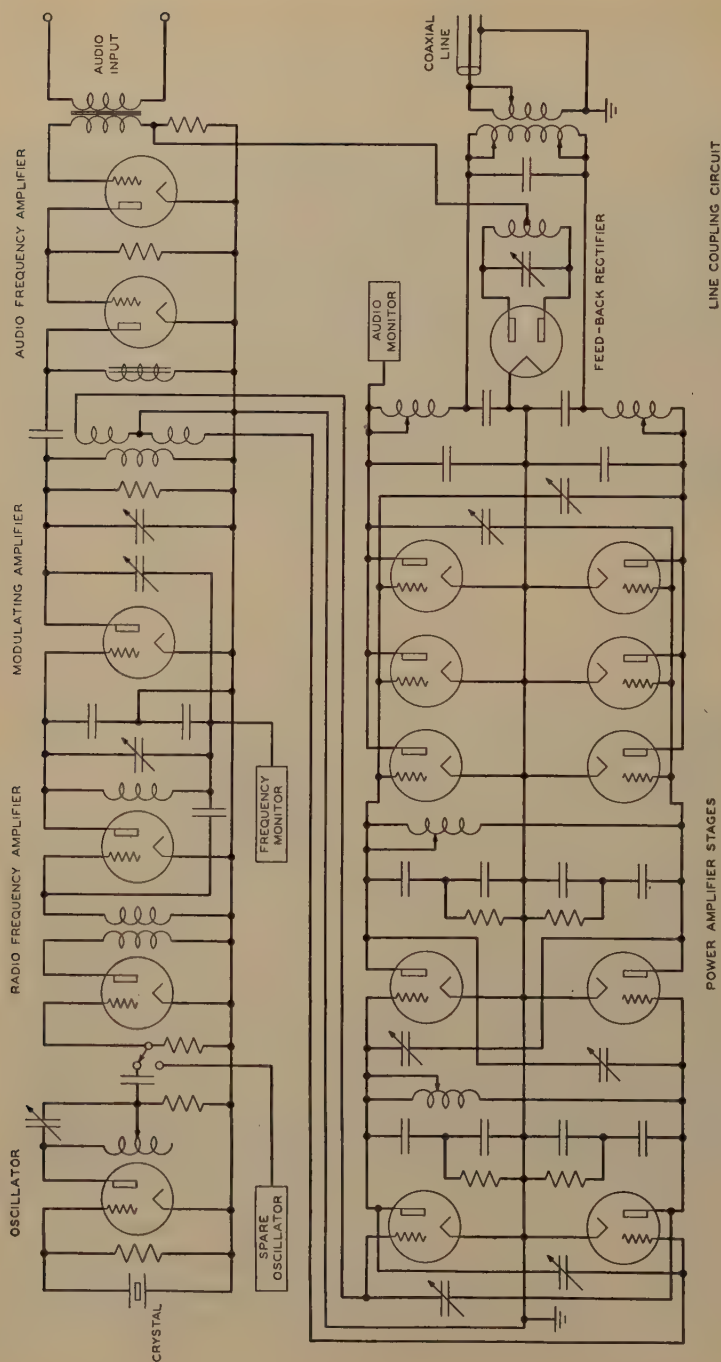


Fig. 7—Fifty-kilowatt transmitter circuits.

and other power needs for the station. The high voltage plate transformers for the fifty-kilowatt transmitter also are installed in this vault.

The fifty-kilowatt transmitter is a Western Electric type 306A modified for high fidelity operation. The circuit essentials of the transmitter are given on Fig. 7. Modulation takes place at low level by the Heising method in a fifty-watt amplifier where the modulating signal is received from the output of a 250-watt tube. The latter is driven by a fifty-watt audio-frequency amplifier, and a fifty-watt radio-frequency amplifier drives the modulating-amplifier tube. A quartz crystal controlled oscillator and a buffer comprise the initial stages of the carrier-frequency circuit, and two stages of intermediate power amplification follow the modulating amplifier stage. The final stage of amplification employs six thirty-five kilowatt vacuum tubes.

This transmitter embodies the first application to broadcasting of the principle of stabilized feedback.<sup>1</sup> This type of feedback effects a marked improvement in frequency response and at the same time greatly reduces the distortion and noise components which appear in the output of conventional amplifiers. In its application at WOR, a small part of the transmitted signal is rectified and reintroduced<sup>2</sup> with, and approximately in phase opposition to, the program signal at the audio input to the transmitter.

Two mercury-vapor tube rectifiers, one producing 1600 volts and the other 17,000 volts direct current, furnish plate power to all tubes. The auxiliaries include motor generator sets for grid-bias and filament supplies, pumps for the water-cooling and circulating system, and the necessary switch gear. The 17,000-volt rectifier employs six twenty-ampere tubes in a conventional circuit. Each tube is equipped with a relay which removes power in case of an arcbreak and indicates its operation by means of a signal light. A spare rectifier tube is kept in readiness for connection into the circuit as a replacement for any of the operating tubes.

Each water-cooled amplifier tube also is equipped with an individual overload relay and signal lamp. These, together with other lamps which indicate various operating conditions, make up a total of thirty-one signal lamps on the control panel, completely supervising operation of the equipment. In addition to the protection afforded by the individual tube overload relays, the apparatus connected between the final amplifier stage and the antenna is protected against damage from

<sup>1</sup> H. S. Black, "Stabilized feedback amplifiers," *Elec. Eng.*, vol. 53, p. 114; January, (1934).

<sup>2</sup> J. C. Schelleng, U. S. Patent No. 1,534,287.



power arcs following a flashover of insulation due to lightning transients or other causes.

This protection is provided by a device which functions to remove the carrier for an instant succeeding a flashover in any part of the circuit. The device makes use of the fact that in the final power amplifier, the grid and plate voltages are proportional and opposite in phase so long as the output circuit is properly adjusted. Two high reactances,  $L_1$  and  $L_2$  in Fig. 8, are connected to the grid and plate circuits, and their common point is connected to ground through a detector. With

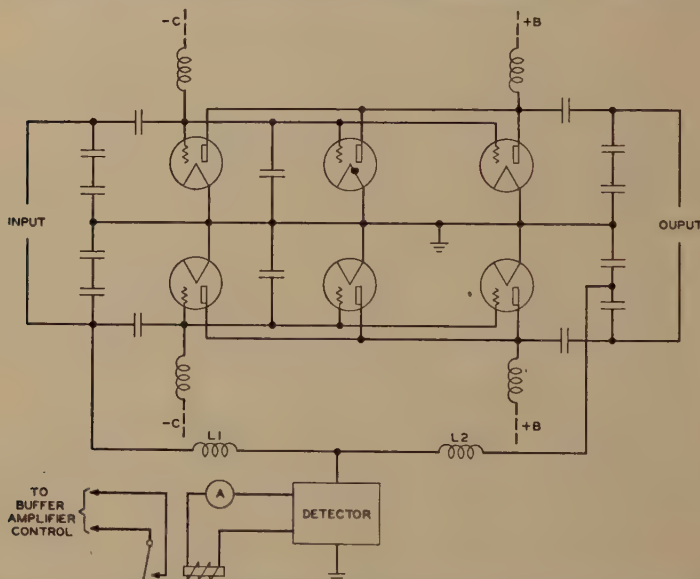


Fig. 8—Circuit of the D-98505 transmission line protection equipment.

the reactances of these coils chosen to be in proportion to the radio-frequency grid and plate voltages, zero output is obtained from the detector when the output circuit is normal. Since the impedance of the output circuit will be changed in magnitude or phase angle, or both, in the event of a flashover in any part of the antenna system, the normal phase and amplitude balance obtained in the detector circuit is destroyed, and the detector functions to operate a relay located in the power amplifier unit. The operation of this relay causes immediate removal of the carrier by removing plate voltage from the amplifier tube immediately following the crystal oscillator. As soon as the carrier is removed the protective system ceases to be energized, and this plate voltage is restored after a delay of approximately a fourth of a second, which permits the arc to clear in the antenna system with an almost



Fig. 9—Rear view of transmitter showing rectifier, switching unit, and high voltage filter.



Fig. 10—Basement view showing motor generators, cooling water hose troughs, and wiring ducts.



unnoticeable interruption of the program. At the same time the operator is informed by a signal light that the protective device has operated.

The apparatus comprising the radio transmitter is mounted on and behind the eight panels, which face the transmitter room. The high voltage rectifier tube unit, filter coil, condensers, and contactors are located within an enclosure formed by these panels on the front and glass partitions on the other three sides. As will be seen in Fig. 9, all busses and transmission lines have been concealed so that no interconnections appear outside the transmitter units.

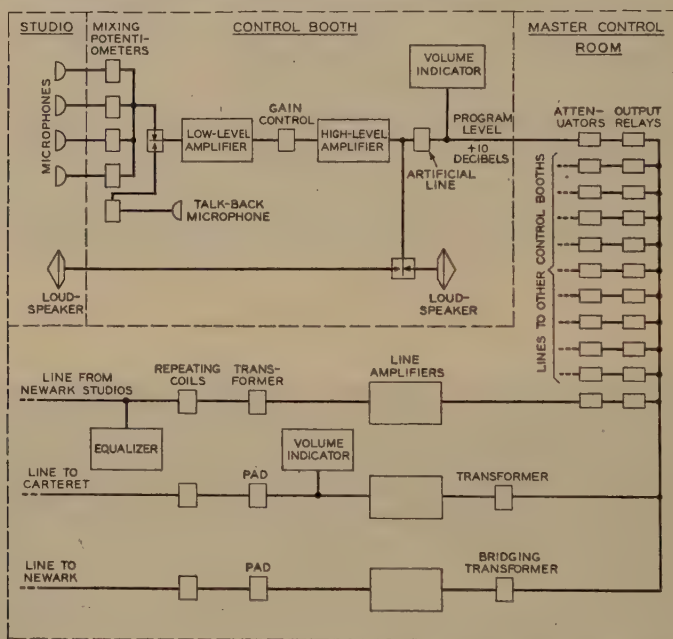


Fig. 11—Diagram of equipment and circuits at New York studios.

Generators, pumps, and power transformers are located in convenient rooms and vaults in the basement. Troughs and metal ducts are suspended from the ceiling below the transmitter units, as shown in Fig. 10, to carry the water hose and interunit wiring. The distilled water flowing through the high power tubes is passed through an inter-cooler in which the heat is transferred to a secondary flow of water and subsequently dissipated in the cooling pond.

The New York studios of WOR are located at 1440 Broadway. Eight studios are provided to accommodate the several types of program, and each is equipped with a control booth from which the operator has a view of the studio through a plate glass window. Fig.

11 is a block schematic diagram of the system installed here with one typical control booth shown in detail. Each control booth with one exception contains a control unit on which is mounted the microphone mixing potentiometers, master gain control, switching keys, the volume indicator and an amplifier bay which contains a low level and a high level amplifier and associated power equipment, a meter for measuring plate currents, a jack panel, and a line equalizer for incoming program lines from remote pickup points. A monitoring loud speaker incorporating a low-frequency and a high-frequency dynamic unit is part of each booth equipment.

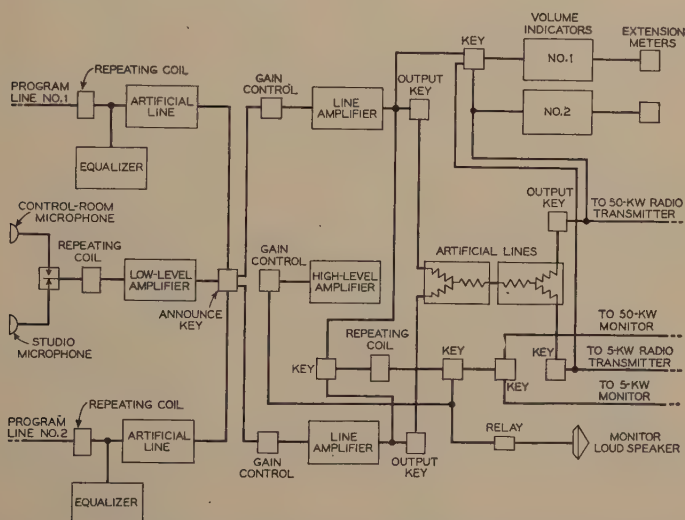


Fig. 12—Diagram of speech input equipment and circuits at the WOR transmitter station, Carteret, New Jersey.

The output of the high level amplifier in each control booth is fed into the master control room, where it is carried through a variable attenuator to a relay which connects it either to the input of the line amplifier or to a 500-ohm resistor depending upon whether or not the studio is supplying program. Eleven of these attenuators and relays are provided in the master control room; eight are connected to local studios, two are used for incoming chain programs or remote pickups, and one is connected to the program line from the Newark studios, programs of which are transmitted through the New York control room. The relay circuits are connected to the line amplifier which feeds the direct line to Carteret. Another similar amplifier is bridged across the output circuit and supplies programs over an emergency circuit routed through Newark to Carteret.



A block diagram of the station speech input equipment at Carteret is shown on Fig. 12. This consists of two identical amplifier channels, one connected to the regular program circuit and the other to the emergency circuit. The program circuits, shunted by line equalizers, are connected through impedance matching networks and gain controls to the line amplifier. The output terminals of the amplifiers are connected to two branches of a Y type resistance network, the third branch of which feeds a second Y type network. The other two branches of the latter supply audio input to the fifty-kilowatt transmitter and to the five-kilowatt emergency transmitter. By means of switches either

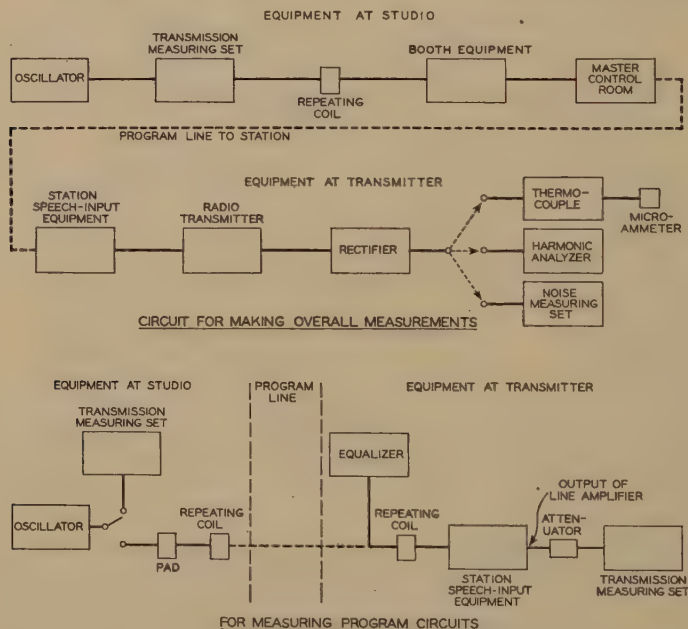


Fig. 13—Circuits used for measurements.

program channel may be connected to either radio transmitter. Monitoring loud speakers similar to those in the studios are used both in the control and in the transmitter room for aural monitoring. These loud speakers may be used to monitor the program either at the input or at the output of the radio transmitter. Provision has been made for the use of local microphones at the station for programs which it may be desirable to originate there and in case of emergency. A studio room with full acoustic treatment has been provided for this purpose.

In order to insure that all parts of the system were properly coordinated and adjusted, extensive measurements were made as soon as the equipment was completed.

The method of making these measurements and the circuit for obtaining the over-all characteristics of the system is given on Fig. 13. In measuring the program circuits a transmission measuring set was used at each end of the circuit. This is a thermocouple type instrument with self-contained calibrating circuit and a meter calibrated in decibels above and below one milliwatt. The range of the instrument is extended by means of a pad, so that levels ten decibels above one milliwatt may also be measured. In making the measurements the oscillator output was adjusted to provide a one-milliwatt level into the line repeating coil at the various frequencies for which the characteristic was required. At the receiving end an attenuator between the line amplifier and the transmission measuring set was adjusted to give a

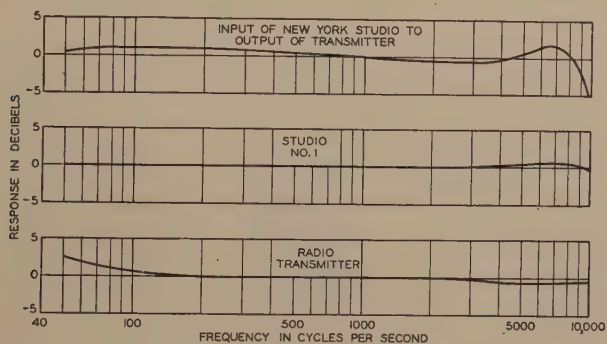


Fig. 14—Frequency response curves.

satisfactory reading on the meter of the set. The output was read directly on the instrument for the various frequencies. In making the over-all measurements the input of the booth equipment was connected to a special transmission measuring set. The output of the equipment was transmitted through the master control room and the program line to the radio transmitter. A portable modulation meter was coupled to the output of the radio transmitter and served the double purpose of indicating percentage modulation and rectifying the carrier to supply audio frequencies for the measuring equipment.

For the frequency characteristic measurements a thermocouple connected to a microammeter was used to indicate the output level. During these measurements the modulation was held constant and the input necessary in New York to maintain a constant output at Carteret was recorded. The over-all frequency characteristic is shown at the top of Fig. 14, with that of Studio No. 1 and the fifty-kilowatt transmitter below.

For the distortion measurements a harmonic analyzer was con-



nected to the output terminals of the modulation meter. The audio-frequency input to the radio transmitter was adjusted to give 100 per cent modulation, as indicated by a cathode-ray oscillograph. The percentage of modulation was determined by readings of a Western Electric 700-A volume indicator for other levels at which distortion measurements were made. The accuracy of this instrument is within two per cent for comparative readings. The distortion produced by the transmitter when modulated by various frequencies ranging from fifty to 7500 cycles is plotted in Fig. 15. The increase in distortion at low frequencies is due in the main to characteristics of the power supply, which can probably be modified to effect an improvement. The rise at the high-frequency extreme is of little significance, because these frequencies rarely, if ever, appear at levels which produce the high degrees of modulation shown.

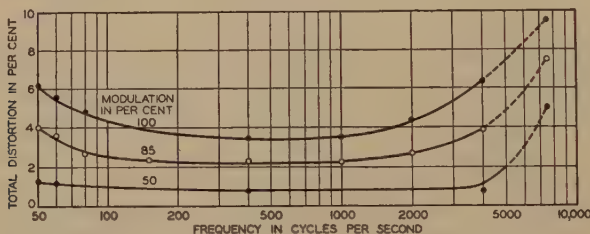


Fig. 15—Audio distortion measurements.

Noise levels were measured with a program circuit noise meter connected to the output terminals of the modulation meter. This instrument contains a weighting network which has been found upon exhaustive program tests to simulate the interfering effect of noise components upon the average listener.<sup>3</sup> The radio transmitter was modulated at 100 per cent with a 1000-cycle signal, and the audio-frequency output level was measured. The modulation was then removed, and the gain of the noise meter was increased until the same meter reading was obtained. The level of the noise below complete modulation was equal to the difference in settings of the attenuator of the instrument. Noise measurements were made by beginning with the transmitter and adding an element of the system with each reading until the entire system was included in the circuit under measurement. The noise level of the entire system from microphone to antenna was found to be approximately sixty-two and five-tenths decibels down

<sup>3</sup> E. L. Owens, "The relative importance of frequency components of noise in radio broadcasting equipment," *Pick-Ups*, February, (1936).

from the level required for complete modulation. In the transmitter alone the noise level measured in a similar manner was seventy-six decibels down.

The concluding test of system performance was a field intensity survey conducted to determine the actual distribution of ground plane radiation from the antenna array. A large number of readings were taken about the antenna at distances ranging from one-half to one and one-half miles. These observed values were corrected for distance to correspond to the intensity at one mile from the antenna but not cor-

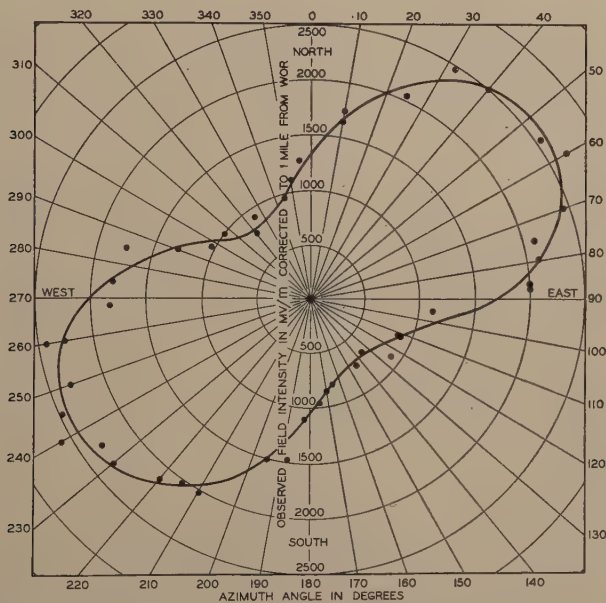


Fig. 16—Observed distribution of radiation from the WOR directional array.

rected for attenuation. While it is generally necessary to correct also for attenuation, preliminary tests showed that this factor was negligible at the distances at which measurements were made. The distribution pattern resulting from this test is shown on Fig. 16.

This station was placed in regular service March 4, 1935. An extensive field survey covering a number of states was made during May and June, 1935, which shows that the selection of station site and antenna type fulfills all expectations. Listener response has been very satisfactory, and an analysis of the statistics has shown excellent correlation with the survey.



## ULTRA-HIGH-FREQUENCY TRANSMISSION BETWEEN THE RCA BUILDING AND THE EMPIRE STATE BUILDING IN NEW YORK CITY\*

By

P. S. CARTER AND G. S. WICKIZER

(R.C.A. Communications, Inc., Rocky Point and Riverhead, L.I., N.Y.)

**Summary**—*Propagation between these two buildings at a frequency of 177 megacycles has been studied with the object of providing a radio circuit with flat response over three megacycles. It was found that the received signal arrived over several paths, some of which were due to reflections from ground and from near-by buildings. The effects on the indirect rays of horizontal and vertical directivity, and change in angle of polarization were observed. The theoretical response curve for an assumed combination of rays was compared with the curves obtained experimentally.*

THE propagation studies discussed in this paper were undertaken in connection with providing a radio circuit for the transmission of television images from the studios in the RCA Building to the transmitter in the Empire State Building. A relatively high carrier frequency was required to transmit both side bands at modulation frequencies up to 1.5 megacycles, and to minimize man-made noises generated in electrical equipment. A frequency of 177 megacycles was selected to avoid possible interference from the Empire State television and sound transmitters which will operate in the neighborhood of fifty megacycles.

The two buildings are approximately 4600 feet apart, and are considerably higher than the buildings lying directly between them. Over this relatively short path, between high buildings, the signal at the receiver would be expected to consist of a direct and a number of reflected rays. The effect of this combination of rays on the radio circuit response curve was investigated in an effort to provide a flat response curve over a frequency band at least three megacycles in width.

During this investigation, the receiving antenna was located in a small balcony outside of the eighty-fifth floor, on the north side of the Empire State Building. The transmitting antenna and transmitter were located first on top of an elevator shaft at the fourteenth floor level of the RCA Building, and later moved to a large balcony at the sixty-seventh floor.

The transmitter was a line controlled master oscillator, followed by a power amplifier stage. Frequency variation was accomplished by

\* Decimal classification: R113.7×R423.5. Original manuscript received by the Institute, June 22, 1936.

a micrometer adjustment on the oscillator line, and the power output was held constant by adjusting the output coupling for constant antenna meter reading.

The receiver was a double superheterodyne, equipped with heterodyne oscillator, followed by an audio measuring unit. Both diode current and heterodyne output were observed as a check on the receiver output. The receiving antenna was located a fraction of a wave length from the building wall. At this small distance the phase change between direct and reflected waves is small for a frequency range of three or four per cent.

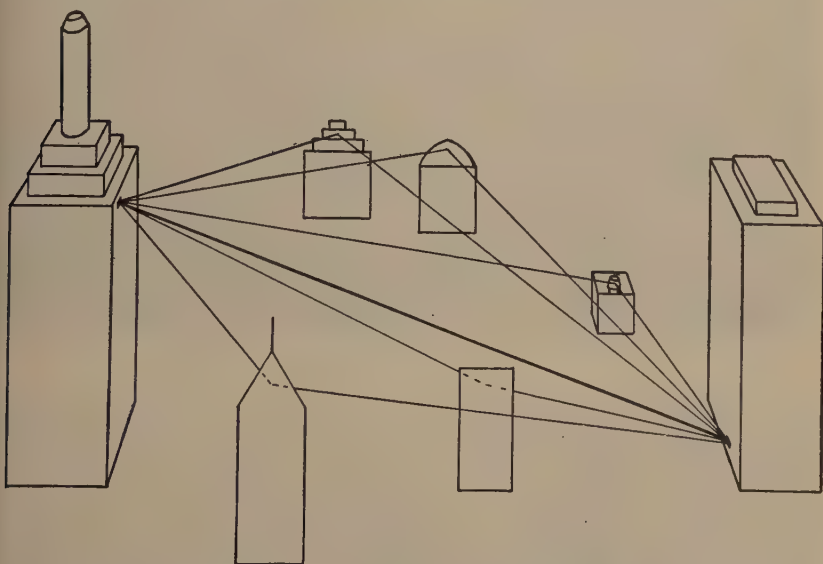


Fig. 1—Direct and reflected ray paths.

Fig. 1 is a sketch showing the direct path and some of the possible indirect paths when transmitting from the fourteenth floor of the RCA Building to the eighty-fifth floor of the Empire State Building. The actual conditions are very much more complex than shown here. Fig. 2 is a photograph looking toward the RCA Building taken from the eighty-fifth floor of the Empire State Building, while Fig. 3 is a photograph taken from the fourteenth floor of the RCA Building looking in the opposite direction. From an inspection of these pictures it is apparent that the signal at the receiver might be made up of a large number of rays. This is possible because there exist surfaces on the various buildings, which lie at almost every conceivable angle. With the transmitter located at a relatively low level, the length of the path



Fig. 2—View from receiver toward transmitter.



Fig. 3—View from transmitter toward receiver.



of the indirect ray lying in the vertical plane is not greatly different from that of the direct ray. However, reflected rays from objects lying off to the sides from the direct path may be of much greater length than the direct ray.

Fig. 4 is a response curve when using simple half-wave dipoles at both ends of the circuit. It was found necessary to install a copper sheet reflector behind the transmitting antenna, to eliminate reflections from the building wall, which was several wave lengths behind

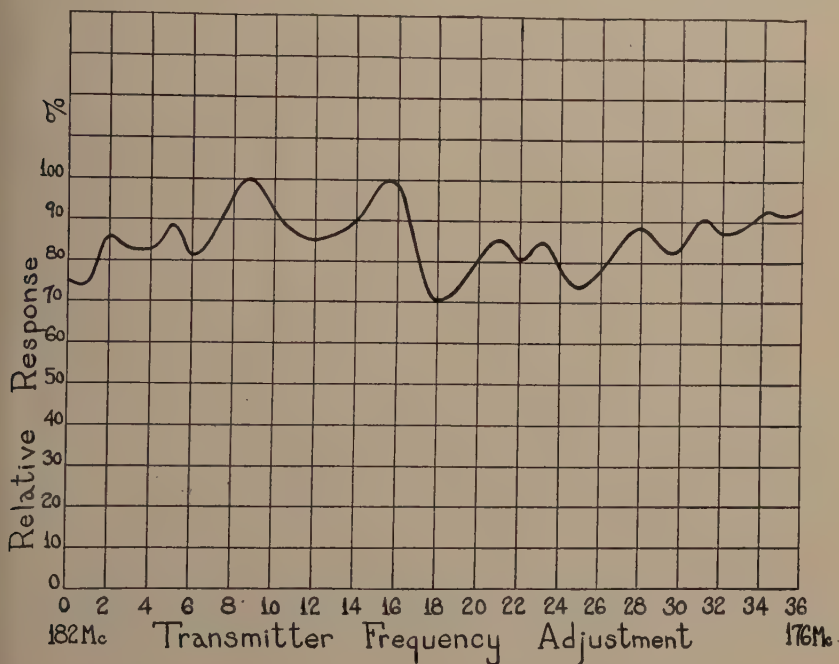


Fig. 4—Response curve with half-wave dipoles at transmitter and receiver. Horizontal polarization, transmitter at fourteenth floor.

the antenna. With such an antenna system, the transmitted pattern is independent of reflecting surfaces behind the antenna. At first sight this curve appears difficult to interpret, there being no definite regularity to the maxima or minima. Let us for a moment consider the process of combination of the various rays making up the resulting received signal. A disturbance leaving the transmitting antenna at the time  $t$  will arrive at the receiving antenna at the time  $t + d/c$  where  $d$  is the distance traveled and  $c$  the velocity of light. If we represent the electric field of the wave at the transmitter by  $E\epsilon^{j\omega t}$  then, at the receiver it will be represented by  $E\epsilon^{j\omega(t+d/c)}$  or, in other words, the phase lag in traveling the distance  $d$  is  $\omega(d/c)$ . Now, if we have two rays

which travel distances differing by a distance  $X$ , the phase angle difference  $\phi$  then becomes

$$\phi = \frac{\omega X}{c} + \alpha = \frac{2\pi f}{c} X + \alpha$$

where  $\alpha$  is the phase change due to reflection from any surface. Then

$$d\phi = \frac{2\pi X}{c} df = \frac{2\pi X}{\lambda} \cdot \frac{df}{f} \text{ radians.}$$

Expressed otherwise, the change in phase angle  $d\phi$ , for a change in frequency  $df$ , is equal to the product of the path difference expressed

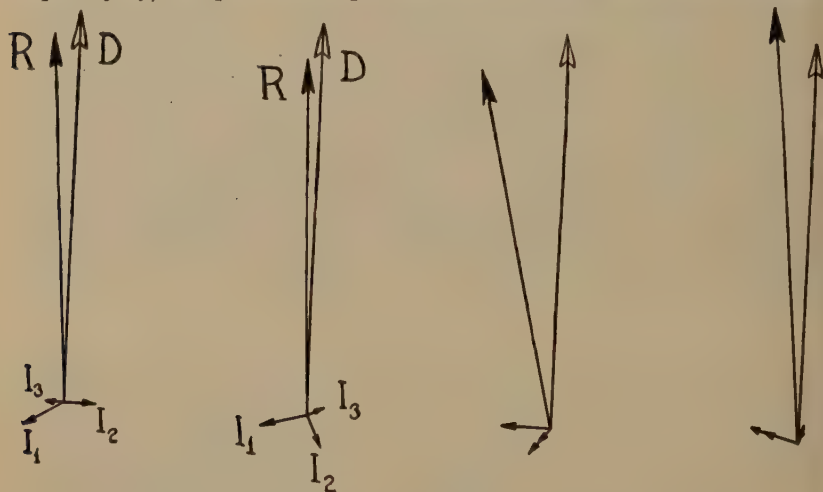


Fig. 5—Vector diagrams showing change in resultant voltage with frequency variation when reflected rays are present.

in terms of angle, multiplied by the ratio of the change in frequency to the frequency. For instance, if we have a path difference of ten wavelengths or 3600 degrees between two rays, a one per cent change in frequency will cause a phase change of approximately thirty-six degrees.

The signal strength resulting from the combination of a direct and several indirect rays is equal to the vector sum of a fixed vector and several other vectors rotating at angular velocities corresponding to the rate of change of phase with frequency given by the above relation.

Fig. 5 shows four combinations of a fixed vector of unit amplitude and three rotating vectors having amplitudes of  $1/8$ ,  $1/12$ , and  $1/20$ ; and angular velocities in the ratios of three, thirteen, and thirty-one. Between successive diagrams, the angle of the slowest rotating vector

has been advanced fifteen degrees which, for a 0.1 per cent change in frequency corresponds to a path difference of 41.7 wave lengths. The continuous curve of the resultant obtained from this process is shown in Fig. 6. Comparing this curve with Fig. 4, certain similarities will be noted which indicate that the experimental curve is the resultant of a direct and several indirect rays having considerable difference in length of path. With the particular conditions existing in these tests, such

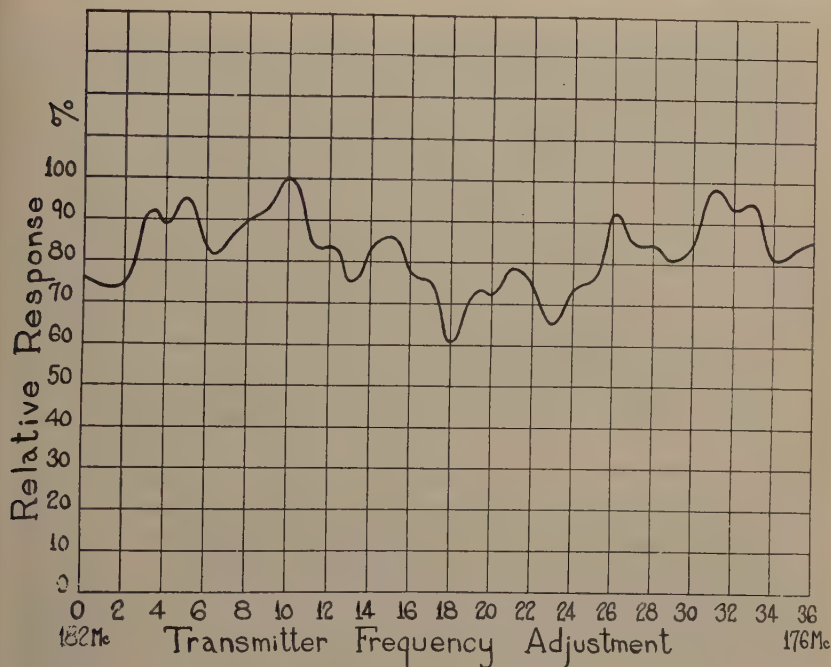


Fig. 6—Curve constructed from vector diagrams shown in Fig. 5.

differences in path would be expected only between rays arriving at relatively wide angles.

From the frequency range between successive maxima of this type of curve, the limits of variation in angle at which the indirect rays are arriving may be estimated. Theoretically, an indirect ray having a given length of path might be reflected from any point on an ellipsoid having the transmitting and receiving antennas as foci. However, when the antennas have reflectors behind them, the angles of the indirect rays with respect to the direct ray are limited to values less than ninety degrees. In a plane containing the two antenna wires this angle is further limited due to the fact that little radiation or reception is obtained at angles in the vicinity of ninety degrees to the direct ray.



Since the curve of Fig. 4 indicates indirect rays arriving at wide angles, the introduction of moderate directivity at either or both transmitter and receiver should materially reduce the rapid variations in the response characteristic. In order to study the effect of an increase in directivity in the horizontal plane, a transmitting antenna having a radiator one wave length long, fed at the center and located in front of a copper reflector, was set up as shown in Fig. 7. The response curve

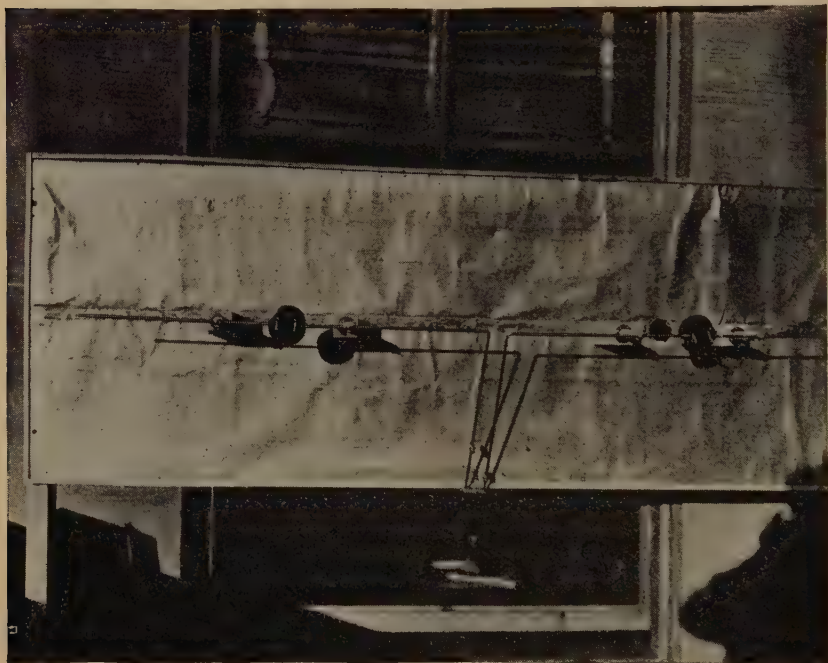


Fig. 7—Experimental directive transmitting antenna with reflector.

obtained with this antenna is shown in Fig. 8. It is apparent that the rapid variations have been considerably reduced, but there are certain frequency ranges where the variation in signal strength has been increased. From a study of vector diagrams such as previously described, it can be shown that although the removal of one or more indirect rays will usually give a general improvement over a wide range of frequency, such a removal may cause wider variation over certain small frequency ranges.

To reduce further the strength of the indirect rays, a directive antenna arrangement was placed at the receiver. This consisted of two half-wave dipoles lying end to end and separated by a distance of one and one-half wave lengths between centers. Using this antenna and the

directive transmitting antenna previously described, the curve shown in Fig. 9 was obtained. It will be noted that this curve shows considerably less variation than the curve of Fig. 8.

Since the reflections in these tests come from surfaces having all sorts of shapes and positions, we should expect a difference in the results with a change in the polarization. To investigate such a change, a half-wave dipole was arranged vertically in front of a copper reflec-

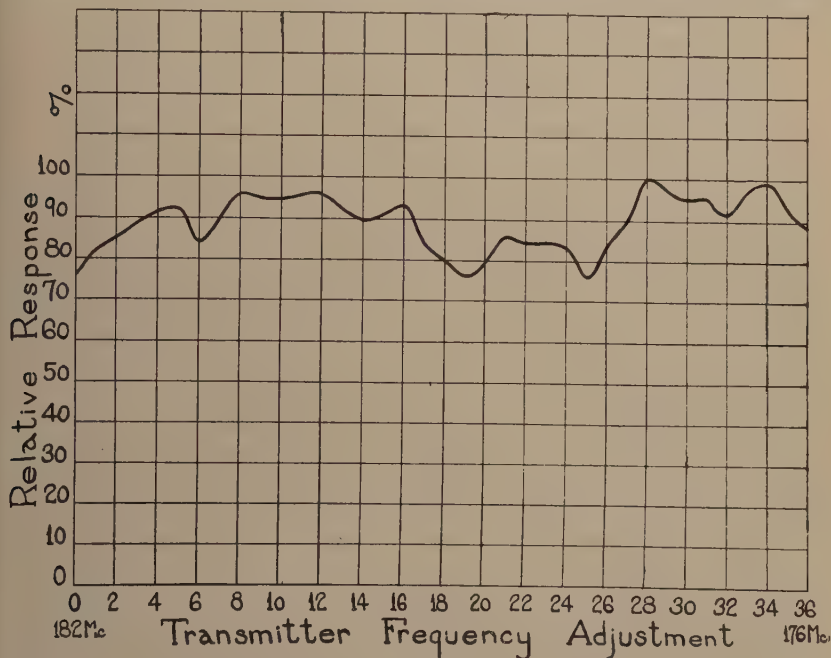


Fig. 8—Response curve with directive transmitting antenna and half-wave receiving dipole. Horizontal polarization, transmitter at fourteenth floor.

tor, for transmission. For reception, a vertical half-wave dipole was placed a few feet from the building. The results are shown in Fig. 10. This curve is of a different shape and has a much greater variation than the curve of Fig. 4 taken with the same antennas oriented to give horizontal polarization. This difference is probably due to a number of factors, among which are some change in directivity, and changes in both phase and amplitude upon reflection. In general, the phase of a wave after reflection, when polarized in the plane of incidence is opposite to the phase when polarized at right angles to the plane of incidence.

When the receiving and transmitting antennas are both at great heights above the intervening buildings, the geometry of the ray paths is considerably different than that where one antenna is at a relatively

low altitude. The path lengths for indirect rays, lying in the vicinity of the vertical plane passing through the transmitter and receiver, are greatly increased and become a major factor in the determination of the resulting signal strength. Also, there is an increase in the number of surfaces having proper angles to reflect energy to the receiver because of the fact that a large number of objects, which were formerly obscured by near-by buildings, are now brought into view from the transmitter location.

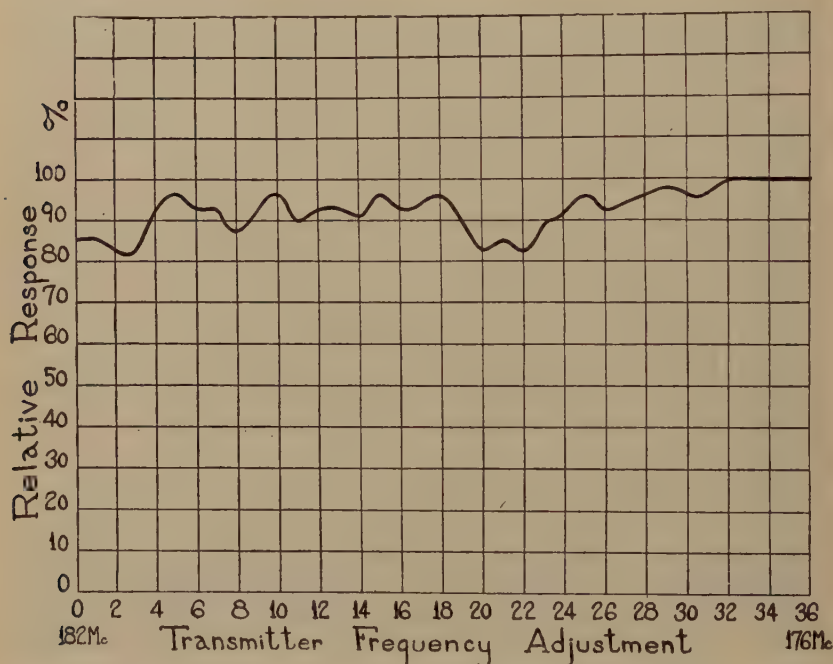


Fig. 9—Response curve with directive transmitting and receiving antennas. Horizontal polarization, transmitter at fourteenth floor.

These effects were investigated by locating the transmitter on a balcony at the sixty-seventh floor of the RCA Building. When facing the Empire State Building at this height, one gets an impression of practically all other buildings being down rather than off to the sides. This impression of height is conveyed by the photograph taken from the Empire State Building.

With the same horizontally polarized directive antennas referred to in connection with Fig. 7, the data shown in Fig. 11 were obtained. The receiving antenna was a single half-wave dipole. It will be noted that the slower variation is of considerable magnitude, and corresponds to a path difference of approximately  $59\lambda$  or about 328 feet. With the



transmitter at a height of 900 feet, the receiver at a height of 1000 feet, and a distance between buildings of 4600 feet, this path difference might naturally be assumed to be due to reflection from a horizontal surface at a height of about 100 feet and located in the vicinity of 2200 feet from the RCA Building. The angle of such a ray would be about 20.5 degrees to the horizon. If such an assumption is correct, a receiving antenna which has minimum pickup at this angle in the vertical plane should eliminate this variation in signal strength.

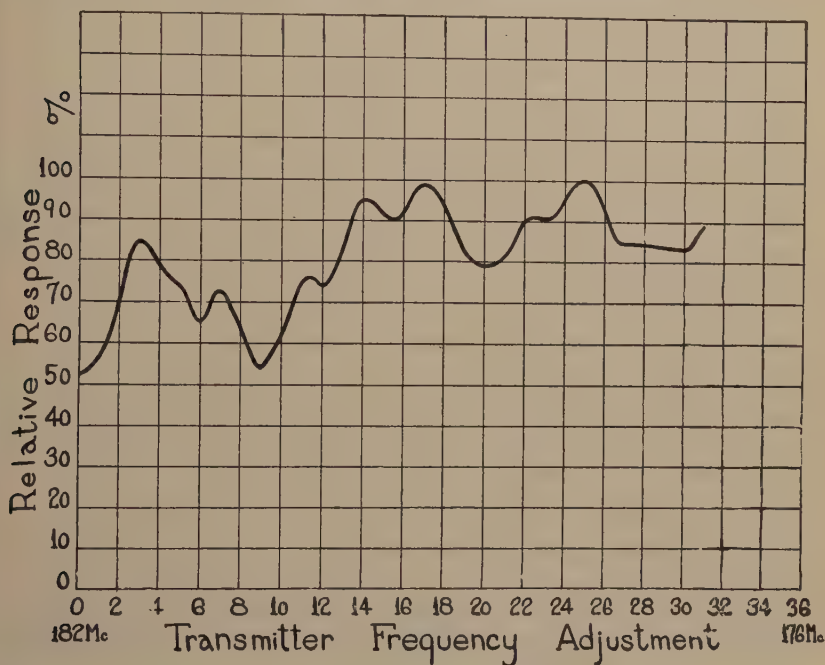


Fig. 10—Response curve with half-wave dipoles at transmitter and receiver. Vertical polarization, transmitter at fourteenth floor.

Accordingly, an antenna consisting of two parallel horizontal dipoles spaced 1.43 wave lengths to give zero reception at an angle of 20.5 degrees to the horizon was erected. Fig. 12 shows the curve resulting from the use of this antenna in conjunction with the same transmitting antenna used for Fig. 11. It is evident that the indirect ray which was assumed to be coming from a building roof lying in a line between the two buildings, has been entirely eliminated. However, the curve is still quite irregular due to side reflections.

Horizontal directivity at both ends was also tried for this height. The rapid variations were fairly well smoothed out as can be seen from Fig. 13. If the proper vertical directivity had been included with the



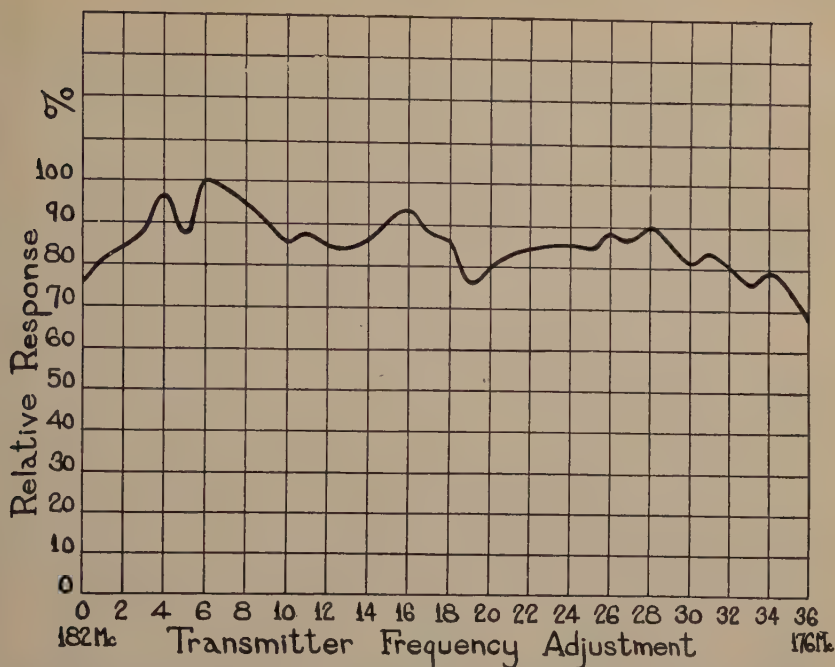


Fig. 12—Response curve with directive transmitting antenna and vertical directivity at receiver. Horizontal polarization, transmitter at sixty-seventh floor.

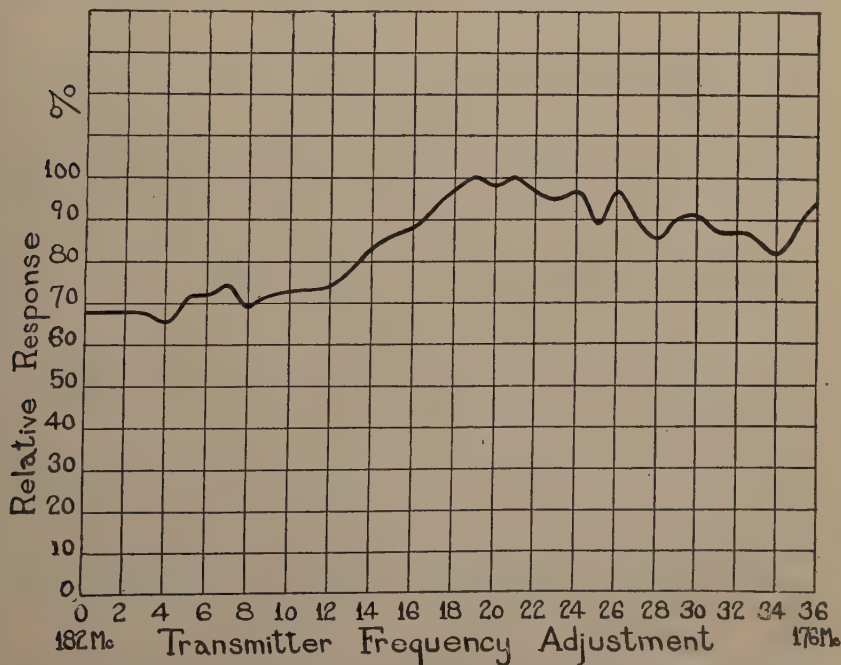


Fig. 13—Response curve with directive transmitting antenna and horizontal directivity at receiver. Horizontal polarization, transmitter at sixty-seventh floor.



The conditions encountered in this investigation fall far short of such ideal assumptions, as is evident from the curve of Fig. 14, which was taken with both transmitting and receiving antennas oriented at an angle of forty-five degrees to the horizon.

The investigation which has been discussed, shows that, where the frequency band is a substantial percentage of the carrier frequency, variation in signal strength within the band may occur unless special precautions are taken to eliminate the effects of indirect rays. A few

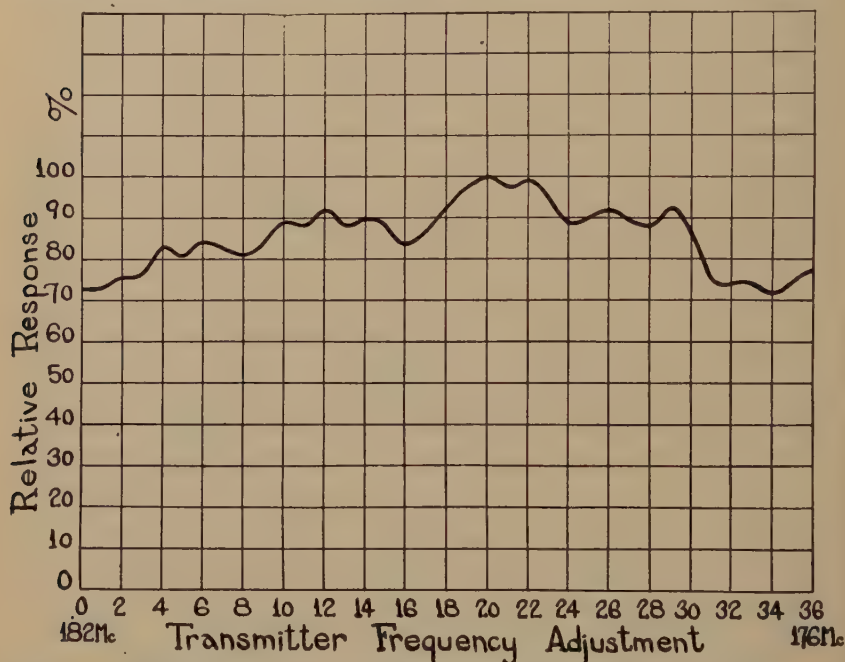


Fig. 14—Response curve with directive transmitting antenna and half-wave dipole at the receiver. Polarization forty-five degrees to the horizon, transmitter at sixty-seventh floor.

indirect rays having amplitudes of the order of ten per cent or less of the amplitude of the direct ray, may cause considerable variation in the received signal.

#### ACKNOWLEDGMENT

The authors wish to acknowledge the valuable assistance given them by W. C. Resides, T. J. Buzalski, and other members of the Development Division of the National Broadcasting Company, and J. W. Conklin of RCA Communications, who designed the special transmitter.

## ELECTRON OPTICAL SYSTEM OF TWO CYLINDERS AS APPLIED TO CATHODE-RAY TUBES\*

By

D. W. EPSTEIN

(RCA Manufacturing Company, Inc., Camden, N. J.)

**Summary**—The electron beam of a cathode-ray tube is usually focused by means of an electron optical system of two coaxial cylinders. This paper presents a detailed treatment of such a focusing system and is divided into two parts.

Geometric electron optics of axially symmetric electrostatic fields is presented in Part I. This part deals with (1) the analogy between light and electron optics, (2) motion of electrons in axially symmetric electrostatic fields, (3) definition and determination of positions of cardinal points due to axially symmetric electrostatic fields, and (4) thick and thin lenses.

The lenses equivalent to the electrostatic fields of two coaxial cylinders are discussed in Part II. This part deals with (1) positions of cardinal points due to two coaxial cylinders of various diameters and at various voltages, (2) use of such cardinal points, (3) experimental determination of positions of cardinal points, and (4) spherical aberration of electrostatic field due to two cylinders.

The results are applied to the cathode-ray tube, throughout the discussion.

### INTRODUCTION

THE exacting demands on cathode-ray tubes used for present-day purposes require that the tube designer have a clear and detailed understanding of the operation of the tube. It is very convenient to treat the operation of a cathode-ray tube in terms of geometric electron optics. In geometric electron optics use is made of the well-known fact that the trajectory of an electron in electrostatic fields is similar to the trajectory of a ray of light in refractive media. Because of this similarity the concepts of geometric optics such as lens, focal length, etc., may be transferred to electrostatic fields. From this point of view a cathode-ray tube is nothing else but an axially symmetric optical system.

Fig. 1 gives the cross section through the axis of a cathode-ray tube. The whole electrostatic focusing system associated with the various electrodes may be considered as two axially symmetric electrostatic lenses, one existing close to the cathode and caused by the potentials on the cathode grid and first anode, and the other existing near the end of the first anode and caused by the difference in potential between the first and second anodes.

\* Decimal classification: R388. Original manuscript received by the Institute, June 22, 1936.

Presented to the Faculty of the Moore School of Electrical Engineering of the University of Pennsylvania in partial fulfillment of the requirements for the degree of Doctor of Philosophy.

The discussion in this paper will be limited to the second lens. For the purposes of this paper the first lens<sup>1</sup> may be considered as concentrating the electrons emitted by the cathode into a small new source which serves as the object for the second lens. The second lens then images this object on the fluorescent screen producing the visible spot.

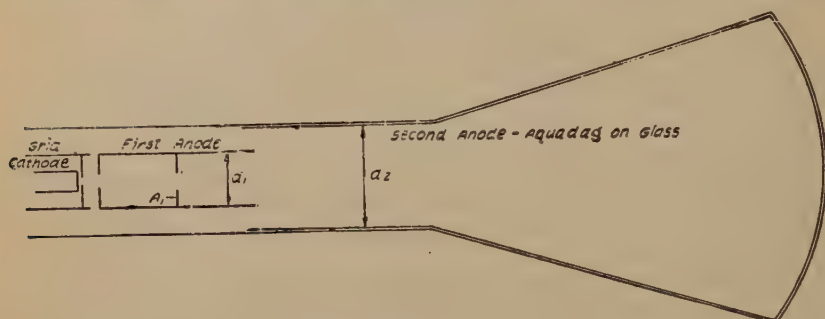


Fig. 1—Cathode-ray tube.

## I. ELECTRON OPTICS OF AXIALLY SYMMETRIC ELECTROSTATIC FIELDS<sup>2</sup>

In the early part of the nineteenth century, William Hamilton showed that a strict analogy exists between the path of a ray of light passing through refracting media and the path of a particle passing through conservative fields of force. The track of an electron moving through electrostatic and magnetostatic fields is, therefore, similar to the track of a ray of light passing through refracting media. Geometrical electron optics is the name given to the subject dealing with the paths of electrons in electrostatic and magnetostatic fields when considered from the point of view of geometrical optics.

### *Analogy of Electron and Light Optics*

The principle of least time may be taken as the basis of geometrical optics. This principle states that the path of a ray of light from point *A* to point *B* is always such as to make the integral an extremal (usually a minimum) with respect to all neighboring paths for rays of the same frequency. The principle is usually stated as,

<sup>1</sup> For an analysis of the first lens see I. G. Maloff and D. W. Epstein, "Theory of electron gun," *Proc. I.R.E.*, vol. 22, pp. 1386-1411; December, (1934).

<sup>2</sup> The theory of geometrical electron optics has been developed by H. Bush, *Ann. der Phys.*, vol. 81, p. 976, (1926); *Archiv. für Elekt.*, vol. XVIII, p. 583, (1927).

J. Picht, *Ann. der Phys.*, vol. 15, p. 926, (1932).

W. Glaser, *Zeits. für Phys.*, vol. 80, p. 451, (1933); *Zeits. für Phys.*, vol. 81, p. 647, (1933); *Zeits. für Phys.*, vol. 83, p. 104, (1933).



$$\delta \int_A^B \mu(\nu, x, y, z) ds = 0 \quad (\nu = \text{constant}). \quad (1)$$

The principle of least action for electron velocities less than one tenth the velocity of light states that an electron of total energy  $E$ , kinetic energy  $T$ , and mass  $m$  moves through an electrostatic field with potential energy  $V(x, y, z)$  in such a way as to make the action integral,

$$s = \int_A^B 2T dt = \int_A^B [2m(E - V)]^{1/2} ds$$

over the actual path between the two points  $A$  and  $B$  an extremal as compared with its value for all adjacent paths for the same value of  $E$ . As the integrand  $[2m(E - V)]^{1/2}$  is identical with the *absolute* value of the momentum  $p$  which the electron would assume at  $(x, y, z)$ , the principle may be stated as

$$\delta \int_A^B p(E, x, y, z) ds = 0 \quad (E = \text{constant}). \quad (2)$$

A comparison of (1) and (2) shows that the paths of an electron in an electrostatic field may be identified with the rays of light in geometrical optics if the index of refraction is chosen to be

$$\mu = k'[E - V]^{1/2} = k'p = kv \quad (3)$$

where  $k$  is a constant of proportionality and  $v$  is the speed of the electron. So the index of refraction at any point of an electrostatic field is proportional to the speed of the electron at the point. If, as is customarily done, the index of refraction is taken as a pure numeric then  $k$  must have the dimensions of  $1/v$ . The value assigned to  $k$  is of no importance since only the ratio of  $\mu$  at two different places is used, so that if  $\mu_1$  and  $\mu_2$  are the indexes of refraction at two different places, the relative index of refraction is,

$$\frac{\mu_2}{\mu_1} = \frac{kv_2}{kv_1} = \frac{v_2}{v_1}. \quad (4)$$

Since the potential function  $V(x, y, z)$  is a continuous scalar function of position it follows from (3) that the index of refraction of an electrostatic field is also a continuous function of position. Optically speaking, this means that an electrostatic field constitutes an isotropic, nonhomogeneous medium for electrons (corresponding to a medium of uniformly variable density for light rays.)

If a magnetostatic field be also present then the index of refraction is<sup>3</sup>

$$\mu = k \left[ v - \frac{e}{|v| m} (\vec{v} \cdot \vec{A}) \right] \quad (5)$$

where  $(\vec{v} \cdot \vec{A})$  stands for the scalar product of the vectors  $\vec{v}$  and  $\vec{A}$ , where  $\vec{A}$  is vector potential defined by the relation

$$\vec{H} = \text{curl } \vec{A}.$$

Equation (5) shows that  $\mu$  is a function not only of position but also of direction. This shows that a magnetostatic field constitutes an anisotropic medium for electrons (corresponding to a crystalline medium for light.)

Here, the interest lies in electrostatic fields only and, therefore, no more will be said of magnetostatic fields.

### *Axially Symmetric Focusing Systems*

Therefore, certain forms of electrostatic fields will act as focusing systems or "lenses" for electron beams, just as certain forms of refracting media act as focusing systems for light beams. The forms of fields required will depend upon the type of focusing.

For many purposes, as in the cathode-ray tube, the interest lies in an electron focusing system having axial symmetry. Most optical systems for light consist of a series of spherical refracting surfaces having a common axis of symmetry called the optical axis. In the case of light, however, the optical systems are usually such that the index of refraction changes abruptly as light passes from one medium to the other. In the case of electron optics, the index of refraction is a continuous function of position.

Fig. 2 represents a cross section through the axis of an electron focusing system; the heavy lines represent two cylindrical, metallic electrodes at the potentials  $V_1$  and  $V_2$ , the light lines represent the equipotential surfaces in the space (vacuum) between the electrodes. From (3) it follows that each equipotential surface represents a surface of constant index of refraction. In Fig. 2 there are shown only a few

<sup>3</sup> The Lagrangian function for an electron moving with the velocity  $v$  ( $< 0.1c$ ) through electrostatic and magnetostatic fields is

$$L = \frac{1}{2}mv^2 - V - e(\vec{v} \cdot \vec{A}).$$

From which it follows that

$$\int p ds = \int \frac{\partial L}{\partial v} ds = \int \left\{ mv - \frac{e}{v} (\vec{v} \cdot \vec{A}) \right\} ds$$

and hence equation (5).

of the equipotential surfaces, actually there are, of course, an infinite series of equipotential surfaces having a common axis. The electron focusing system of Fig. 2 may, therefore, be considered as a very large number of coaxial refracting surfaces.

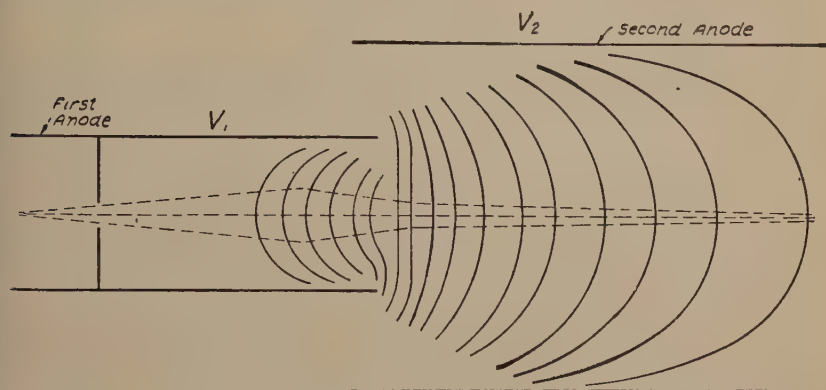


Fig. 2—Equipotential line plot of two cylinders.

To illustrate the focusing action of the electrostatic field consider the artificial case of a spherical surface separating two media of different indexes of refraction. Let  $S$  of Fig. 3 be such a surface, and let  $R$

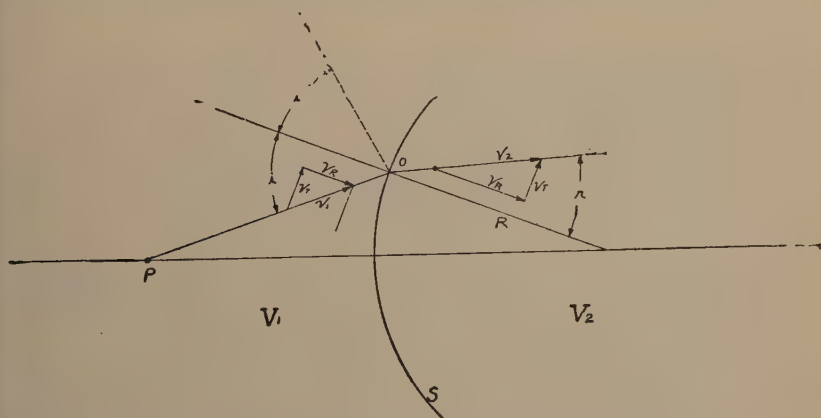


Fig. 3—Electron refraction and reflection at spherical surface.

be its radius; further let the electrostatic potential to the left of  $S$  be  $V_1$  and to the right  $V_2$ . Now consider an electron moving in the direction  $PO$  with the velocity  $v_1$ . As it arrives at the surface a force normal to the surface in the direction of  $R$  will act on it, and when it has passed through the surface its velocity will have changed to, say,  $v_2$ . The



force being normal to the surface, only the component of initial velocity  $v_R$  normal to the surface will change; the tangential component of velocity  $v_T$  will be the same on both sides of the surface. From Fig. 2 it thus follows that

$$v_T = v_1 \sin i = v_2 \sin r$$

where  $i$  and  $r$  are the angles of incidence and refraction, respectively. Hence,

$$\frac{\sin i}{\sin r} = \frac{v_2}{v_1} = \mu \quad (a \text{ constant}). \quad (6)$$

So, if  $v_2/v_1$  be the index of refraction then (6) is the well-known law of refraction.

It is instructive to express (6) in a different form. The work done by the field on the electron when it goes from the first to the second medium is  $e(V_2 - V_1)$ . Then from the law of conservation of energy it follows that

$$\frac{1}{2}mv_2^2 = \frac{1}{2}mv_1^2 + e(V_2 - V_1)$$

so,

$$\mu = \frac{v_2}{v_1} = \sqrt{1 + \frac{e(V_2 - V_1)}{\frac{1}{2}mv_1^2}}. \quad (7)$$

If, further, the initial velocity of the electron  $v_1$  is that corresponding to the voltage  $V_1$ , then  $\frac{1}{2}mv_1^2 = eV_1$  and

$$\mu = \frac{v_2}{v_1} = \sqrt{1 + \frac{(V_2 - V_1)}{V_1}} = \sqrt{\frac{V_2}{V_1}}. \quad (8)$$

If  $V_2 < V_1$ , then  $V_2 - V_1$  is negative and if in absolute magnitude it is larger than  $\frac{1}{2}m(v_1 \cos i)^2$ —the part of the kinetic energy of the electron corresponding to the normal component of its velocity—then the electron will be shot back from the surface with its normal velocity component reversed. The direction of the reflected electron makes with the normal to the surface the same angle  $i$  as that of the incident ray.

### *Potential of Axially Symmetric Electrostatic Fields*

To determine the potential distribution in space due to assigned potentials on axial symmetric electrodes it is necessary to solve the reduced Laplace equation

$$\frac{\partial^2 V}{\partial r^2} + \frac{1}{r} \frac{\partial V}{\partial r} + \frac{\partial^2 V}{\partial z^2} = 0 \quad (9)$$

subject to the boundary conditions that  $V$  assume the given values of potential on the electrodes. In general, it has not been found possible to obtain a simple analytical solution of (9) subject to the actually existing boundary conditions. However, the required solution of (9) subject to the existing boundary conditions is easily obtained experimentally. The equipotential line plot shown in Fig. 2 was thus obtained.<sup>4</sup>

Of great significance is the fact that the potential distribution in space is uniquely determined if the distribution of potential along the axis together with its even derivatives are known. This is shown as follows: Let  $V(r, z)$  be the required solution of (3), then due to the axial symmetry one can expand  $V(r, z)$  into an infinite series containing only even powers of  $r$ ; i.e.,

$$V(r, z) = V_0(z) + r^2 V_2(z) + r^4 V_4(z) + \cdots + r^{2n} V_{2n}(z) + \cdots \quad (10)$$

Substituting (10) into (9) and equating the coefficients of equal powers of  $r$  to zero there results that

$$\begin{aligned} V(r, z) = & V_0(z) - \frac{r^2}{2^2} V_0''(z) + \frac{r^4}{2^4 4^2} V_0^{(4)}(z) + \cdots \\ & + \frac{(-1)^{nr^{2n}}}{2^2 \cdot 4^2 \cdots (2n)^2} V_0^{2n}(z) + \cdots \end{aligned} \quad (11)$$

By setting  $r=0$  in (11) note that  $V(0, z) = V_0(z)$ ; i.e.,  $V_0(z)$  represents the distribution of potential along the axis. So if the function  $V_0(z)$  together with all its even derivatives are known, then the potential distribution off the axis can be found by means of (11).

### *Equations of Motion of Electron*

The equations of motion of an electron moving in a meridian plane are

$$\begin{aligned} m \frac{d^2 z}{dt^2} &= e \frac{\partial V}{\partial z} \\ m \frac{d^2 r}{dt^2} &= e \frac{\partial V}{\partial r} \end{aligned} \quad (12)$$

In terms of the axial distribution of potential these equations become from (11)

<sup>4</sup> E. D. McArthur, "A method of experimentally determining potential distribution," *Electronics*, p. 192, June, (1932).

$$\begin{aligned}
m \frac{d^2 z}{dt^2} &= e \left[ V_0'(z) - \frac{r^2}{2^2} V_0^{(3)}(z) + \dots \right. \\
&\quad \left. + \frac{(-1)^n r^{2n}}{2^2 \cdot 4^2 \cdot \dots \cdot (2n)^2} V_0^{(2n+1)}(z) + \dots \right] \\
m \frac{d^2 r}{dt^2} &= e \left[ -\frac{r}{2} V_0''(z) + \frac{r^3}{2^2 \cdot 4} V_0^{(4)}(z) + \dots \right. \\
&\quad \left. + \frac{(-1)^n r^{2n-1}}{2^2 \cdot 4^2 \cdot \dots \cdot (2n-1)^2 \cdot 2n} V_0^{(2n)} + \dots \right].
\end{aligned} \tag{13}$$

### Energy Equation

Adding the two equations (12) we have

$$m \left[ \frac{dz}{dt} d\left(\frac{dz}{dt}\right) + \frac{dr}{dt} d\left(\frac{dr}{dt}\right) \right] = e \left( \frac{\partial V}{\partial z} dz + \frac{\partial V}{\partial r} dr \right) = e dV. \tag{14}$$

Equation (14) is exact and its solution is

$$\frac{1}{2} m v^2 = \frac{1}{2} m \left[ \left( \frac{dz}{dt} \right)^2 + \left( \frac{dr}{dt} \right)^2 \right] = eV + C.$$

If the velocity of the electron is zero when  $V=0$  then  $C=0$  and

$$\frac{1}{2} m v^2 = \frac{1}{2} m \left[ \left( \frac{dz}{dt} \right)^2 + \left( \frac{dr}{dt} \right)^2 \right] = eV \tag{15}$$

and,

$$v = \sqrt{2 \frac{e}{m} V} = 5.95 \times 10^7 \sqrt{V} \text{ volts cm/sec.} \tag{16}$$

If  $v=v_0$  when  $V=0$  then  $c=\frac{1}{2}mv_0^2$  and

$$\frac{1}{2} m (v^2 - v_0^2) = eV.$$

If further the velocity  $v_0$  be given in equivalent volts then  $\frac{1}{2}mv_0^2 = e(V_0/300)$  and

$$v_0 = \sqrt{2 \frac{e}{m} \frac{(V + V_0)}{300}} = 5.95 \times 10^7 \sqrt{(V + V_0)} \text{ volts cm/sec.} \tag{17}$$



*Differential Equation of Trajectory of Electron*

It will now be shown that the trajectory of an electron traversing an axially symmetric electrostatic field described by the potential function  $V(r, z)$  satisfies the following differential equation:

$$\frac{d^2r}{dz^2} + \frac{\left[1 + \left(\frac{dr}{dz}\right)^2\right]}{2V} \frac{\partial V}{\partial z} \frac{dr}{dz} - \frac{\left[1 + \left(\frac{dr}{dz}\right)^2\right]}{2V} \frac{\partial V}{\partial r} = 0. \quad (18)$$

To show this note that

$$\begin{aligned} \frac{d^2r}{dt^2} &= \frac{d}{dt} \left( \frac{dr}{dt} \right) = \frac{dz}{dt} \frac{d}{dz} \left( \frac{dr}{dz} \frac{dz}{dt} \right) \\ &= \left( \frac{dz}{dt} \right)^2 \frac{d^2r}{dz^2} + \frac{dr}{dz} \frac{dz}{dt} \frac{d}{dz} \left( \frac{dz}{dt} \right) \end{aligned} \quad (9)$$

$$\frac{d^2z}{dt^2} = \frac{d}{dt} \left( \frac{dz}{dt} \right) = \frac{dz}{dt} \frac{d}{dz} \left( \frac{dz}{dt} \right) \quad (20)$$

and that (15) may be written as

$$\frac{1}{2} m \left( \frac{dz}{dt} \right)^2 \left[ 1 + \left( \frac{dr}{dz} \right)^2 \right] = eV. \quad (21)$$

From (19), (20), and (21) it follows that

$$\frac{d^2r}{dt^2} = \frac{2 \frac{e}{m} V}{\left[ 1 + \left( \frac{dr}{dz} \right)^2 \right]} \frac{d^2r}{dz^2} + \frac{dr}{dz} \frac{d^2z}{dt^2}. \quad (22)$$

Inserting into (22) the values of  $d^2r/dt^2$  and  $d^2z/dt^2$  as given by (12), there results (18).

It is of interest to note that  $e/m$  does not appear in (18), signifying that the trajectory is the same for *any* charged particle. Further, it is to be noted that (18) is homogeneous in  $V$  so that if the voltages on the electrodes are all increased by a constant factor the trajectory of the electron will remain unaltered. Equation (18) is also homogeneous in  $r, z$  so that if all dimensions are increased by a constant factor then the trajectory is also increased by the same factor.

### Paraxial Electrons

An optical system is usually described in terms of paraxial or first order imagery. Actual imagery departs from paraxial imagery. Such departures are described as aberrations.

The focusing action of an electrostatic field is similarly described to a first approximation by considering only paraxial electrons. Paraxial electrons are characterized by the fact that in calculating their paths it is assumed that their distances from the axis,  $r$ , and their inclination toward the axis,  $dr/dz$ , are so small that the second and higher powers of  $r$  and  $dr/dz$  are negligible.

For the case of paraxial electrons (11), (13), and (15) become

$$V(r, z) = V_0(z) \quad (11p)$$

$$\left. \begin{aligned} m \frac{d^2 r}{dt^2} &= -e \frac{r}{2} V_0''(z) \\ m \frac{d^2 z}{dt^2} &= e V_0'(z) \end{aligned} \right\} \quad (13p)$$

$$\frac{1}{2} m v^2 = \frac{1}{2} m \left( \frac{dz}{dt} \right)^2 = e V_0(z) \quad (15p)$$

and the differential equation for the trajectory traversed by a paraxial electron becomes from (18)

$$\frac{d^2 r}{dz^2} + \frac{V_0'}{2V_0} \frac{dr}{dz} + \frac{V_0''}{4V_0} r = 0. \quad (18p)$$

The letter  $p$  after the equation number is to indicate that the equations so lettered are valid for paraxial electrons only.

Equation (18p) (or equations (13p)) may be taken as the fundamental equation of the electron optics of axially symmetric electrostatic fields.

### The Two Fundamental Trajectories

Multiplying (18p) by  $\sqrt{V}$  there results the self-adjoint<sup>5</sup> equation<sup>6</sup>

$$\begin{aligned} L(r) &= \sqrt{V} \frac{d^2 r}{dz^2} + \frac{V'}{2\sqrt{V}} \frac{dr}{dz} + \frac{V''}{4\sqrt{V}} r \\ &= \frac{d}{dz} \left( \sqrt{V} \frac{dr}{dz} \right) + \frac{V''}{4\sqrt{V}} r = 0. \end{aligned} \quad (23p)$$

<sup>5</sup> See E. L. Ince, Ordinary Differential Equations, p. 215.

<sup>6</sup> For the remainder of this paper  $V$  stands for the axial distribution of potential.

Let  $r_1(z)$  and  $r_2(z)$  be two independent solutions of (18p) representing the trajectories of two electrons then,

$$r_2 L(r_1) - r_1 L(r_2) = \frac{d}{dz} \left\{ \sqrt{V} \left( r_2 \frac{dr_1}{dz} - r_1 \frac{dr_2}{dz} \right) \right\} = 0. \quad (24p)$$

Integrating this equation between the limit  $a$  and  $b$  there results that<sup>7</sup>

$$\int_a^b \{r_2 L(r_1) - r_1 L(r_2)\} dz = \left[ \sqrt{V} \left( r_2 \frac{dr_1}{dz} - r_1 \frac{dr_2}{dz} \right) \right]_a^b = 0$$

substituting the limits,

$$\begin{aligned} & \sqrt{V(b)} \{r_2(b)r_1'(b) - r_1(b)r_2'(b)\} \\ &= \sqrt{V(a)} \{r_2(a)r_1'(a) - r_1(a)r_2'(a)\}. \end{aligned} \quad (25p)$$

In particular let  $r_1(z)$ ,  $r_2(z)$ ,  $r'(z)$ , and  $r_2'(z)$  assume the following values at  $a$  and  $b$ :

$$\begin{aligned} r_1(a) &= h_1 & r_1(b) &= 0 \\ r_1'(a) &= 0 & r_1'(b) &= \tan \beta_2 \\ r_2(a) &= 0 & r_2(b) &= -h_2 \\ r_2'(a) &= \tan \beta_1 & r_2'(b) &= 0 \end{aligned} \quad (26p)$$

then (25p) reduces to

$$\sqrt{V(b)} h_2 \tan \beta_2 = \sqrt{V(a)} h_1 \tan \beta_1. \quad (27p)$$

The two trajectories  $r_1(z)$  and  $r_2(z)$  satisfying (26p) will be called the two fundamental trajectories. Fig. 4 shows two fundamental trajectories. Any two independent trajectories may be taken as the fundamental pair; this particular pair is chosen because by means of this pair the usual optical relations are easily obtained. Thus, (27p) corresponds to Lagrange's law

$$\mu_2 h_2 \tan \beta_2 = \mu_1 h_1 \tan \beta_1.$$

Let  $f_1$  and  $f_2$  be the focal lengths of the focusing system then (see Fig. 4)

$$f_1 = -\frac{h_2}{\tan \beta_1} \quad \text{and} \quad f_2 = \frac{h_1}{\tan \beta_2} \quad (28p)$$

<sup>7</sup> This discussion is limited to electrostatic fields having finite extension; i.e.,  $V=V(z)$  for  $\alpha \leq z \leq \beta$  and  $V=\text{constant}$  for  $\alpha \geq z \geq \beta$  and further  $a \leq \alpha$  and  $b \geq \beta$ .



by definition. Inserting (28p) into (27p) there results that

$$\frac{f_2}{f_1} = - \sqrt{\frac{V(b)}{V(a)}}. \quad (29p)$$

Equation (29p) corresponds to the well-known optical relation that the ratio of the focal lengths of a system is equal to the ratio of the indexes of refraction on the two sides of the system.

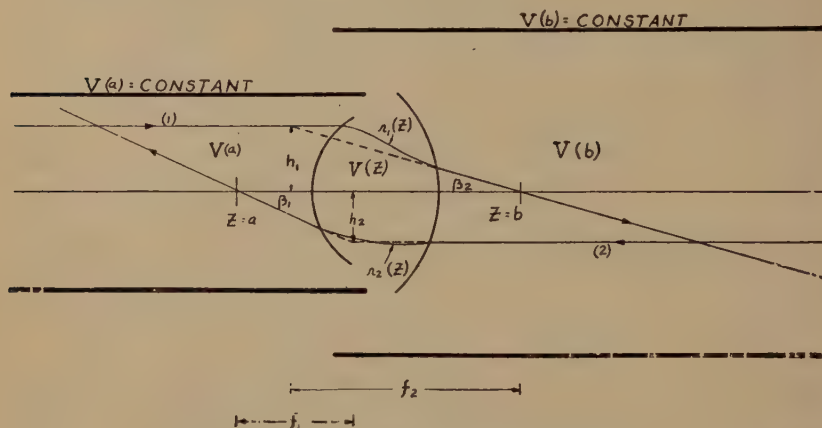


Fig. 4—Two fundamental trajectories.

Further let

$$X_1 = \frac{h_1}{\tan \beta_1} \quad \text{and} \quad X_2 = - \frac{h_2}{\tan \beta_2}, \quad (30p)$$

then from (30p) and (28p) it follows that

$$X_1 X_2 = f_1 f_2. \quad (31p)$$

$X_1$  is the distance between an object and the first focal point and  $X_2$  is the distance between the image and the second focal point, if  $h_1$  is the height of the object and  $h_2$  is the height of the image. The magnification is from (28p) and (30p)

$$m = \frac{h_2}{h_1} = - \frac{f_1}{X_1} = - \frac{X_2}{f_2}. \quad (32p)$$

The points  $F_1$ ,  $F_2$ ,  $H_1$ , and  $H_2$  shown in Fig. 5 constitute the set of cardinal points of the focusing system.  $F_1$  and  $F_2$  are the first and second focal points and  $H_1$  and  $H_2$  are known as the first and second principal points, respectively.

### Equivalent Lens of Axially Symmetric Field

By determining the two fundamental trajectories  $r_1(z)$  and  $r_2(z)$  one is enabled to determine the location of the cardinal points of the focusing system; i.e., the location of the focal and principal points. A knowledge of the location of these cardinal points is sufficient for the determination of the paraxial focusing action of the field. It is therefore permissible to replace the electrostatic field by the set of cardinal points. This set of cardinal points constitutes a lens which may be called the equivalent lens of the field.

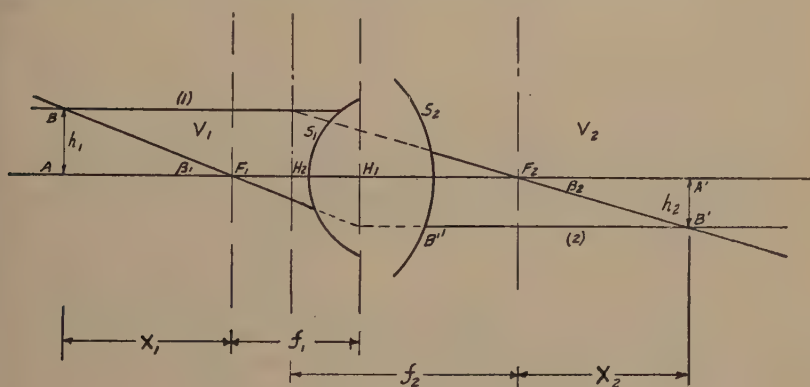
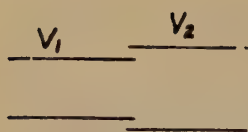


Fig. 5—Location of cardinal points.

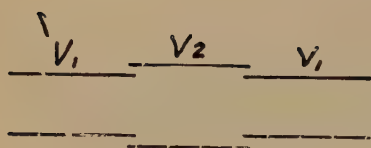
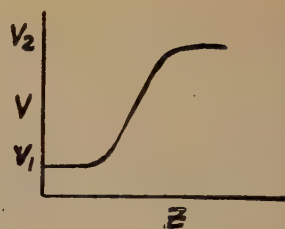
It is thus seen that an electrostatic field having axial symmetry will bring a paraxial electron beam to a focus. Fields possessing axial symmetry may be produced by applying various voltages to electrodes having geometric axial symmetry, such as coaxial cylinders, cones, disks with apertures, etc. Fig. 6 gives the axial cross sections of several focusing electrode combinations, together with the distribution of potential along the axis.

### Determination of Cardinal Points

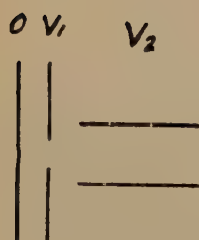
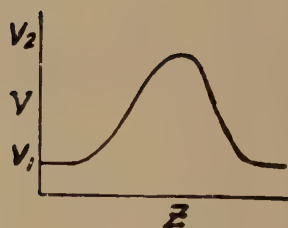
It is now appropriate to consider in some detail how to evaluate the focusing action of an axially symmetric electrostatic field; i.e., how to find the cardinal points of the equivalent lens. Referring to Fig. 5 let  $S_1$  and  $S_2$  be two equipotential surfaces such that the space to the left of  $S_1$  is equipotential and is at potential  $V_1$  and the space to the right of  $S_2$  is equipotential and at the potential  $V_2$ . The potential in the region between  $S_1$  and  $S_2$  varies continuously, in some such manner as indicated in Fig. 2. Then the paraxial electron (1) moving parallel to the axis in the equipotential space to the left of  $S_1$  will, after passing



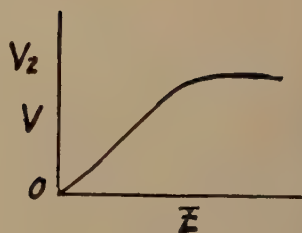
(a)



(b)



(c)



(d)



Fig. 6—Types of electrostatic lenses.



through the focusing system move in a direction inclined at an angle to the axis and will pass through the axial point  $F_2$ . All paraxial electrons moving parallel to the axis in the object space<sup>8</sup> will pass through  $F_2$ . The point  $F_2$  is known as the second focal point. The plane passing through the second focal point and perpendicular to the axis of symmetry is known as the second focal plane.

The plane perpendicular to the axis and passing through the point of intersection of the original and final directions of motion of the electron (1) is known as the second principal plane. The point of intersection  $H_2$  between the second principal plane and the axis is known as the second principal point. The distance  $H_2F_2$  denoted by  $f_2$  is known as the second focal length.

Similarly, the paraxial electron (2) moving parallel to the axis in the image space will after passing through the focusing system move in a direction inclined to the axis, and will pass through the point  $F_1$  in the object space.  $F_1$  is known as the first focal point.  $F_1$  may also be considered as that axial point in the object space from which all electrons, after passing through the focusing system, are parallel to the axis in the image space.

The plane perpendicular to the axis of symmetry and passing through the first focal point is known as the first focal plane. The plane perpendicular to the axis and passing through the point of intersection of the original and final directions of motion of the electron (2), is known as the first principal plane. The point of intersection,  $H_1$ , of the first principal plane and the axis is known as the first principal point.

It is to be noted that in Fig. 5 the principal planes are crossed, that is, the object and image spaces overlap. This is a characteristic of lenses having indexes of refraction different on the two sides. As any two electrode electrostatic lenses will have the indexes of refraction (i.e., the speeds of the electrons) different on the two sides of the lens, it follows that any two electrode electrostatic lens will have its principal planes crossed.

### *Use of Cardinal Points*

Having the cardinal points of the lens one may now obtain either graphically or by means of (31*p*) and (32*p*) the position and magnification of a given object. Thus, in Fig. 5 let  $AB$  be an object from which electrons issue (to make it more concrete let the object  $AB$  be an aperture through which electrons are passing). Then a paraxial elec-

<sup>8</sup> The region to the left of the plane  $H_1$  is the object space and the region to the right of  $H_2$  is the image space.

tron coming from  $B$  and moving parallel to the axis will after passing through the lens go in the direction  $F_2B'$ . A paraxial electron issuing from  $B$  in the direction  $BF_1$  will after passing through the lens go in the direction  $B''B'$ . Similarly, for every point of the object  $AB$ , and so the inverted image  $A'B'$  is obtained. The ratio  $A'B'/AB$  gives the magnification. The electron image of  $AB$  becomes visible if a fluorescent screen be placed in the plane of  $A'B'$ .

Instead of obtaining the position and magnification of the object graphically one can more simply obtain them with the aid of (31p) and (32p). Thus, since the values of  $X_1$ ,  $f_1$ , and  $f_2$  are known,  $X_2$  the distance between the second principal plane and the image is calculated from (31p) as  $X_2 = f_1 f_2 / X_1$  and the magnification  $m$  is by (32p)

$$m = -\frac{f_1}{X} = -\frac{X_2}{f_2}.$$

Similarly, if the position and size of the image are known, then (31p) and (32p) determine the position and size of the object.

### *Types of Electrostatic Lenses*

For purposes of identification several different types of electrostatic lenses may be distinguished. By a unipotential lens shall be meant one for which the potential (or the index of refraction) on the two sides of the lens is the same. Whereas, if the potential on the two sides of the lens is different, the lens will be called a bipotential lens. It is to be noted that all two electrode lenses are bipotential. (See Fig. 6(a) and (b).)

There is a third type of lens which is of importance in the field of cathode-ray tubes; this is the immersion lens. This lens is characterized by the fact that the object is immersed in the lens. This is the lens existing at the cathode of most cathode-ray tubes.<sup>1</sup> (See Fig. 6(c).)

A fourth type of lens which is mentioned but which is of little interest here is the so-called aperture lens—see Fig. 6d. The only reason it is here mentioned is that it is the only electrostatic lens of those mentioned that can be made convergent or divergent. The unipotential, bipotential and immersion lenses are always *convergent*.

### *Thin Lens*

In general, all lenses are "thick lenses." A knowledge of the positions of the focal and principal points is sufficient for the determination

<sup>1</sup> *Loc. cit.*, Fig. 11.

of the focusing action of a "thick lens." To compute the positions of the cardinal points it is necessary to determine the fundamental trajectories. The calculation of the fundamental trajectories is accomplished by the integration of (18p).

A considerable simplification is effected by considering a lens as "thin." A thin lens is one having negligible thickness along the axis of symmetry and is characterized by the fact that the two principal planes are assumed to coincide with (say, center of) the lens. The paraxial focusing action of a thin lens may, therefore, be completely determined as soon as the location of the lens and one of the focal lengths, say  $f_1$ , is known, for by (29p),  $f_2$  also becomes known.

Since for only a lens of zero thickness will the two principal planes coincide with the lens, a practical thin lens will only approximately have the characteristics of the ideal thin lens.

For a thin lens the electrostatic field is confined to such a narrow range of  $z$  that the electron is in the field for such a short time that  $r$  remains sensibly unchanged during the time the electron is in the field. Thus, let  $r=r_0$  be the value of  $r$  when the electron is in the field, so (18p) becomes

$$\frac{d^2r}{dz^2} + \frac{V'}{2V} \frac{dr}{dz} + \frac{V''}{4V} r_0 = 0. \quad (18'p)$$

Let,

$$\frac{\sqrt{V}}{r_0} \frac{dr}{dz} = P$$

then (18'p) becomes

$$\frac{dP}{dz} + \frac{V''}{4\sqrt{V}} = 0.$$

Let the electrostatic field be confined within the narrow range  $a \leq z \leq b$  then integrating between these limits

$$P_b - P_a + \int_a^b \frac{V''}{4\sqrt{V}} dz = 0.$$

Now consider an electron in the object space  $z \leq a$  moving parallel to the axis at the distance  $r_0$  from the axis then at  $a$   $dr/dz=0$  and so  $P_a=0$ . At  $b$  the electron issues from the lens still at the distance  $r_0$  but with the slope  $dr/dz = -r'(b)$  so that

$$P_b = - \frac{\sqrt{V_b}}{r_0} r'(b) = - \frac{\sqrt{V(b)}}{r_0}$$



since,

$$\frac{1}{f_2} = \frac{r'(b)}{r_0} \text{ by definition}$$

so,

$$\frac{1}{f_2} = \frac{1}{4\sqrt{V(b)}} \int_a^b \frac{V''}{\sqrt{V}} dz. \quad (33p)$$

From (33p) and (29p) it follows that

$$\frac{1}{f_1} = - \frac{1}{4\sqrt{V(a)}} \int_a^b \frac{V''}{\sqrt{V}} dz. \quad (34p)$$

By partial integration it may be deduced that

$$\int_a^b \frac{V''}{\sqrt{V}} dz = \frac{1}{2} \int_a^b \frac{(V')^2}{\sqrt{V^3}} dz.$$

So (33p) and (34p) become

$$\frac{1}{f_2} = \frac{1}{8\sqrt{V(b)}} \int_a^b \frac{(V')^2}{\sqrt{V^3}} dz \quad (35p)$$

$$\frac{1}{f_1} = - \frac{1}{8\sqrt{V(a)}} \int_a^b \frac{(V')^2}{\sqrt{V^3}} dz. \quad (36p)$$

## II. OPTICS OF TWO OVERLAPPING COAXIAL CYLINDERS

The electron beam of a cathode-ray tube used for present-day purposes is usually focused by means of two slightly overlapping coaxial cylinders. Such a focusing system is shown in Fig. 2. As was shown in Part I, one may, for paraxial purposes, replace this focusing system by its four cardinal points constituting the equivalent thick lens.

In order to determine the fundamental trajectories, it is necessary to solve (18p) or (9p). An exact solution of these equations is obtainable only for simple expressions for  $V(z)$ . The distribution of potential along the axis due to two coaxial cylinders of various diameters is not represented by these simple expressions. If an analytical expression for  $V$  is available, then (18p) may be integrated in the form of an infinite series.

There is no analytical expression for  $V(z)$  available in the case of two long coaxial cylinders of different diameters. However,  $V(z)$  may be obtained experimentally. But before (18p) is ready for solution, it is necessary to know  $V'(z)(=dV/dz)$  and  $V''(z)(=d^2V/dz^2)$ . These

may be obtained by graphical or numerical differentiation of  $V(z)$ . With  $V(z)$ ,  $V'$ , and  $V''$  known (18p) or (9p) may be integrated by any step-by-step method of approximation.

If  $V(r, z)$ , such as shown in Fig. 2, is determined experimentally then one may measure the radii of curvature of the equipotential surfaces along the axis and obtain a relation between  $V'$  and  $V''$  which one may use as a check on the graphical or numerical differentiation. The relation between the radii of curvature  $\rho$  along the axis and  $V'$  and  $V''$  is<sup>1</sup>

$$\rho = \frac{2 V'(z)}{V''(z)}.$$

### *Electrostatic Field of Two Cylinders*

Consider the bipotential lens (Fig. 2) due to two long metallic cylinders of diameters  $d_1$  and  $d_2$ , and charged to potentials  $V_1$  and  $V_2$ .<sup>9</sup>

If one of the diameters, say  $d_1$ , is chosen as the unit of length (in both the  $r$  and  $z$  directions) then a given ratio of cylinder diameters,  $d_2/d_1$  always represents the same configuration of electrodes; i.e., two cylinders, one having a diameter of unit length and the other having a diameter of  $d_2/d_1$  units of length. This unit we shall designate as the gun diameter.

A given ratio of diameters,  $d_2/d_1$ , will for given voltages  $V_2$  and  $V_1$  always produce the same distribution of potential. Thus, Fig. 2 represents the potential distribution for any  $d_1$  and  $d_2$  for which  $d_1$  is taken as the unit of length and  $d_2/d_1$  is that given in Fig. 2. The use of the gun diameter as the unit of length greatly simplifies the presentation of information. Thus the two fundamental trajectories and the accompanying cardinal points determined for given cylinder diameters  $d_2$  and  $d_1$  are also the fundamental trajectories for all cylinder diameters  $d_2'$  and  $d_1'$  for which  $d_2'/d_1' = d_2/d_1$ .

The differential equation (18) for the trajectory of an electron remains unchanged if one replaces  $V$  by  $kV$  where  $k$  is a constant. Hence, the trajectory of an electron will remain unaltered if the voltages on the electrodes are all multiplied by the same factor. The two fundamental trajectories and the accompanying cardinal points depend, therefore, not on  $V_1$  or  $V_2$  but on  $V_2/V_1$ . So that if the cardinal points are determined for given potentials  $V_1$  and  $V_2$  they remain the same for any  $V_1'$  or  $V_2'$  so long as  $V_2'/V_1' = V_2/V_1$ . Hence, a given voltage ratio and a given diameter ratio uniquely determine the positions of the

<sup>1</sup> *Loc. cit.*, Appendix II.

<sup>9</sup> The potential of the cathode is here taken as the reference of potential.

cardinal points of the electrostatic field if the gun diameter be used as a unit of length.

From the fact that the potential function is relative, it follows that a given equipotential plot such as that shown in Fig. 2 is independent of  $V_1$  or  $V_2$  but depends solely upon  $V_1 - V_2$ . So that a given equipotential plot may be used for the determination of the fundamental trajectories for any voltage ratio  $V_2/V_1$ .

Hence, the important result that a given axial distribution of potential (such as shown in Fig. 2) determined for two cylinders of

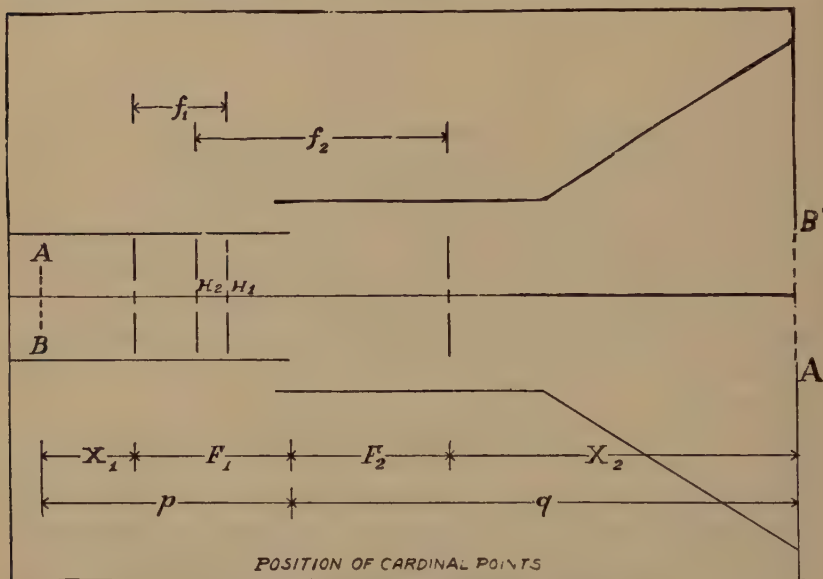


Fig. 7—Position of cardinal points.

diameters  $d_1$  and  $d_2$  and charged to potentials  $V_1$  and  $V_2$  enables one to determine the positions of the cardinal points of an electrostatic lens made up of two cylinders of diameters  $d_2'$  and  $d_1'$  if  $d_2'/d_1' = d_2/d_1$  and with any voltages on the electrodes.

#### Cardinal Points of Electrostatic Field of Two Cylinders

From the equipotential line plots such as shown in Fig. 2, the fundamental trajectories are calculated and the positions of the cardinal points are determined for a series of values of voltage ratios and diameter ratios.

Fig. 7 shows the position<sup>10</sup> of the cardinal points for a given voltage ratio and diameter ratio.

<sup>10</sup> It is convenient to locate the focal points,  $F_1$  and  $F_2$ , by their distances from the end of the gun. Starting with Fig. 7,  $F_1$  and  $F_2$  are therefore indicated as lengths.

It is to be noted from Fig. 7 that (1) the principal planes are crossed, that is, the object and image space overlap, (2) the focal length of the image space  $f_2$  is greater than the focal length of the object space  $f_1$ ;

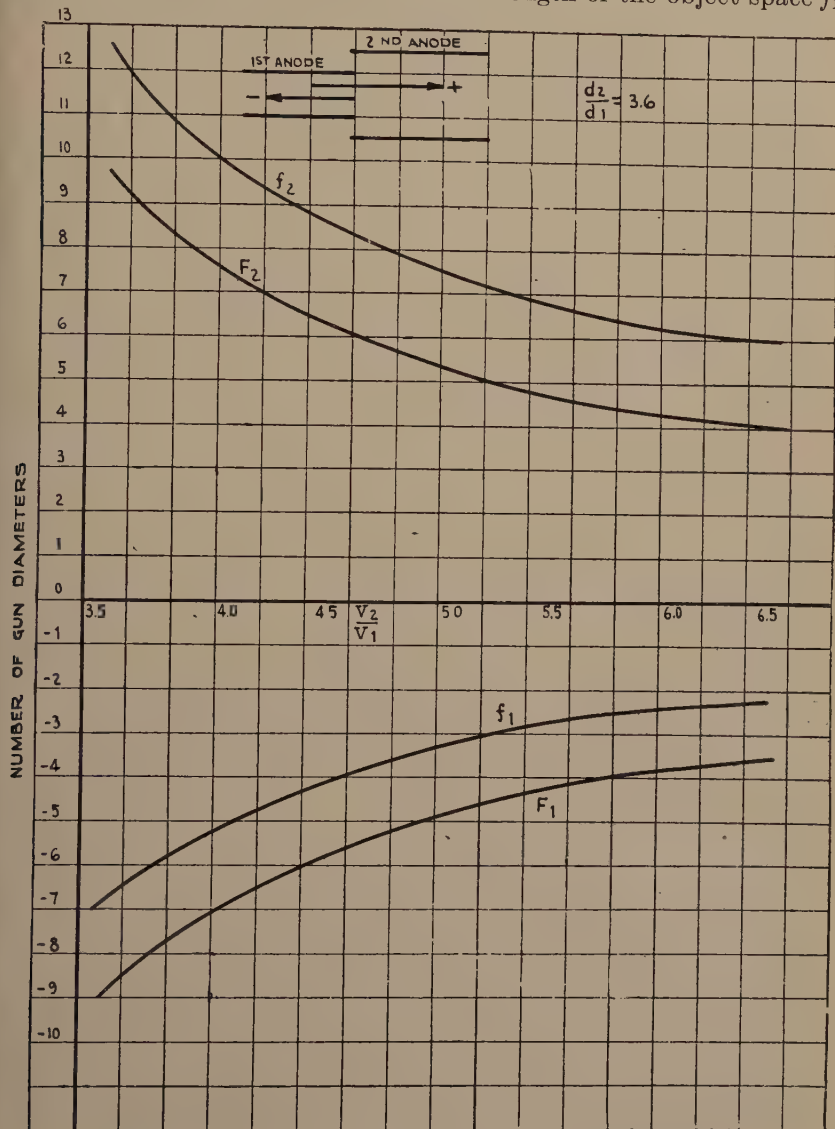


Fig. 8—Variation of optical constants with voltage ratio.

(3) the principal planes are located inside the first anode (for  $V_1 < V_2$ ). These properties are inherent in a bipotential lens.

Fig. 8 shows how the cardinal points vary with the voltage ratio



for a diameter ratio 3.60. It is seen that the focal lengths decrease, i.e., the power of the lens increases, as the voltage ratio is increased. Figs.

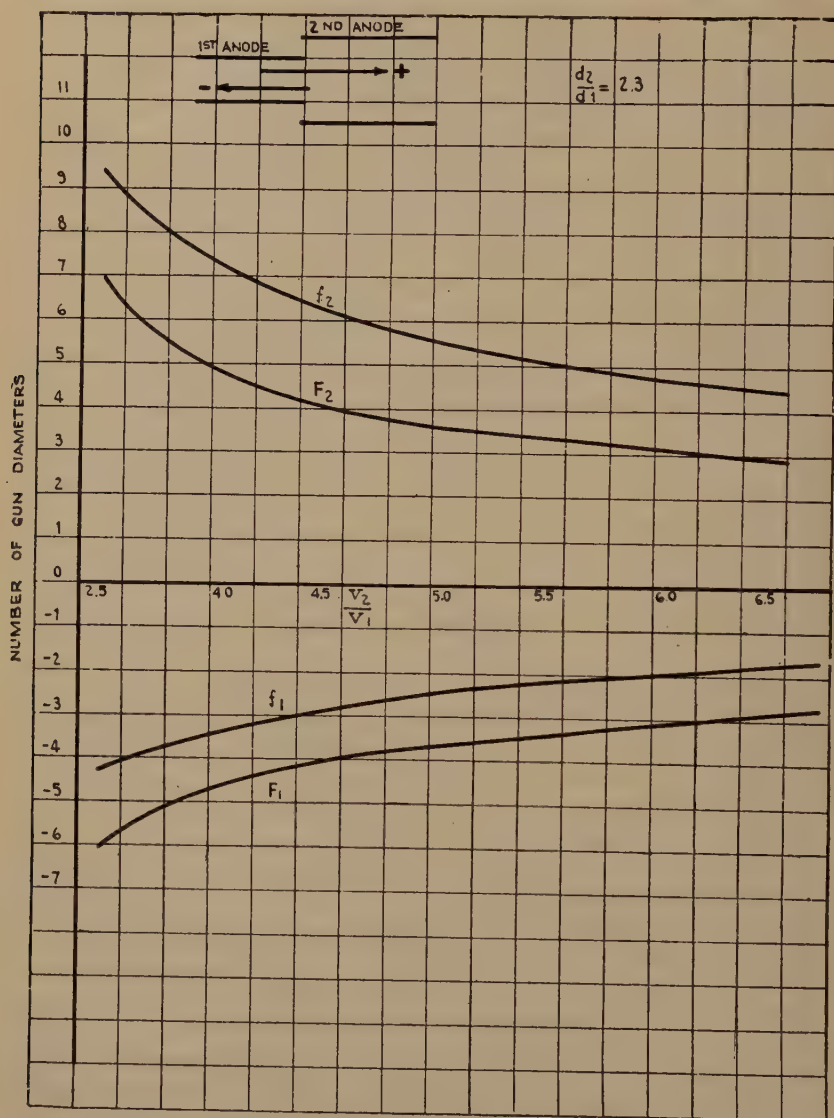


Fig. 9—Variation of optical constants with voltage ratio.

9, 10, and 11 show the variation of positions of the cardinal points with voltage ratio for different diameter ratios. Fig. 12 shows how the cardinal points vary with the diameter ratio for a given voltage ratio.

It should be clear that to a given voltage ratio and diameter ratio there corresponds but one set of cardinal points if the gun diameter

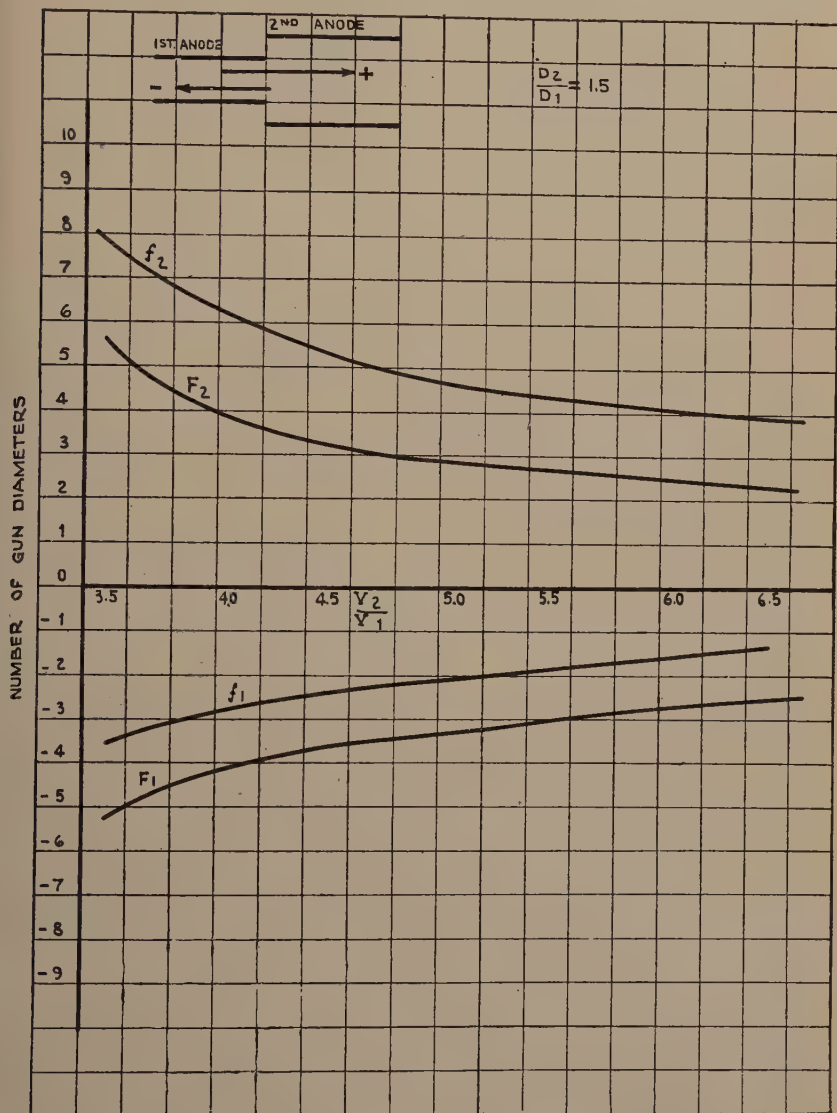


Fig. 10—Variation of optical constants with voltage ratio.

be chosen as the unit of length. It is worth noting that a given ratio of diameters determines the shape (curvature) and the distance between the refractive (equipotential) surfaces (see Fig. 2), while the voltage

ratio determines the indexes of refraction between the various surfaces.

The curves of Figs. 8, 9, 10, and 11 show how the cardinal points

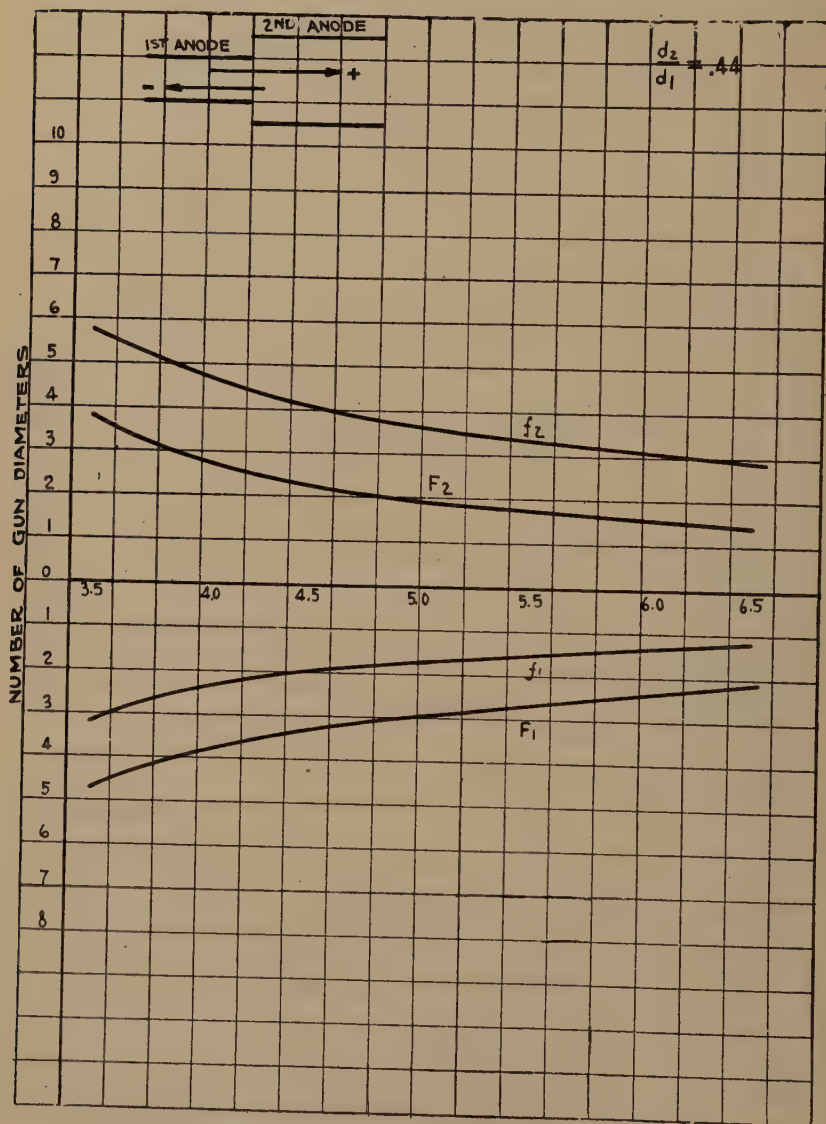


Fig. 11—Variation of optical constants with voltage ratio.

vary when  $V_2/V_1$  and  $d_2/d_1$  are varied. From these curves one can determine how the cardinal points vary by varying only one of the variables  $V_1$ ,  $V_2$ ,  $d_1$ , and  $d_2$  and keeping the other three constant. Thus

by increasing  $V_2$ , keeping  $V_1$ ,  $d_1$ , and  $d_2$  constant,  $V_2/V_1$  increases and the focal lengths decrease, by increasing  $V_1$  the focal lengths are increased. By increasing  $d_2$ ,  $d_2/d_1$  increases and so the focal lengths

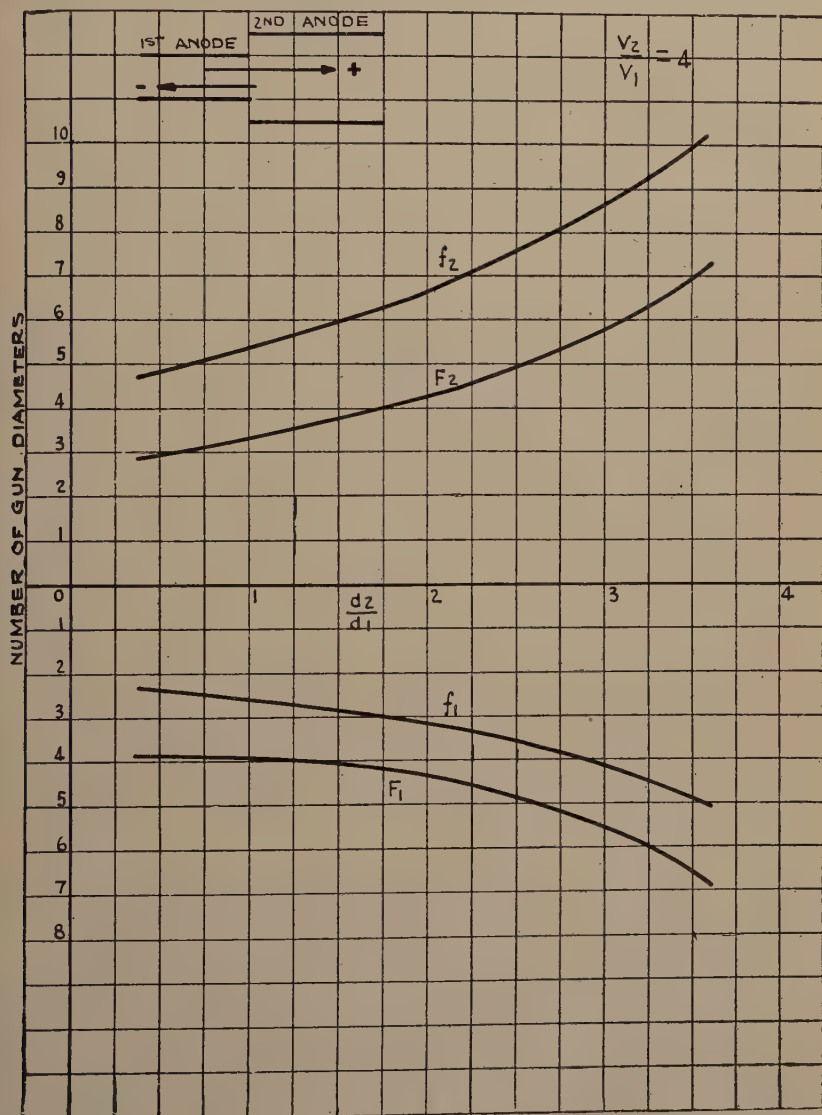


Fig. 12—Variation of optical constants with diameter ratio.

are increased, and by increasing  $d_1$ ,  $d_2/d_1$  decreases and so decrease the focal lengths. It must be carefully noted, however, that by increasing  $d_1$  the unit of length is increased.



*Use of Curves of Cardinal Points*

As an example to illustrate the use of the curves of Figs. 9 to 12 consider the cathode-ray tube shown in cross section in Fig. 1. Suppose it were found that in order to obtain the minimum spot on the screen with 1000 volts on the first anode it is necessary to have 5000 volts on the second anode. Further let  $d_2 = 3.5$  cm and  $d_1 = 1.5$  cm. Then from Fig. 9 note that for  $d_2/d_1 = 2.3$  and  $V_2/V_1 = 5$ .

$$f_1 = -2.5 \text{ gun diameters} \quad F_1 = -3.7 \text{ gun diameters}$$

$$f_2 = +5.6 \text{ gun diameters} \quad F_2 = +3.5 \text{ gun diameters}$$

(It must be remembered that these cardinal points hold only for paraxial electrons; in order to use these cardinal points it is, therefore, necessary to have the aperture  $A_1$  sufficiently small so as to permit only paraxial electrons to enter the lens.)

Let  $q$ , the distance between the screen and end of gun, be 15 gun diameters, then,

$$|X_2 = q - F_2 = 15 - 3.5 = 11.5 \text{ gun diameters:}$$

So by (31p)

$$X_1 = \frac{f_1 f_2}{X_2} = \frac{-2.5 \times (+5.6)}{+11.5} = -1.2 \text{ gun diameters.}$$

and  $p$ , the distance between object and end of gun is

$$p = X_1 + F_1 = -1.2 - 3.7 = -4.9 \text{ gun diameters.}$$

By means of (32p) the magnification of the object is determined. Thus,

$$m = -\frac{f_1}{X_1} = -\frac{2.5}{1.2} = -2.1$$

and if the size of the spot on the screen is measured to be 0.5 mm then the size of the object being imaged on the screen is  $0.5/2.1 = .24$  mm. So by knowing  $V_2/V_1$ ,  $d_2/d_1$ ,  $q$  and the size of the spot one can by means of the curves of Figs. 8 to 11 and equations (31p) and (32p) determine the position and the size of the object that is imaged on the screen.

A knowledge of the positions of the cardinal points permits one to give quantitative answers to the following questions: What will be the effect on the spot size of a given tube if

- (1) the length of the first anode is varied
- (2) the diameter of the first anode is varied
- (3) the diameter of second anode is varied
- (4) the ratio of voltages on the two anodes is varied
- (5) the distance between the screen and gun end is varied.

It is to be noted, however, that in order to keep the object focused on the screen (minimum spot on the screen) it is necessary to change at least two of these variables. Thus, if in the above example, the length

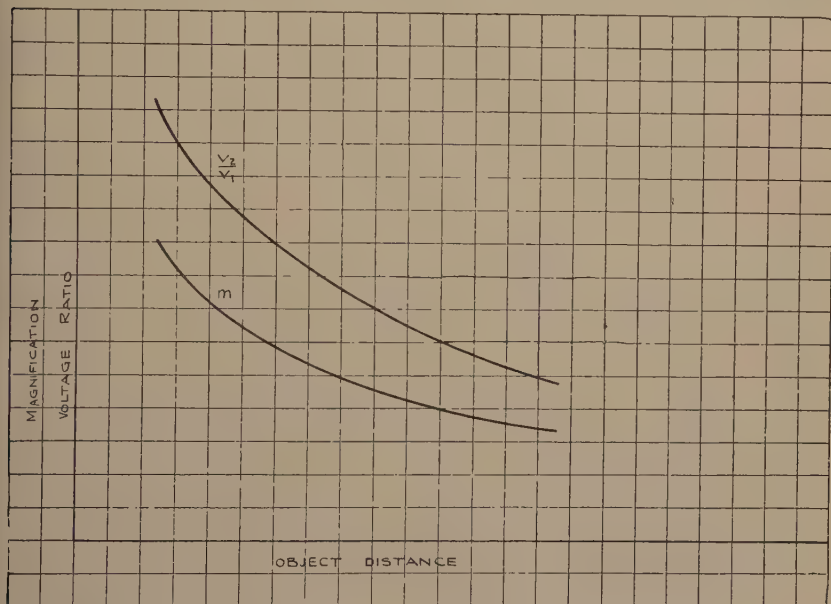


Fig. 13—Magnification and voltage ratio vs. object distance.

of the first anode is changed, it will be necessary to change  $V_2/V_1$  or gun screen distance in order to keep the minimum spot on the screen.

The calculation of the effect of the various variables is, therefore, not straightforward but requires several trials. Thus, in order to use the curves of Figs. 8 to 11 to calculate the effect on the spot size if the length of the first anode is changed, while the remaining dimensions in the tube remain unaltered, it is first necessary to know the voltage ratio for the new object distance at which the spot is focused. To get around this difficulty note that with a given ratio  $d_2/d_1$  and given  $q$   $V_2/V_1$  can be calculated as a function of  $p$  and to each  $p$  (and the corresponding  $V_2/V_1$ ) a magnification can be calculated so that the curves shown in Fig. 13 may be plotted. Fig. 13 then gives the change in spot

size and voltage ratio caused by a given change in object distance. The curves of Fig. 13 hold for a given image distance; similar curves can be calculated for other image distances.

### *Thin Lens*

If the object and image are at large distances from the end of the gun then to a fair approximation the two principal planes may be assumed to coincide and to be located at the end of the gun. Under these circumstances, the following simple formulas apply:

$$\frac{\sqrt{V_a}}{p} + \frac{\sqrt{V_b}}{q} = \frac{\sqrt{V_a}}{f_1} = \frac{\sqrt{V_b}}{f_2} \quad (37p)$$

and,

$$m = -\frac{q}{p} \sqrt{\frac{V_a}{V_b}} \quad (38p)$$

where  $p$  and  $q$  are the object and image distances measured from the end of the gun and  $f_1$  is the first focal length which may be calculated from the formula for the focal length of a thin lens given by (33p). For this case it is not necessary to determine the fundamental trajectories.

A much better approximation is to consider the lens thin, that is, to assume that the two principal planes coincide, but to assume the thin lens to be situated between the two principal planes of the thick lens. Here the above formulas still apply if  $p$  and  $q$  are measured from the assumed position of the thin lens instead of from the end of the gun. For this case it is necessary to determine one fundamental trajectory. It is seen from Figs. 8 to 12 that this thin lens is situated about 1.5 gun diameters inside the first anode.

### *Experimental Determination of Cardinal Points*

The position of the cardinal points may be determined experimentally if the magnification is known for two given positions of object and image. Thus, in Fig. 7 let  $AB$ , representing a fine wire mesh of known dimensions, be the object. The object is "illuminated" with electrons originating at a cathode to the left of  $AB$ , and is imaged on a fluorescent screen. Let the distance between the mesh  $AB$  and end of gun be  $p$ , the distance between end of gun and fluorescent screen be  $q$ , and the magnification with which the mesh is imaged on the screen be  $m$ . Then from Fig. 7 and the relation for magnification

$$m = -\frac{f_1}{X_1} = -\frac{X_2}{f_2} \quad (32p)$$

it follows that

$$p = X_1 + F_1 = \frac{-f_1}{m} + F_1 \quad (39p)$$

$$q = X_2 + F_2 = -mf_2 + F_2. \quad (40p)$$

Then if  $p_1$ ,  $q_1$ , and  $m_1$  correspond to one position of the object and  $p_2$ ,  $q_2$ , and  $m_2$ , correspond to another position of the object (for the same lens; i.e., the voltage ratio and diameter ratio being fixed), then it follows that

$$f_1 = m_1 m_2 \left( \frac{p_1 - p_2}{m_1 - m_2} \right) \quad (41p)$$

$$f_2 = \frac{q_1 - q_2}{m_2 - m_1} \quad (42p)$$

$$F_1 = \frac{m_1 p_1 - m_2 p_2}{m_1 - m_2} \quad (43p)$$

$$F_2 = \frac{m_2 q_1 - m_1 q_2}{m_2 - m_1}. \quad (44p)$$

Equations (41p) to (44p) allow one to determine the positions of all the cardinal points provided the sets of conjugate quantities  $p_1 q_1 m_1$  and  $p_2 q_2 m_2$  are known. An obvious method for determining these quantities is to use a tube having two independently moving parts; the object mesh and the fluorescent screen on which to image the mesh. It is very difficult to build a tube with two independently moving parts which move over considerable distances.

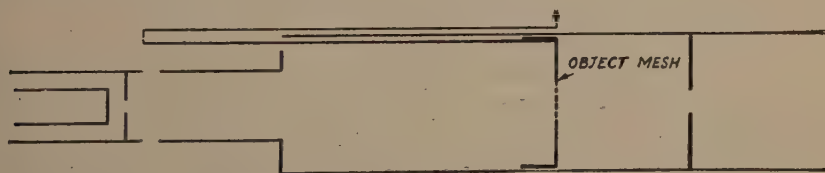


Fig. 14—Gun with sliding mesh.

It is relatively simple, however, to build a tube with one moving part and especially so if the moving part is the object mesh. Fig. 14 shows the cross section of a gun having a moving mesh. The mesh is welded onto an aperture cup which slides inside the gun by merely tilting the tube. The position of the mesh inside the gun is indicated by an index on the outside of the gun which is calibrated.



To determine the two sets of quantities  $p_1q_1m_1$  and  $p_2q_2m_2$  by means of a tube having only a moving object, one may proceed as follows: The gun is inserted inside a glass blank with the screen at a known distance, say  $q_1$ , from the end of the gun. The voltage ratios required to focus the mesh on the screen and the magnifications of the mesh are then noted for various known positions of the mesh. The results are then plotted as shown by the curves  $p_1$  and  $m_1$  of Fig. 15. The same gun is then inserted into a blank with the screen at a different distance, say  $q_2$ , from the end of the gun. The measurements are repeated with

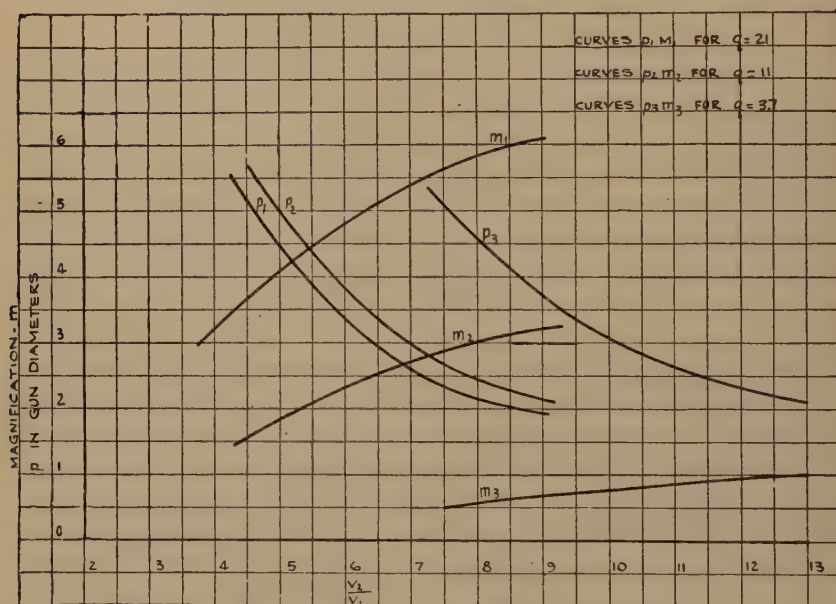


Fig. 15—Magnification and object distance vs. voltage ratio.

this blank and the results plotted as given by the curves  $m_2$  and  $p_2$  of Fig. 15.

The positions of the cardinal points may then be calculated by means of (41p) to (44p) and the four curves ( $p_1$ )( $m_1$ )( $p_2$ )( $m_2$ ) of Fig. 15. To do this it is necessary to choose the quantities  $m$  and  $p$  along a vertical line corresponding to a given voltage ratio.

The curves of Fig. 15 were determined, by the method just described, for a lens corresponding to a diameter ratio of 1.5.

The accuracy of determining the positions of the cardinal points by means of (41p) to (44p) depends greatly upon the accuracy with which the quantities  $p_2-p_1$ ,  $q_2-q_1$ , and  $m_2-m_1$  may be determined

from the curves of Fig. 15. A glance at the curves will show that the accuracy of the quantity  $p_2 - p_1$  is rather poor, since it is the differ-

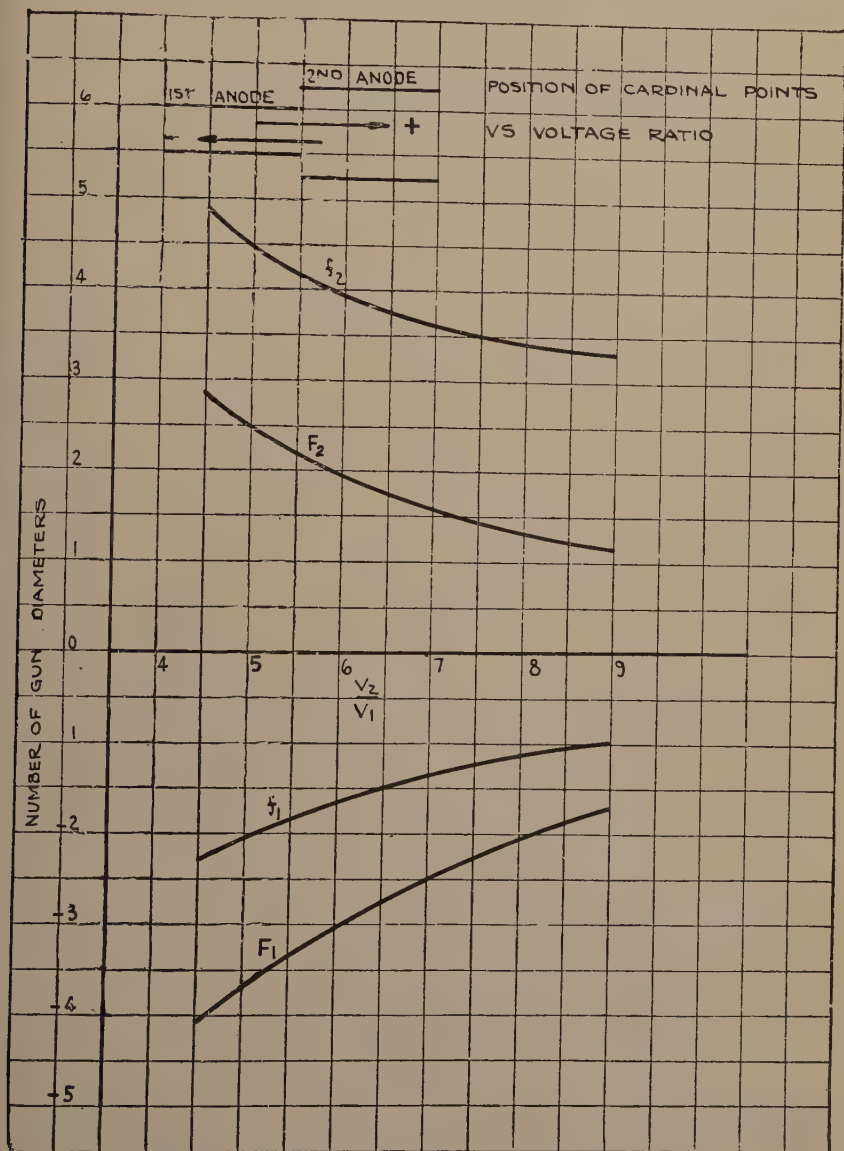


Fig. 16—Position of cardinal points vs. voltage ratio.

ence of two nearly equal quantities. The quantities  $q_2 - q_1$  and  $m_2 - m_1$  are quite accurate, however.

To avoid the use of the quantity  $p_2 - p_1$  one may, instead of using (41p) to (44p) proceed as follows: Determine  $f_2$  by means of

$$f_2 = \frac{q_1 - q_2}{m_2 - m_1} \quad (42p)$$

$f_1$  is then determined by the relation

$$f_1 = \frac{-1}{\sqrt{\frac{V_2}{V_1}}} f_2 \quad (29p)$$

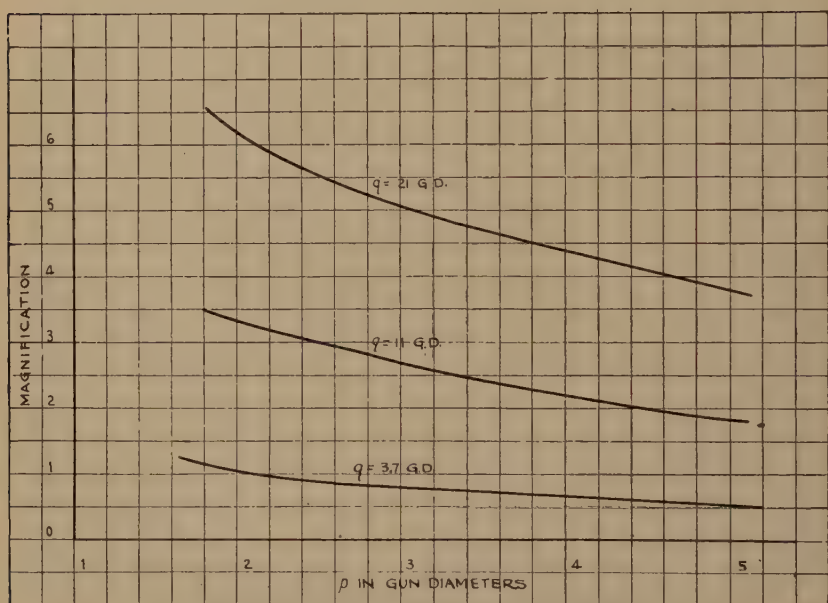


Fig. 17—Magnification vs. object distance.

and the quantities  $F_1$  and  $F_2$  are determined by

$$F_1 = p_1 + \frac{f_1}{m_1} = p_2 + \frac{f_1}{m_2} \quad (45p)$$

$$F_2 = q_1 + m_1 f_2 = q_2 + m_2 f_2 \quad (46p)$$

wherein  $f_2$  and  $f_1$  are the values obtained by means of (42p) and (29p).

The focal lengths and the positions of the focal points determined as described above are shown plotted in Fig. 16. In Table I, the values of  $f_1$ ,  $f_2$ ,  $F_1$ , and  $F_2$  determined from the experimental data are compared with the theoretical values taken from the curves of Fig. 10. The agreement is within experimental error.

The data as plotted in Fig. 15 are useful only for the determination of the positions of the cardinal points. The data have been replotted in Figs. 17 and 18 showing how the magnification and the focusing voltage ratio vary with the position of the object (or gun lengths) for three positions of the screen (or gun-screen distances). These curves are very useful as gun design information.

The method described above determines the positions of all the cardinal points and, therefore, determines the thick lens equivalent to the focusing field. If the object and image are sufficiently distant

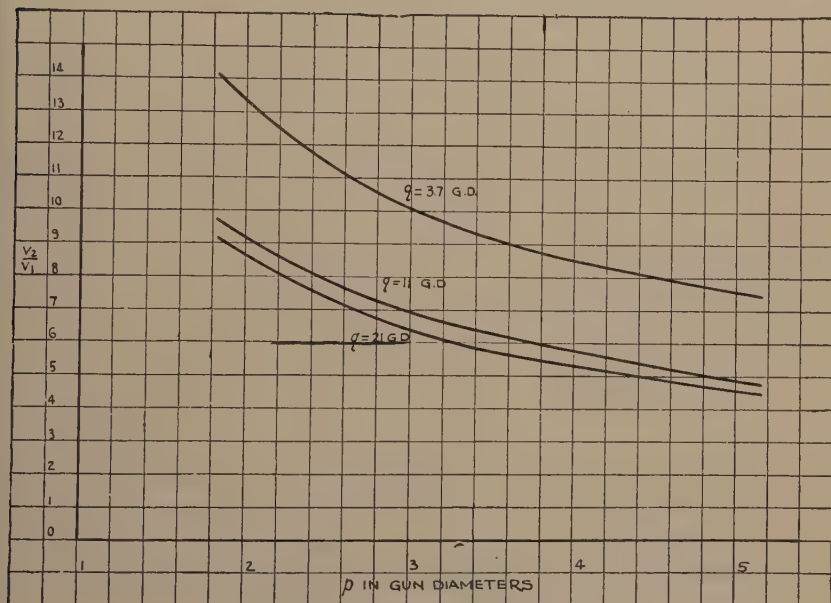


Fig. 18—Voltage ratio vs. object distance.

from the lens we may to a fair approximation consider the lens as thin and situated between the two principal planes of the thick lens. The position and the focal lengths of the thin lens may be determined experimentally by simply noting the distance between object and image, magnification, and voltage ratio at which the object is focused on the screen.

Thus, in Fig. 19 let  $L$  be the equivalent thin lens and let  $u$  and  $v$  be the object and image distances measured from the thin lens. The following thin lens relations then apply

$$\frac{1}{u} + \frac{1}{v} \sqrt{\frac{V_2}{V_1}} = \frac{1}{f_1} \quad (47p)$$



$$\frac{v}{u} = m \sqrt{\frac{V_2}{V_1}} \quad (48p)$$

Besides these the following two relations also hold:

$$u + v = d \quad (49p)$$

$$\frac{f_2}{f_1} = - \sqrt{\frac{V_2}{V_1}} \quad (50p)$$

where  $d$  is the distance between object and image.

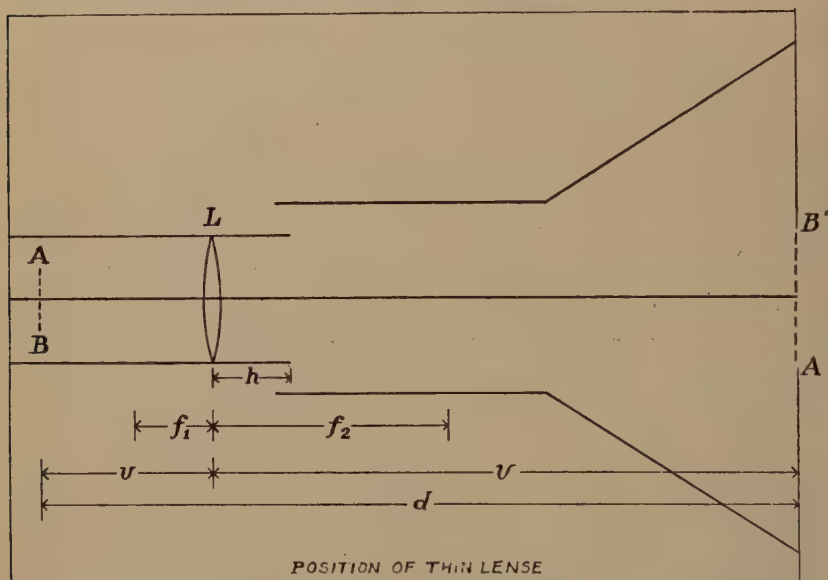


Fig. 19—Position of thin lens.

It follows from (48p) and (49p) that

$$u = \frac{d}{1 + m \sqrt{\frac{V_2}{V_1}}} \quad (51p)$$

TABLE I

$V_2/V_1$	$f_2$		$f_1$		$F_2$		$F_1$	
	Experimental	Theoretical	Exp.	Theo.	Exp.	Theo.	Exp.	Theo.
4.5	4.9	5.1	-2.3	-2.4	2.9	3.2	-4.1	-3.8
5.0	4.4	4.7	-2.0	-2.1	3.0	2.9	-3.7	-3.4
5.5	4.2	4.3	-1.8	-1.9	2.3	2.7	-3.3	-3.1
6.0	4.0	4.1	-1.7	-1.7	2.0	2.4	-3.0	-2.8
6.5	3.8	3.9	-1.5	-1.5	1.8	2.1	-2.7	-2.6

As  $u$  is the distance between object and lens, (51p) permits one to determine the position of the lens. Substituting (51p) and (49p) into (47p) there results that

$$f_1 = \frac{d}{1 + m\sqrt{\frac{V_2}{V_1}}} \frac{m}{m+1} = u \frac{m}{m+1} \quad (52p)$$

Equation (52p) determines the first focal length; it is seen from (52p) that for large magnifications

$$f_1 \approx u. \quad (53p)$$

The second focal length is determined by (50p).

It is thus seen that to obtain the position of the thin lens and the two focal lengths  $f_1$  and  $f_2$  it is merely necessary to know (1)  $d$ , the distance between the object (mesh) and the image (screen), (2)  $m$ , the magnification of the object, and (3)  $V_2/V_1$  the voltage ratio required to focus the mesh on the screen.

Using the data of Fig. 15, the position and focal lengths of the thin lens were calculated by means of the above relations. Fig. 20 gives the position and the focal lengths as functions of the voltage ratio. Comparing Figs. 10 and 20, it is seen that the thin lens is situated between the two principal planes of the thick lens.

### *Defects of Electron Focusing System*

The defects may be roughly classified as:

- (1) Those associated with construction.
- (2) Those associated with aberrations.
- (3) Those associated with space charge or mutual repulsion between the electrons in the beam.

The defects of the first class may be caused by:

- (a) The two focusing cylinders not being coaxial.
- (b) Cylinders being out of round.
- (c) Cylinders and apertures not being coaxial, etc.

These defects may all be overcome by a more careful construction of the tube. In what follows it will be assumed that the tube is well constructed.

The defects due to space charge will not be discussed in this paper.

### *Aberration*

In optics it is customary to speak of first, third, fifth, etc., order of imagery; paraxial imagery being synonymous with first order imagery. Third order imagery is usually considered as first order imagery upon

which are superimposed third order monochromatic aberrations. Similarly, with the fifth and higher orders of imagery. The number and

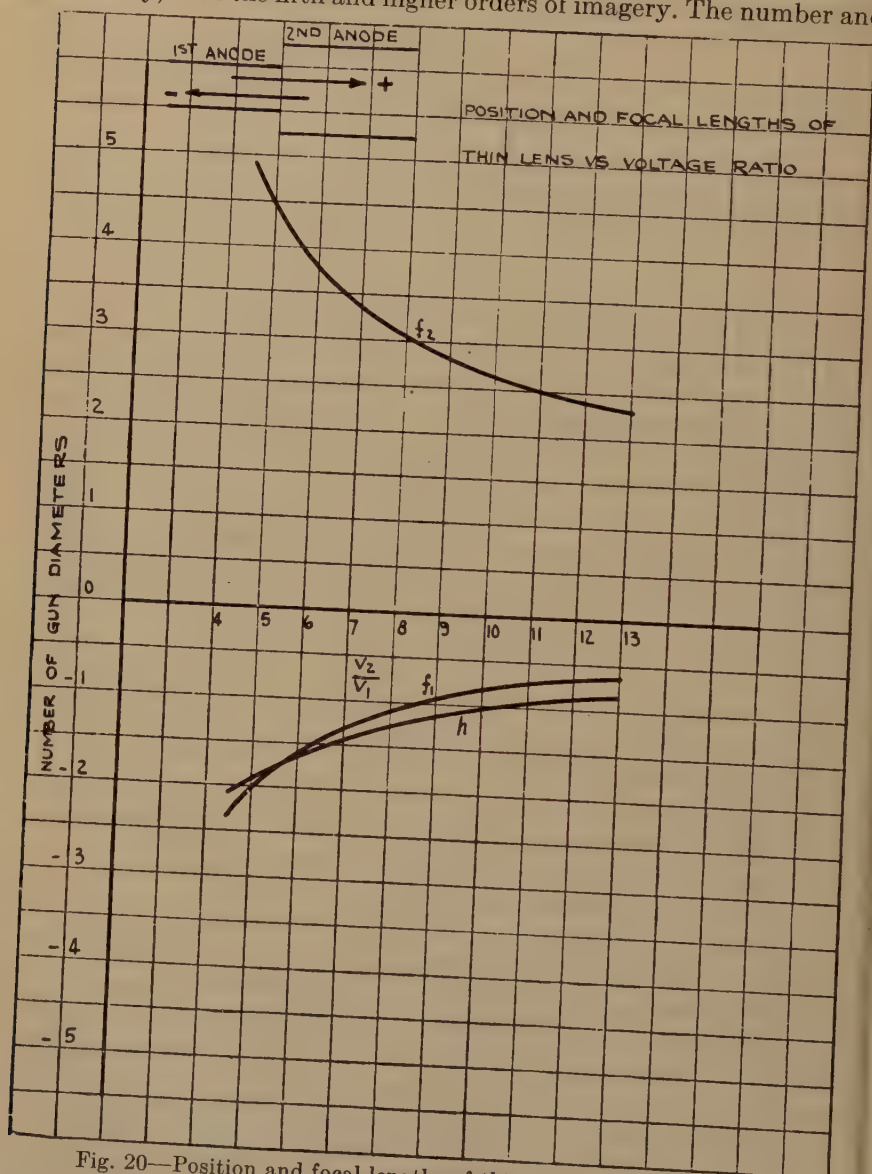


Fig. 20—Position and focal lengths of thin lens vs. voltage ratio.

complexity increase rather rapidly with the order of imagery, so that the usual treatment of the aberrations limits itself to the aberrations of the third order.

There are five monochromatic aberrations due to third order imagery. These are:

- (1) Spherical aberration
- (2) Coma
- (3) Astigmatism
- (4) Curvature of the field
- (5) Distortion.

Besides these monochromatic there are two chromatic aberrations. For these it is usual to assume paraxial imagery and to deduce the aberrations from the variation of the indexes of refraction with the wave length of light.

Similarly, one may speak of first and higher orders imagery in electron optics. Thus, one may speak of the various orders of imagery according to the number of terms that one uses in the expansion for the potential (equation (11) ). For first order imagery (paraxial) only the first term was used, assuming that the radial force on an electron (equation (13*p*)) is proportional to its distance from the axis. For third order imagery the second term would be included, etc.

A first order or paraxial discussion of a focusing system is an approximate description of the imagery which is very useful for most purposes, but is not sufficiently complete to serve as a basis for the final design of a cathode-ray tube. The assumptions underlying paraxial imagery are true only if the aperture of the lens and the size of the object are very small. To obtain the necessary current in the beam it is necessary to have quite a large aperture. Therefore, the imagery actually existing in cathode-ray tubes departs from paraxial. For a final design it is, therefore, necessary to know the aberrations of the focusing field.

The task of theoretically determining any of the monochromatic aberrations for a particular case is extremely difficult and of little use. The only practical method available for determining the aberrations in any particular case is the experimental. The chromatic aberrations are negligible in cathode-ray tubes.

Of the five monochromatic aberrations enumerated above, it is only the first three that affect the definition of the image points. The last two affect only the position of the image point. The size of the object of the final focusing field of a well-designed cathode-ray tube is about 0.1 millimeter. If the gun is well lined up one may consider the small object to lie wholly on the axis. In this case, the electrostatic lens focusing the very small object will display spherical aberration only. If the gun is not well lined up, then the small object will lie off the axis and the lens will also display coma and astigmatism. Coma



and astigmatism may be present even though no spherical aberration is present.

### *Spherical Aberration*

In the case of a well-designed and well-constructed cathode-ray tube, the only aberration (neglecting space charge) damaging the spot size is spherical aberration. It is, therefore, essential to determine the amount of spherical aberration present in various lenses, used in various manners. Third order imagery limits itself to small apertures.

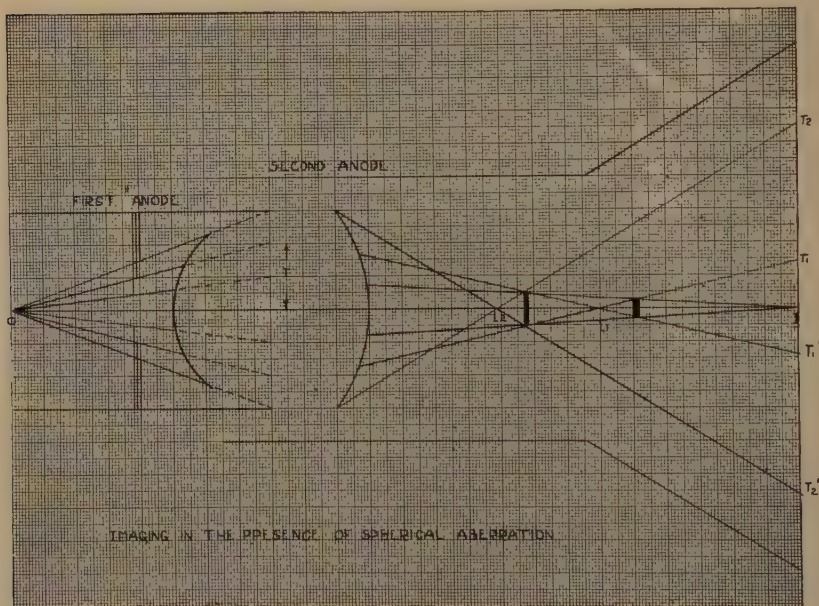


Fig. 21—Imaging in the presence of spherical aberration.

In the experimental determination of the spherical aberration, it is not necessary to limit oneself to the third order imagery.

In the presence of spherical aberration, all electrons coming from an object point on the axis do not recombine at one point on the axis, as paraxial theory predicts, but rather intersect the axis at various distances as shown in Fig. 21. In Fig. 21,  $I$  represents the paraxial image of  $O$ , and  $IL_1$ ,  $IL_2$  are defined as the longitudinal spherical aberrations and  $IT_1$ ,  $IT_2$  are defined as the transverse spherical aberration for the various apertures. The longitudinal spherical aberration is said to be positive if as in Fig. 22  $L_1$  and  $L_2$  are to the left of  $I$  and negative if to the right of  $I$ . The transverse spherical aberration is said to be

positive for electrons  $T_1$  and  $T_2$  and negative for  $T_1'$  and  $T_2'$ . The heavy vertical lines in the image space represent the disks of least confusion.

Let  $r$  be the distance between any electron and the axis at the end of the gun (see Fig. 21) and let  $L$  be the longitudinal spherical aberration for the electron of height  $r$ , then,

$$L = a_2 r^2 + a_4 r^4 + a_6 r^6 + \dots$$

That  $L$  is a function of only the even powers of  $r$  follows from the fact that  $L$  is the same for plus or minus  $r$ ; i.e.,  $L$  is the same for an electron above or below the axis. Similarly if  $T$  represents the transverse spherical aberration then

$$T = a_1 r + a_3 r^3 + a_5 r^5 + \dots$$

since a change in the sign of  $r$  changes the sign of  $T$  only.

It is to be noted that the effect of spherical aberration is perfectly symmetrical, that is, the disks of least confusion, which represent the minima spots possible with the given amount of aberration, are perfectly symmetrical about the axis.

#### *Experimental Determination of Transverse Spherical Aberration*

The type of gun used in the determination of the transverse spherical aberration is shown in Fig. 22. Fig. 23(a) represents the appearance of the spots on the screen when  $V_2 = V_1$ . If there were no spherical aberration all the spots would, on focusing, unite to form the small paraxial image spot. Fig. 23(b) shows the appearance of the screen when the electrons issuing from the central 0.040-inch aperture are focused. In Fig. 23(b) it is seen that due to the spherical aberration the nonparaxial electrons are already overfocused when the axial electrons (those passing through the central 0.040-inch aperture) are just focused. The transverse spherical aberration is thus directly obtained from Fig. 23(b).

Fig. 24 shows how the transverse spherical aberration for the various image distances and diameter ratios varies with the width of the beam at the end of the gun. The curves of Fig. 24 may be fairly well represented by the first two terms of (2). The width of the beam at the end of the gun is obtained from Fig. 23(a) and from the given positions of aperture and screen.

As shown in Fig. 21 the plane containing the disk of least confusion occurs nearer the lens than that predicted by paraxial theory. If the focusing voltage ratio is set for the paraxial image, then the disk of least confusion will occur between the end of the gun and the screen.

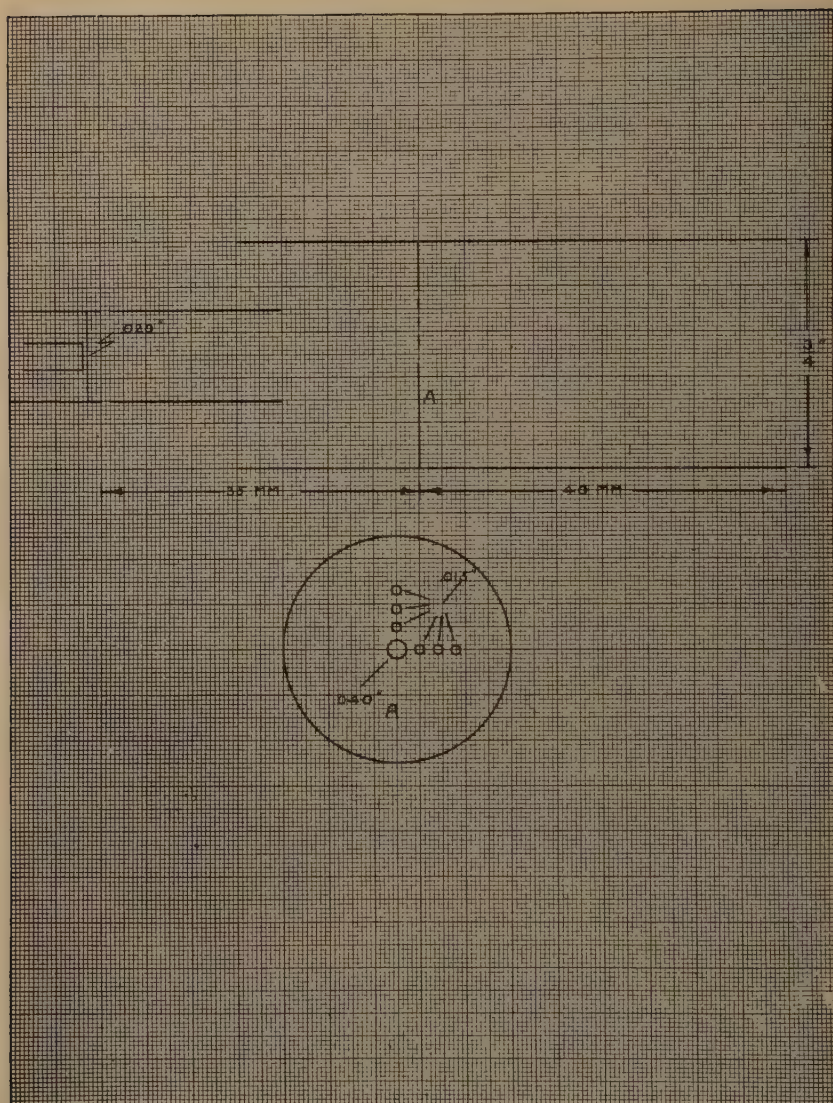


Fig. 22—Gun used for determination of spherical aberration.



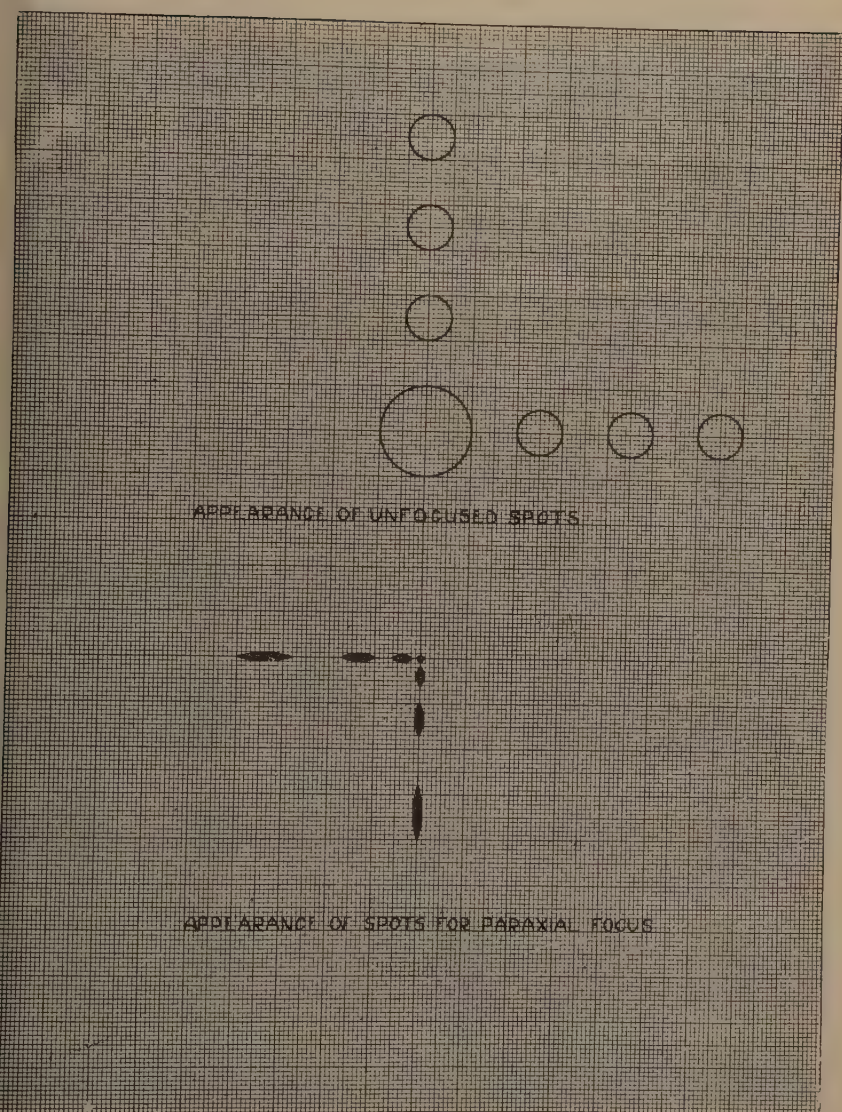


Fig. 23(a)—Appearance of unfocused spots.

Fig. 23(b)—Appearance of spots for paraxial focus.



In other words, the spot on the screen is overfocused. To focus the disk of least confusion on the screen, it will be necessary to lower the voltage

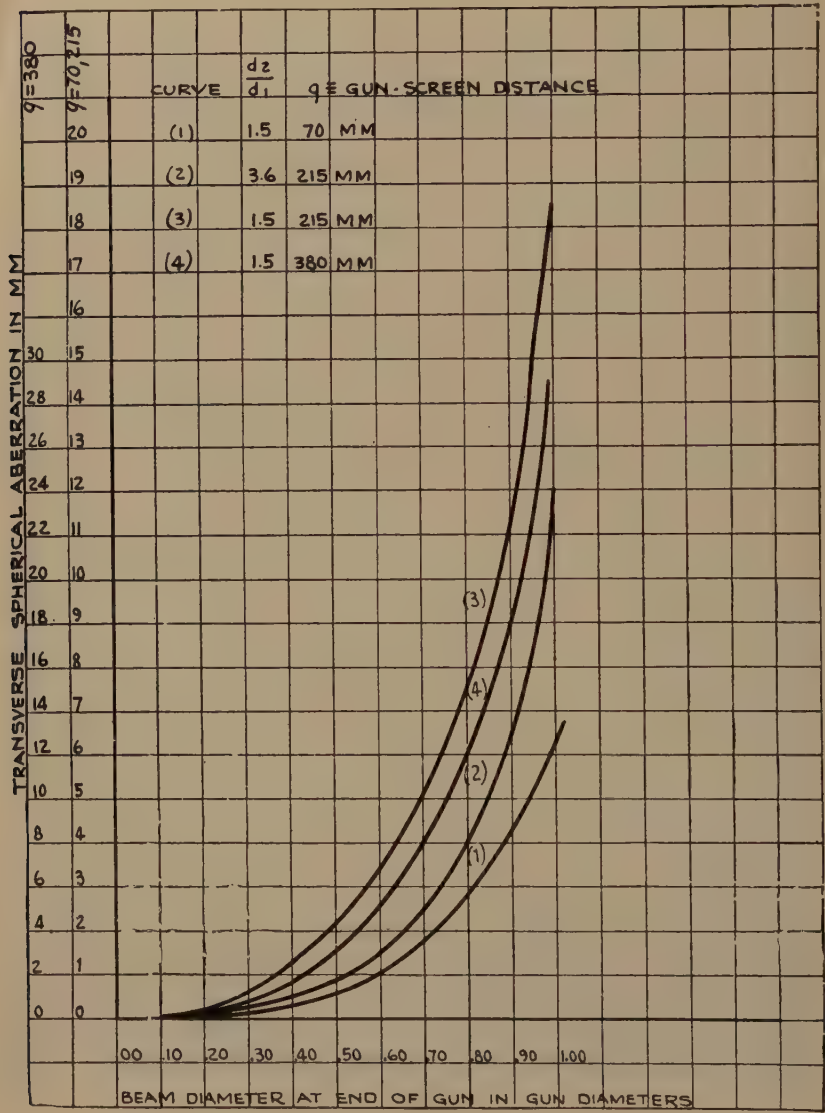


Fig. 24—Spherical aberration vs. beam width.

ratio. Fig. 25 shows the variation of the voltage ratio required to focus the disk of least confusion for various beam widths. The voltage ratio

required to focus the disk of least confusion and the size of the disk were determined by simultaneously focusing to a minimum spot the

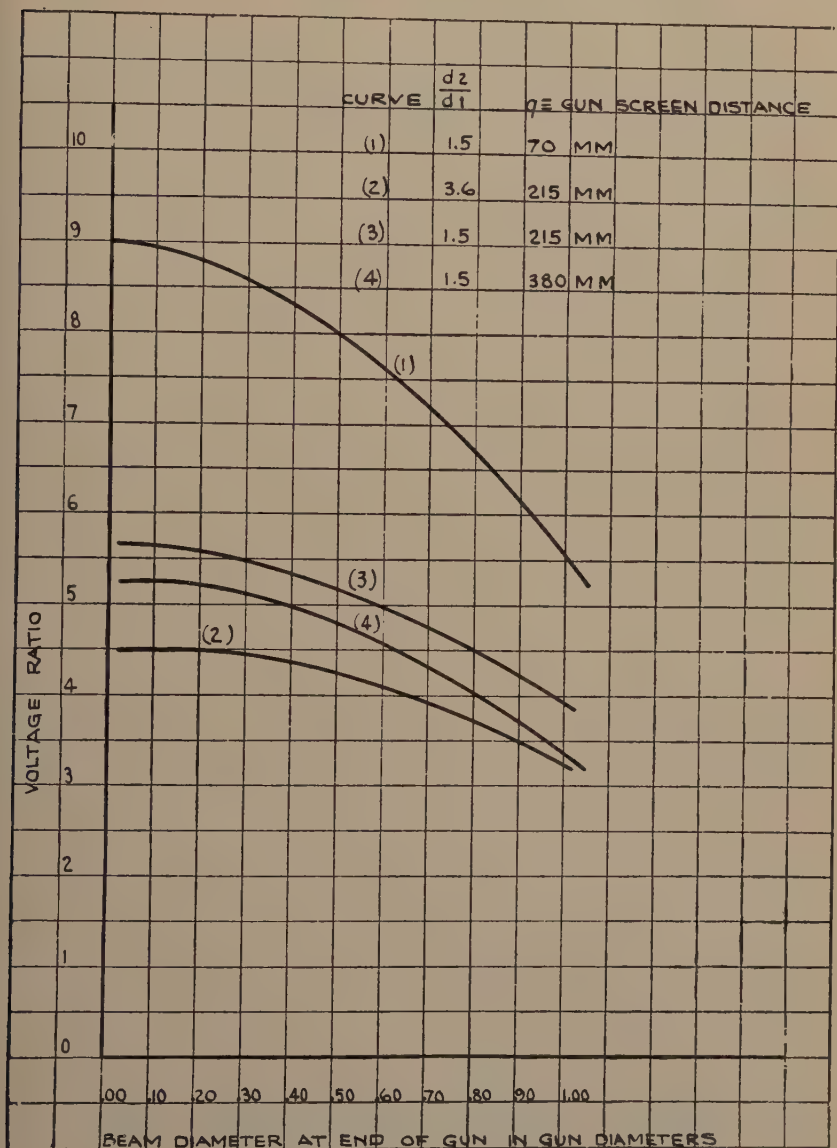


Fig. 25—Voltage ratio vs. beam width.

beams passing through the central 0.040-inch aperture and two or more of the other apertures, considering the center of the central spot (spot

formed by beam through 0.040-inch aperture) as the center of the disk of least confusion.

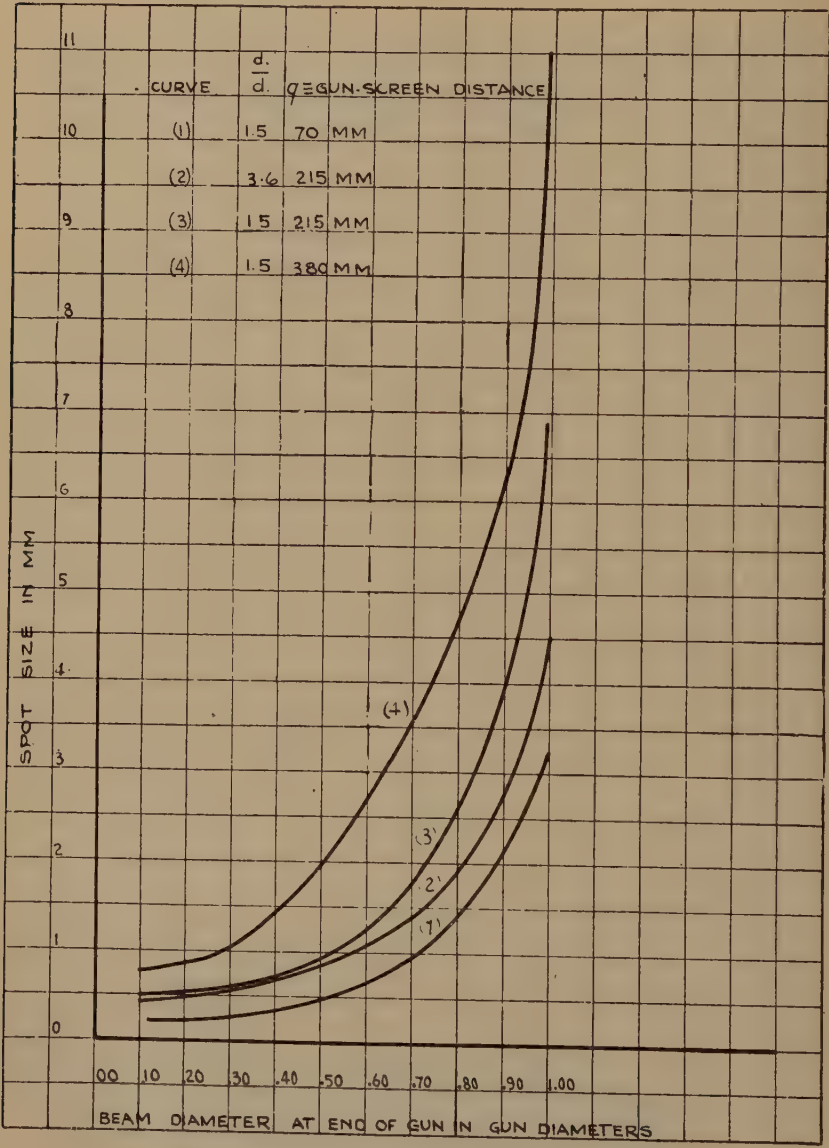


Fig. 26—Minimum spot size vs. beam width.

The size of the disk of least confusion represents the minimum spot obtainable. Fig. 26 shows the variation of the size of the disk of

least confusion with the ratio of the beam diameter at the end of the gun to the gun diameter.

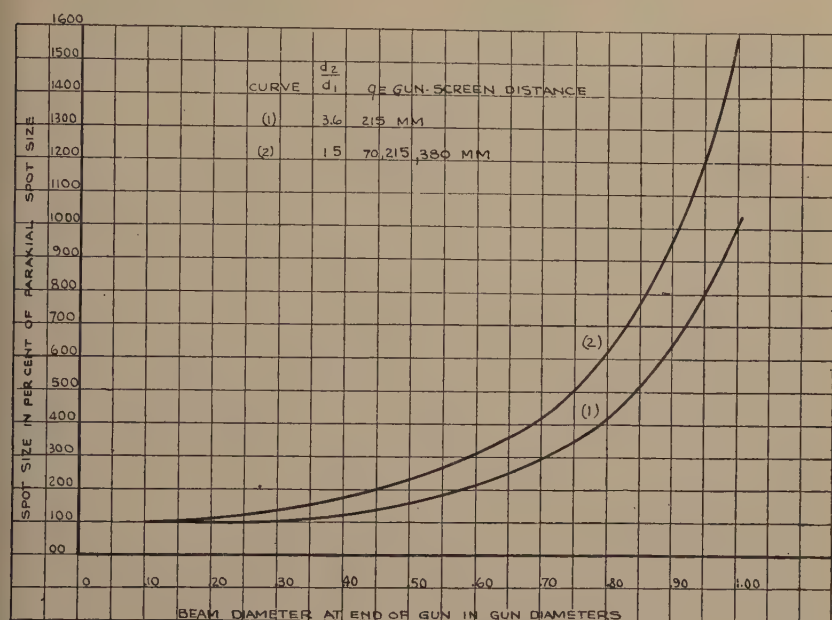


Fig. 27—Minimum spot size vs. beam width.

Fig. 27 shows the same curves given in Fig. 26 plotted in terms of the paraxial image size. Fig. 27 shows the very interesting results that the disk of least confusion, measured in terms of the paraxial size of the image, is independent of the image distance; i.e., of the type of tube.





## MAGNETRON OSCILLATORS FOR THE GENERATION OF FREQUENCIES BETWEEN 300 AND 600 MEGACYCLES\*

By

G. R. KILGORE

(Radiotron Division, RCA Manufacturing Company, Inc., Harrison, New Jersey)

**Summary**—The need for vacuum tube generators capable of delivering appreciable power at frequencies from 300 to 600 megacycles is pointed out and the negative resistance magnetron is suggested as one of the more promising generators for this purpose.

An explanation of the negative resistance characteristic in a split-anode magnetron is given by means of a special tube which makes possible the visual study of electron paths. In this manner it is demonstrated how most of the electrons starting toward the higher potential plate reach the lower potential plate.

From the static characteristics it is shown how the output, efficiency, and load resistance can be calculated, and from this analysis it is concluded that the negative resistance magnetron is essentially a high efficiency device at low frequencies.

Measurements of efficiency at ultra-high frequencies are given for several magnetrons under various operating conditions. It is concluded from these measurements that the decrease of efficiency at very high frequencies is mainly due to electron-transit-time effects. A general curve is given showing efficiency as a function of the "transit-time ratio." This curve indicates that for a transit time of one-fifteenth of a period, approximately fifty per cent efficiency is possible; for one-tenth of a period, thirty per cent; and for one-fifth of a period, the efficiency is essentially zero.

Two methods are described for increasing the plate-dissipation limit. One method is that of increasing the effective heat-dissipating area by the use of an internal circuit of heavy conductors. The other method is that of a special water-cooling arrangement which also makes use of the internal circuit construction.

Examples of laboratory tubes are illustrated, including a radiation-cooled tube which will deliver fifty watts at 550 megacycles and a water-cooled tube which will deliver 100 watts at 600 megacycles.

### I. INTRODUCTION

THE demand for more ultra-high-frequency channels has necessitated the development of generators for frequencies of higher and higher order. This development has progressed in two directions; the extension of the upper frequency limit of conventional oscillators and amplifiers, and the investigation of other types of generators especially adapted to ultra-high frequencies, such as Barkhausen-Kurz oscillators,<sup>1</sup> and magnetron oscillators.

\* Decimal classification: R355.9. Original manuscript received by the Institute, March 10, 1936. Presented before Tenth Annual Convention, Detroit, Michigan, July 1, 1935.

<sup>1</sup> H. Barkhausen and K. Kurz, "Shortest waves obtainable with valve generators," *Phys. Zeit.*, vol. 21, pp. 1-6; January, (1920).

A review of the work done shows a tendency to concentrate on the second line of development with an emphasis on obtaining the very highest frequencies rather than on obtaining appreciable power at frequencies just above the limit of conventional tubes. As a result little work has been done until very recently towards the generation of power at frequencies between 300 and 600 megacycles.

At the same time the advancement of the receiving tube art with the introduction of the "acorn" type tube<sup>2,3</sup> has made it possible to build practical receivers for frequencies somewhat above 300 megacycles. This fact brings nearer the practical utilization of these frequencies and makes it more important to obtain satisfactory generators.

While considerable progress has been made in extending the usefulness of the feed-back oscillator above 300 megacycles, the possibilities of other means of generation cannot be disregarded. One of the less conventional means which shows promise from the standpoint of output and efficiency is the magnetron oscillator.

Magnetron oscillators for generation of ultra-high frequencies can be classed as "electronic oscillators"<sup>4,5,6,7,8,9</sup> and "negative resistance" oscillators,<sup>10</sup> the former being of little importance in the frequency range under consideration. However, for the sake of clearness both types will be defined.

An *electronic magnetron* oscillator can be defined as one which operates by reason of electron-transit-time phenomena and in which the frequency is essentially determined by the electron-transit time. Although this type of oscillator is capable of generating the very highest frequencies obtainable with vacuum tubes, it has an inherently low

<sup>2</sup> B. J. Thompson and G. M. Rose, Jr., "Vacuum tubes of small dimensions for use at extremely high frequencies," *Proc. I.R.E.*, vol. 21, pp. 1707-1721; December, (1933).

<sup>3</sup> B. Salzberg and D. G. Burnside, "Recent developments in miniature tubes," *Proc. I.R.E.*, vol. 23, pp. 1142-1157; October, (1935).

<sup>4</sup> This type of magnetron oscillator was first described in the literature by Zacek<sup>5</sup> in 1924, and was later discussed in papers by Okabe,<sup>6</sup> Yagi,<sup>7</sup> Kilgore,<sup>8</sup> Megaw,<sup>9</sup> and others. It is sometimes referred to as a "Magnetostatic oscillator."<sup>8</sup>

<sup>5</sup> A. Zacek, "A method of generating short electromagnetic waves," *Casopis pro Pestovani Matematiky a Fysiky* (Prague), vol. 53, p. 378; June, (1924); (summary in *Zeit. für Hochfrequenz.*, vol. 32, p. 172, (1928)).

<sup>6</sup> K. Okabe, "Ultra-short waves from magnetrons," *Jour. I.E.E.* (Japan), p. 575, June, (1927).

<sup>7</sup> H. Yagi, "Beam transmission of ultra-short waves," *Proc. I.R.E.*, vol. 16, pp. 715-740; June, (1928).

<sup>8</sup> G. R. Kilgore, "Magnetostatic oscillators for generation of ultra-short waves," *Proc. I.R.E.*, vol. 20, pp. 1741-1751; November, (1932).

<sup>9</sup> E. C. S. Megaw, "An investigation of the magnetron short-wave oscillator," *Jour. I.E.E.* (London), vol. 72, pp. 326-348; April, (1933).

<sup>10</sup> Otherwise referred to as a "dynatron magnetron"<sup>9</sup> and as a "Habann generator."

efficiency (approximately ten per cent) and a very limited output. At frequencies between 300 and 600 megacycles, the possible output is much smaller than that obtainable from the negative resistance magnetron.

A *negative resistance magnetron oscillator* is defined as one which operates by reason of a static negative resistance between its electrodes and in which the frequency is equal to the natural period of the circuit. In its usual form it consists of a cylindrical plate and coaxial filament, the plate being split into two or more segments. Both the two-segment and the four-segment<sup>11, 12, 13, 14</sup> form are being used with success, but in this paper the discussion will be limited to the two-segment type.

The basic idea of the negative resistance magnetron was disclosed by Habann<sup>15</sup> in 1924. Since that time a number of papers on the subject have appeared; notably those of Spitzer and McArthur,<sup>16</sup> Megaw,<sup>9</sup> and Slutzkin<sup>17</sup> and his associates. Although the present paper necessarily covers some of the same ground as the previous papers, it represents an independent investigation of the subject by the writer in the past few years.

It is the object of this paper to discuss the two-segment negative resistance magnetron with regard to mechanism of oscillation, limitations in efficiency and power output at ultra-high frequencies, and its application to generation of large power output at frequencies from 300 to 600 megacycles.

## II. THEORY OF NEGATIVE RESISTANCE MAGNETRON OSCILLATORS

Before considering the negative resistance magnetron at ultra-high frequency it is well to study the fundamental principles underlying its operation.

The usual circuit of a split-anode magnetron oscillator is shown in

<sup>11</sup> The four-segment construction appears to have been first mentioned in the literature by Yagi<sup>7</sup> and later discussed by Posthumous,<sup>12</sup> Runge,<sup>13</sup> and others. Recently there has been considerable discussion as to whether the four-segment tube can be classed as a negative resistance oscillator.<sup>14</sup> The present writer feels that there is enough difference between the two-segment and four-segment tubes at ultra-high frequencies to warrant a separate treatment of the two types.

<sup>12</sup> K. Posthumous, "Oscillations in a split-anode magnetron," *Wireless Engineer*, vol. 12, pp. 126-132; March, (1935).

<sup>13</sup> W. Runge, "Four-segment magnetron," *Telefunken Zeitung*, vol. 15, p. 69; December, (1934).

<sup>14</sup> E. C. S. Megaw and K. Posthumous, "Magnetron oscillators," *Nature*, vol. 135, p. 914; June 1, (1935).

<sup>15</sup> E. Habann, "A new vacuum tube generator," *Zeit. für Hochfrequenz.*, vol. 24, pp. 115-120; 135-141, (1924).

<sup>16</sup> E. D. McArthur and E. E. Spitzer, "Vacuum tubes as ultra-high frequency generators," *Proc. I.R.E.*, vol. 19, pp. 1971-1982; November, (1931).

<sup>17</sup> A. A. Slutzkin, "Theory of split-anode magnetrons," *Phys. Zeit. der Sowietunion*, vol. 6, pp. 280-292, (1934).

Fig. 1. Oscillations can be started by applying a magnetic field of proper magnitude parallel to the filament. The value of magnetic field required is somewhat beyond the "critical" value, which is defined as the field required to cause all of the electrons to miss the plate when both plate halves are at the same potential. The expression for the "critical field"<sup>18</sup> is

$$H_c = \frac{6.72}{R_a} \sqrt{E_0} \quad (1)$$

where,

$R_a$  = anode radius in centimeters

$H_c$  = critical field in gauss

$E_0$  = average plate potential in volts.

During the oscillation cycle, the instantaneous potentials on the plate halves can be represented as shown in Fig. 2.

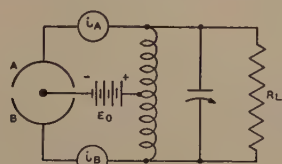


Fig. 1

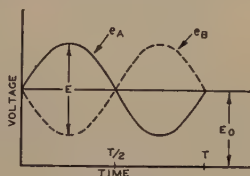


Fig. 2

Fig. 1—Two-segment magnetron oscillator circuit.

Fig. 2—Instantaneous potentials on the plate halves of a two-segment magnetron oscillator.

It is possible to demonstrate the reason for oscillation by referring to the volt-ampere characteristics, which can be shown in a number of ways. Probably the best method of representing these characteristics is illustrated in Fig. 3. For this example, a tube having a 0.5-centimeter diameter plate was used and the curves were taken for the condition of 500 volts average plate potential and a magnetic field equal to approximately 1.5 times the "critical field."

The method of taking these characteristics was to increase the potential of plate A by increments and, at the same time, decrease the potential of plate B by the same increments, so as to simulate conditions during oscillation. When the currents to the plate segments are measured, it is found that more current flows to plate B than to plate A even though plate B is at the lower potential. Furthermore, as the potential difference ( $E_A - E_B$ ) is increased, up to a certain point, the excess of current to plate B increases. The current ( $I_A - I_B$ ) plotted

<sup>18</sup> A. W. Hull, "Effect of a uniform magnetic field on the motion of electrons between coaxial cylinders," *Phys. Rev.*, vol. 18, pp. 31-57; September, (1921).



against the potential ( $E_A - E_B$ ) gives the curve  $OPB$  of Fig. 3, the portion  $OP$  of which represents a negative resistance across the circuit. This negative resistance is sufficient to account for self-sustained oscillations.

To understand why such a characteristic should exist, it is necessary to study the electron paths under various potential conditions. With equal potentials on the plate halves, and with magnetic field beyond the "critical value," the electron paths are symmetrical curves

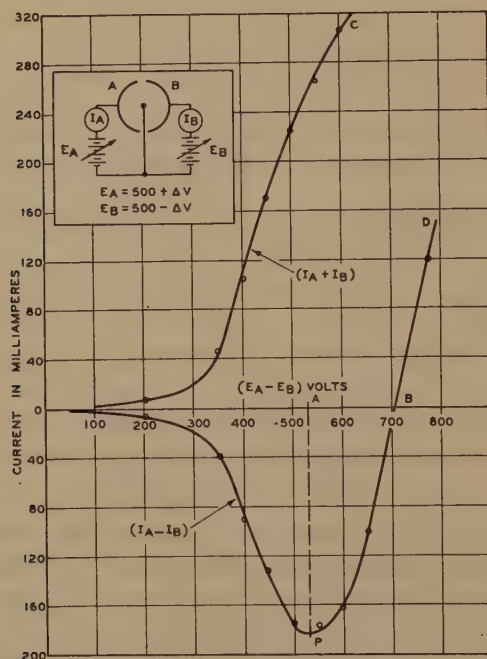


Fig. 3—Static characteristics of a two-segment magnetron.

of the type shown in Fig. 4. However, when the plate halves are at different potentials, say  $E_A = +150$  and  $E_B = +50$ , the paths are more complicated. An approximate idea of what an electron will do in this case can be had by studying an electrostatic-flux plot as shown in Fig. 5. Consider first the case of an electron starting toward the high potential plate. The electron after passing the slot plane will enter a low potential region which *decreases the radius of curvature* and causes the electron to curve back somewhat short of the filament. This results in the electron describing one or more loops, finally landing on the lower potential plate in most cases as shown in Fig. 5.

On the other hand, the electrons which start toward the lower

potential plate will pass the slot plane into a higher potential region with a resulting increase in radius of curvature, and a consequent en-

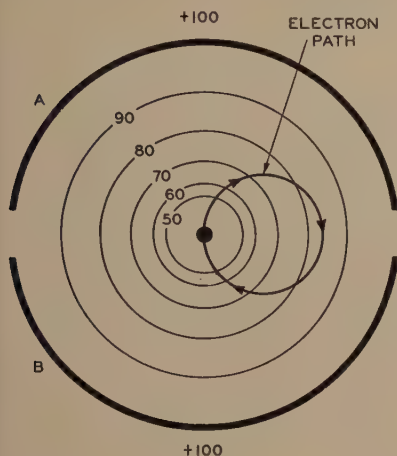


Fig. 4

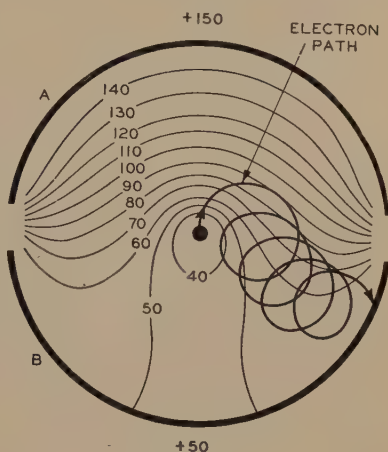


Fig. 5

Fig. 4—Electron path in a two-segment magnetron when the plate halves are at the same potential and the magnetic field is 1.5 times the critical value. (In Figs. 4, 5, and 6 the lightweight lines represent equipotential surfaces.)

Fig. 5—Electron path in a two-segment magnetron when the plate halves are at different potentials and the electron starts toward the higher potential plate. Magnetic field 1.5 times critical value.

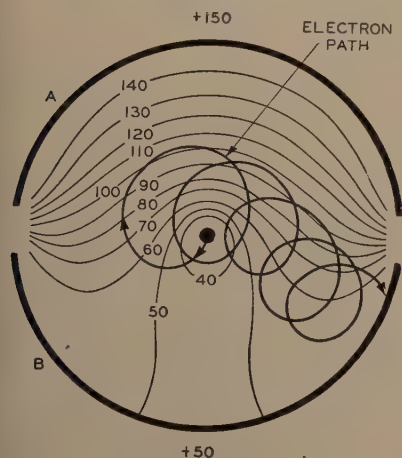


Fig. 6

Fig. 6—Path of an electron starting toward the lower potential plate. Magnetic field 1.5 times critical value.

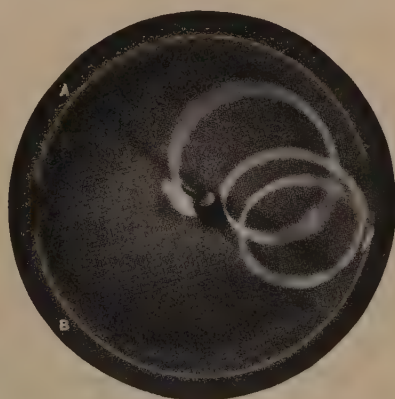


Fig. 7

Fig. 7—Photograph of ionized path of an electron stream starting toward the higher potential plate. Magnetic field 1.25 times critical.  $E_A = +300$  volts,  $E_B = +250$  volts.

circling of the filament as shown in Fig. 6. In this case, it is more difficult to say what the ultimate destination of the electrons will be, but

it appears probable that these electrons will also eventually reach the lower potential plate.

For an experimental check of these predictions, a special magnetron was built which made possible a visual study of electron paths by gas ionization. The cathode was constructed with a small emitting spot and made rotatable so that the electrons starting in any direction could be studied. Argon gas of a few microns pressure was used, which made the electron beam just visible without essentially changing the shape of the beam trace. The terminal spot of the beam was also made visible by coating the plate halves with willemite.

With this tube it was possible to illustrate beautifully the predicted paths of the type shown in Figs. 5 and 6. In some cases of high magnetic field, as many as ten or more loops were observed. A typical photograph of an electron-beam trace is shown in Fig. 7 for the condition of  $E_A = +300$ ,  $E_B = +250$ , and magnetic field equal to about 1.25 times the critical value. A systematic study was made of the electron paths by varying the direction of emission, the ratio of plate potentials, and the strength of magnetic field. The conclusion drawn from these observations is that, for sufficiently high magnetic field (one and one-half to two times critical) and with the ratio of  $E_A$  to  $E_B$  not too high (less than four to one), most of the electrons arrive at the lower potential plate no matter in what direction they started.

However, this fact in itself is not sufficient to explain fully the negative resistance characteristic. In addition, the space-charge effects must be considered. A complete analysis of the space-charge conditions in a magnetron is too involved to be attempted here, but a qualitative picture can be given as follows: With the magnetic field beyond the critical value and the plate halves at the same potential, no electrons will reach either plate; but as soon as  $E_A$  is increased by an increment and  $E_B$  decreased by the same increment, some electrons will flow to plate  $B$  as illustrated above. Because of the space-charge limitation, however, the number of these electrons will be only a small fraction of the total number emitted from the filament. It is clear that the space charge for a given current will be much higher than without magnetic field because the electrons describe several orbits before reaching the plate, thus contributing more to the space charge. Now a study of the electron paths shows that an increase in  $(E_A - E_B)$  causes the electrons to describe fewer orbits. Therefore, an increase in  $(E_A - E_B)$  will result in a smaller space charge and a, consequently, greater current to  $B$ .

This analysis is sufficient to explain the negative resistance characteristic such as is represented by the portion  $OP$  of the  $(I_A - I_B)$

curve in Fig. 3. The other part of the curve, *PBD*, can be explained by the fact that, as the ratio of  $E_A$  to  $E_B$  is increased, electrons eventually begin to arrive at plate *A* until, ultimately, more electrons are arriving at *A* than at *B*.

### III. CALCULATION OF PERFORMANCE FROM THE VOLT-AMPERE CHARACTERISTICS

Having explained the reason for the typical volt-ampere characteristics in a split-anode magnetron it is interesting next to use these characteristics to calculate the oscillator performance. In this analysis, it is assumed that the transit time is very small compared to a period. Referring to the notation of Figs. 1 and 2 and letting  $e_A = E_0 + E/2 \sin \omega t$  and  $e_B = E_0 - E/2 \sin \omega t$ , it is easy to derive the following expressions:

$$\begin{aligned} \text{Plate Loss} &= \frac{1}{T} \int_0^T e_A i_A dt + \int_0^T e_B i_B dt \\ &= \frac{E_0}{T} \int_0^T (i_A + i_B) dt + \frac{E}{2T} \int_0^T (i_A - i_B) \sin \omega t dt. \end{aligned} \quad (2)$$

$$\text{Power Input} = \frac{E_0}{T} \int_0^T (i_A + i_B) dt. \quad (3)$$

$$\text{Power Output } (P_0) = - \frac{E}{2T} \int_0^T (i_A - i_B) \sin \omega t dt. \quad (4)$$

$$\text{Efficiency} = \frac{E}{2E_0} \frac{- \int_0^T (i_A - i_B) \sin \omega t dt}{\int_0^T (i_A + i_B) dt}. \quad (5)$$

$$\text{Load Resistance} = \frac{E^2}{2P_0}. \quad (6)$$

It is clear that curves *OPB* and *OC* of Fig. 3 give all the information necessary to calculate the above quantities. If an amplitude  $E$  is assumed, the instantaneous values of  $(i_A - i_B)$  and  $(i_A + i_B)$  can be read from Fig. 3 and then, by numerical integration, power input and power output can be evaluated from (3) and (4).

The conditions for maximum output and maximum efficiency can be determined by taking several values of amplitude. This analysis was carried out for the example of Fig. 3; the results are shown in Fig. 8. As could be expected, the peak output occurs at an amplitude nearly equal to *OP*, and the maximum efficiency occurs at somewhat lower amplitude.



In general, it is found that as the magnetic field is increased the crossing point *B*, of curve *OPB*, moves further out. The result is an increase in maximum output and efficiency.

In the above example, the maximum efficiency is about thirty-four per cent which by no means represents the best efficiency obtainable in a tube of this type. Unfortunately in the example given, the static curves could not be taken with higher magnetic fields because of problems of oscillation and electron bombardment of the leads. With higher magnetic fields, higher efficiencies may be expected. Megaw,<sup>9</sup> in a similar analysis, has calculated efficiencies as high as forty-five

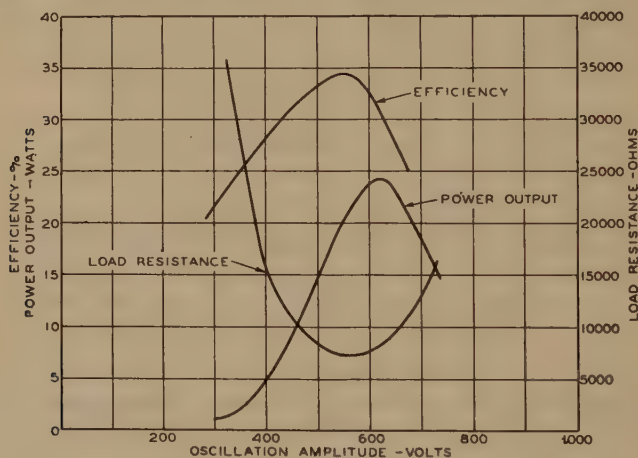


Fig. 8—Performance curves of a two-segment magnetron, calculated from the static characteristics.

per cent for a tube operating under somewhat more favorable conditions than the above example.

#### IV. LIMITATIONS OF EFFICIENCY AT ULTRA-HIGH FREQUENCIES

Measured efficiencies of magnetrons at low and medium frequencies agree well with those predicted from the volt-ampere characteristics, but at very high frequencies it is found that the efficiency is considerably reduced. An experimental study of the efficiency of several magnetrons at very high frequencies was made to determine the main causes of decreased efficiency.

The problem of measuring efficiency at frequencies above 300 megacycles is very difficult because of the lack of a means of measuring power output, which is accurate and at the same time flexible enough to be used under a wide variety of conditions. The method finally

adopted was that of absorbing power in a lamp previously calibrated photometrically on direct current. The obvious error in this method is the nonuniform heating of the lamp filament at high frequencies. However, it is estimated that, by the use of specially designed lamps, the error in the measurements was held to within plus or minus twenty per cent.

Fig. 9 shows the measured efficiency as a function of frequency for plate diameters of 0.5 and 1.0 centimeter. When these curves were taken, the plate potential was held at 500 volts and the magnetic field

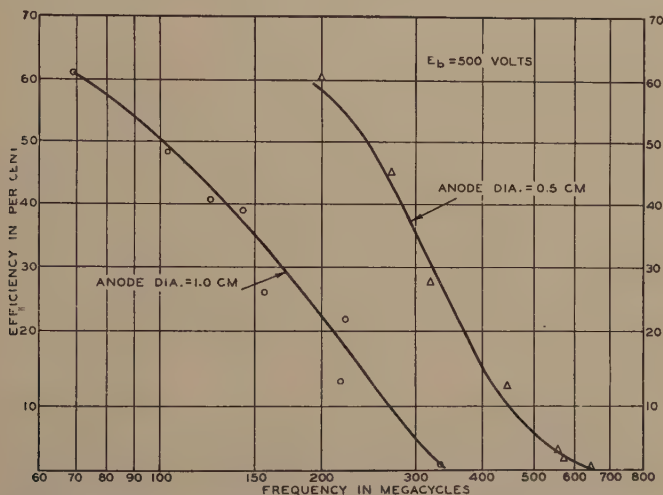


Fig. 9—Efficiency versus frequency for two sizes of magnetrons operating at the same plate potential.

was adjusted to give maximum efficiency at each point. The general shape of the curves for the two tubes is approximately the same; but, at a given efficiency, the frequency for the smaller plate diameter is roughly twice that for the larger. This seems to indicate that the higher efficiency for the smaller diameter tube is due to the shorter electron-transit time, and suggests that the decrease in efficiency at higher frequencies is because of the appreciable transit time.

If the efficiency is mainly a function of the ratio of transit time to period, then it might be expected that, at a given frequency, the efficiency will increase with plate voltage. This is borne out by the curve shown in Fig. 10 where efficiency is plotted as a function of plate voltage for a tube operating at 440 megacycles. The tube used in this test had a plate diameter of 0.5 centimeter and was of the internal

circuit construction described in Part V. The magnetic field for each reading was adjusted for the best efficiency.

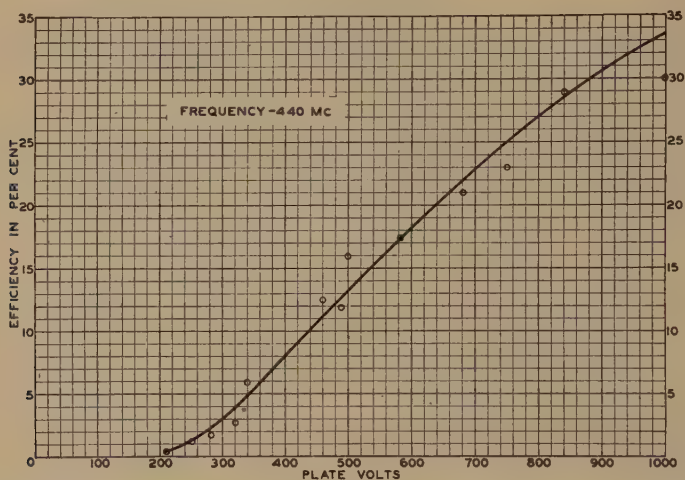


Fig. 10—Efficiency versus plate voltage for a magnetron operating at a frequency near the high-frequency limit.

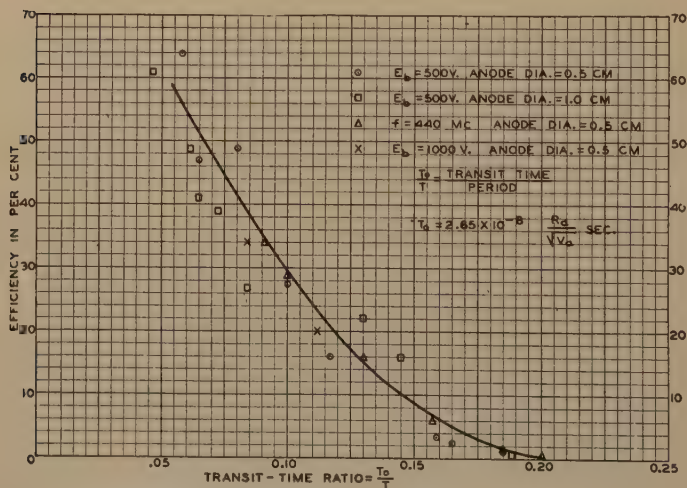


Fig. 11—Combined efficiency data for two-segment magnetrons, plotted as a function of transit-time ratio.

To illustrate further the relation between efficiency and transit time, the efficiency data of Figs. 9 and 10 with some additional data

are plotted as a function of the ratio of transit time to period as shown in Fig. 11. The value of transit time used is an effective direct-current transit time<sup>19</sup> given by the expression,

$$T_0 = 2.65 \times 10^{-8} \frac{R_a}{\sqrt{E_0}} \quad (7)$$

where,

$R_a$  = radius of the plate in centimeters,

$E_0$  = direct-current plate potential in volts,

$T_0$  = effective transit time in seconds.

The fact that all points from the several sources lie fairly close to a smooth curve is good evidence that the decrease in efficiency is, for the most part, due to transit-time effects. Examination of the curve shows that, if the transit-time ratio is below one-fifteenth of a period, efficiencies as high as fifty per cent can be expected, and that, even at one-tenth of a period, thirty per cent efficiency is possible, but that, at one-fifth of a period, the tube will almost fail to oscillate.<sup>20</sup>

As a practical example, an efficiency of thirty per cent can be obtained at 600 megacycles with a tube having a plate diameter of 0.5 centimeter and a plate potential of 1500 volts.

Another factor to be considered in connection with attaining high efficiency at ultra-high frequencies is the value of magnetic field required. It is possible to demonstrate that, for a given efficiency and frequency, the value of the magnetic field is definitely determined, regardless of what plate voltage or plate diameter is used. This can be shown by expressing the transit time as a function of the magnetic field alone. This is possible, since  $E_0$  and  $R_a$  are connected through the relation

$$H = k \frac{6.72}{R_a} \sqrt{E_0} \quad (8)$$

where  $k$  in practice lies between 1.5 and 2.0. Substituting (8) and (7) gives,

$$\frac{T_0}{T} = 1780 \frac{kf}{H} \times 10^{-10} \quad (9)$$

where,

<sup>19</sup> The calculation of this transit time assumes a uniform velocity ( $v_0 = 5.95 \times 10^7 \sqrt{E_0}$ ) and a semicircular path of a diameter equal to  $R_a$ . This transit time is equal to one half the orbital time of an electron traveling with a velocity  $v_0$  in a magnetic field  $H_c = 6.72/R_a \sqrt{E_0}$ .

<sup>20</sup> When this general relation is compared with the data given by Megaw<sup>9</sup> a fairly good agreement is found. A similar comparison with the work of Slutzkin shows much poorer agreement, the efficiencies given by Slutzkin being generally higher.



$f$  = frequency in cycles per second

$H$  = magnetic field in gaussess

$\frac{T_0}{T}$  = ratio of transit time to period.

This expression for transit-time ratio can now be combined with the efficiency curve of Fig. 11 to give the magnetic field for any frequency and efficiency. This relation can best be illustrated by a chart of the type shown in Fig. 12. The values of magnetic field obtained from

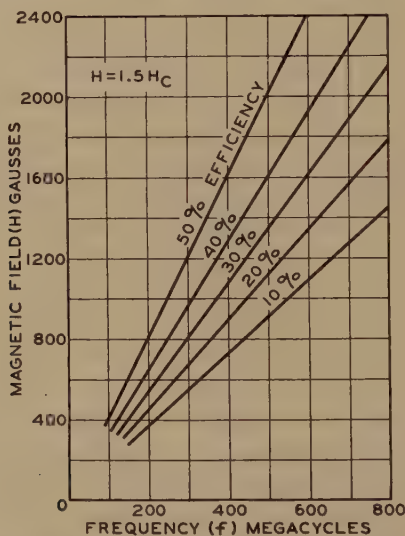


Fig. 12—Constant efficiency curves of a negative resistance magnetron showing the magnetic field strength required for any given efficiency and frequency.

this diagram are only approximate because the value of  $k$  may vary considerably in practice and because the efficiency measurements are subject to a fairly large error.

It is interesting to compare the magnetic field required by a negative resistance oscillator to that required by an electronic oscillator operating at the same frequency. If the comparison is made on the basis of ten per cent efficiency (limit of electronic oscillator) it is found that the negative resistance magnetron requires approximately four times the field strength.<sup>21</sup>

In the discussion so far it has been assumed that circuit loss plays an unimportant role. This is contrary to the statement often made that

<sup>21</sup> This follows from the approximate relation for electronic oscillators that  $H = 12,000/\lambda$  cm.

circuit loss is the limiting factor in magnetron oscillators at ultra-high frequencies. However, it has been the experience of the author that, with proper care in design, circuits can be built which have negligible loss even at 600 megacycles. This is accomplished by using close-spaced leads to reduce radiation and by making the surface area of the leads sufficient to give small high-frequency resistance. A very low loss circuit has been obtained by the use of an internal-copper circuit which will be described in Part V. The conclusion can be drawn that magnetron circuits can be designed so that the real limiting factor is the electron transit time.

#### V. LIMITATIONS IN PLATE DISSIPATION

The preceding analysis has shown that, for high efficiency in the 300- to 600-megacycle range, a small anode diameter is required (about 0.5 centimeter for 1500 volts). It has also shown that a high magnetic field is required, a fact which limits the length of plate to a few centimeters for a magnet of reasonable dimensions. Both of these facts definitely limit the plate size and, consequently, impose a serious limitation on the possible plate dissipation. At first thought, it appears that the maximum dissipation of such a tube would be of the order of ten watts, but further study shows that this value can be increased by a large factor.

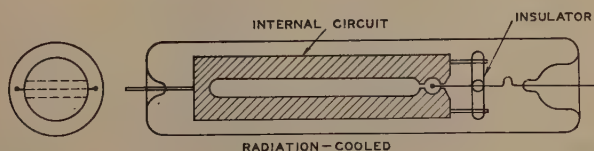


Fig. 13—Sectional view of an internal circuit radiation-cooled magnetron for obtaining high power at ultra-high frequencies.

Although the dimensions of the plate cylinder are small, the radiating surface can be increased considerably by using a heavy walled plate to increase the outside area. The surface can be still further increased by placing the oscillating circuit within the bulb, as illustrated in Fig. 13. When conductors of large cross section and good thermal conductivity are used the whole circuit is essentially at the same temperature, and its entire surface is effective in radiating heat. In this manner the radiating surface can be increased by a factor of the order of twenty to one.<sup>22</sup> Fig. 14 illustrates a tube of this construction which

<sup>22</sup> Shortly prior to the time at which the author constructed the first tube of this type, Mr. P. D. Zottu of this laboratory designed an internal circuit magnetron embodying the principal features described here.

has a safe plate dissipation of 200 watts and will deliver an output of about fifty watts at a frequency of 550 megacycles with an efficiency of about thirty per cent. In this instance, the circuit was made of copper, which not only gives good thermal conductivity but also results in a very low loss circuit. To increase the emissivity the outer surface was carbonized. Incidentally, the carbonization may be expected to cause but little increase in the high-frequency resistance



Fig. 14—Photograph of an internal circuit radiation-cooled magnetron oscillator for 550 megacycles.

because most of the current in such a structure flows on the inner surface. The method of coupling this tube to the load was to use a parallel-wire transmission line, the closed end of which was inductively coupled to the internal circuit of the tube.

It is obvious that the internal circuit construction limits a given tube to operation over a relatively narrow frequency band. However, such a limitation may not be so serious in an ultra-high-frequency tube as it would be in a tube intended for lower frequency applications. Moreover, it may be pointed out that, aside from the advantage

of high dissipation, the internal circuit construction becomes a necessity at frequencies around 400 megacycles, because of the impossibility of building external circuit tubes which will tune to such high frequencies.

To obtain still greater plate dissipation, it is necessary to resort to the use of some cooling liquid such as water. The problem of water-cooling in a split-anode magnetron for very high frequencies is not so simple as in the conventional three-electrode tube. In a magnetron, the power is dissipated over a comparatively small area. This makes it necessary to conduct the heat away to a larger surface which can be effectively water-cooled. There are a number of ways in which this can be accomplished; one example is illustrated by Fig. 15. Here,

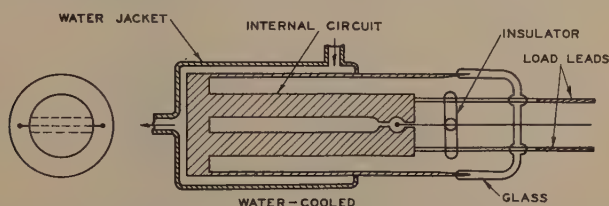


Fig. 15—Sectional view of one type of water-cooled magnetron for high power at ultra-high frequencies.

also, an internal circuit of heavy copper conductors is used, but in this case the circuit is conductively coupled to the load by two leads brought out in a plane at right angles to the plane of the filament leads. Fig. 16 shows a photograph of a laboratory tube of this construction with an internal circuit and plate of approximately the same dimensions as the radiation-cooled tube of Fig. 14. This particular tube will dissipate more than 500 watts and will deliver an output of approximately 100 watts at a frequency of 600 megacycles with an efficiency of about twenty-five per cent.

## VI. MISCELLANEOUS LIMITATIONS

Besides the factors discussed in the previous sections, there are two other factors that limit to some degree the output obtainable from a magnetron oscillator. One of these, existing in radiation-cooled tubes, is the electron bombardment of the glass walls opposite the ends of the plate due to the focusing effect of the magnetic field. A solution to this problem has been found by adding shielding electrodes at the plate ends. Shielding electrodes of this type can be seen in the illustration of Fig. 14.

The other factor which is somewhat more serious is a phenomenon



termed "filament-bombardment effect." This effect, observed by the author several years ago, has been mentioned by a number of writers on magnetrons.<sup>23</sup> The effect manifests itself as an increase of filament temperature under certain conditions of high magnetic field and high

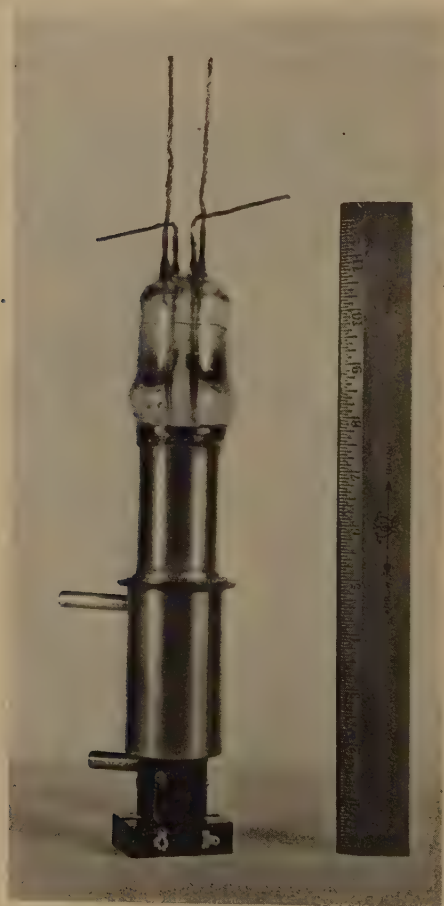


Fig. 16—Photograph of a water-cooled magnetron oscillator for 600 megacycles.

<sup>23</sup> Megaw,<sup>24</sup> Slutzkin<sup>25,26</sup> and others have described this effect and Langmuir and Found<sup>27</sup> have observed a related phenomenon in connection with electron scattering.

<sup>24</sup> E. C. S. Megaw, "A new effect in thermionic valves at very short wave lengths," *Nature*, vol. 132, p. 854; December 2, (1933).

<sup>25</sup> A. A. Slutzkin, S. J. Brande, and I. M. Wigdortschik, "Generation of ion currents in high vacuum by the help of magnetic fields," *Phys. Zeit. der Sowietunion*, vol. 6, pp. 268-279, (1934).

<sup>26</sup> A. A. Slutzkin, et al., "Production of electromagnetic waves below fifty centimeters," *Phys. Zeit. der Sowietunion*, vol. 6, pp. 150-158, (1934).

<sup>27</sup> I. Langmuir, "Scattering of electrons in ionized gases," *Phys. Rev.*, vol. 26, pp. 585-613, (1925).

plate voltage, and sometimes results in unstable operation of the tube. In extreme cases, the filament can receive sufficient energy from the plate circuit to permit operation of the tube with the usual filament supply disconnected. The cause of this phenomenon has not been fully explained, but it appears to be due to a bombardment of the filament by electrons.

Although the filament-bombardment effect is sometimes troublesome, it can generally be avoided by using heavy filaments and by operating the tube at somewhat reduced plate voltage and magnetic field strength.

## VII. CONCLUSION

It has been demonstrated by theory and experiment that the negative resistance magnetron is essentially a high efficiency device at low frequencies, and that the decrease of efficiency at high frequencies is mainly due to transit-time effects. As applied to frequencies between 300 and 600 megacycles, it is shown that this type of oscillator can be expected to give efficiencies of the order of fifty to thirty per cent.

Methods are described by which the inherently small plate-dissipation limit can be extended by twenty to fifty times, and by which it is possible to realize power outputs of the order of fifty to 100 watts in the 300- to 600-megacycle range. The output and efficiencies obtained compare favorably with those of conventional tubes at much lower frequencies, but it is not to be inferred that magnetrons will necessarily supplant other types of generators. Problems of modulation and frequency stability are still to be met and in some applications the supplying of a high magnetic field may be inconvenient.

In conclusion, the author wishes to point out that the specific tubes described are not to be regarded as commercial designs. They are, rather, laboratory tubes built to demonstrate certain principles which, it is hoped, will prove useful in future designs of ultra-high-frequency generators.

## ACKNOWLEDGMENT

The writer desires to express his indebtedness to Mr. B. J. Thompson and Mr. H. C. Thompson for many helpful suggestions, and to Mr. T. H. Clark for his assistance in the experimental work.





## BOOK REVIEWS

**"An Hour a Day with Rider on Resonance and Alignment,"** by John F. Rider, J. F. Rider, 1440 Broadway, New York City. Price 60 cents. 91 pages. Illustrations and oscillograms.

This treatise is one of a series of self-study books prepared under the general title of "An Hour a Day With Rider" and continues the author's endeavor to keep members of the radio service industry informed as to the latest circuits and most approved methods of servicing.

Starting with a nonmathematical description of the general subject of resonance, it proceeds with actual details of aligning all of the usual types of modern receivers. The author has placed emphasis on any special details or processes necessary with unusual circuit features. The book is written in an easily understandable style and presents a clear picture of the subject. It is published in a handy size for convenience in carrying around for odd-moment study.

\*RALPH R. BATCHER

**"The New Acoustics,"** by N. W. McLachlan. Oxford University Press, 114 Fifth Ave., New York City. 166 pages. Price \$2.75.

This book is a nonmathematical survey of the field of applied acoustics with some emphasis on its development in England. The author has covered a very wide field and the book is, therefore, to be noted more for breadth than intensity. The style is sufficiently nontechnical to be intelligible to a reader with a high school training in physics.

After a brief historical introduction, chapters are included on antisubmarine devices, broadcasting, loudspeakers, microphones, phonographs, talking pictures, analysis of sounds, behavior of the ear, deaf aids, auditorium acoustics, and sound absorption coefficients.

This book will be of most interest to the reader who is interested in finding out what some of the accomplishments in acoustics have been during the past ten years, and at the same time would like to have a not too detailed physical picture of the means which have been used to obtain the results.

†IRVING WOLFF

**"1934 Report of C.C.I.R. Meeting at Lisbon."** Government Printing Office, Washington, D.C. 413 pages. Price 50 cents.

The report of the C.C.I.R. meeting at Lisbon in 1934 has recently been published. This is the Report of the Delegation of the United States of America and Appended Documents, Third Meeting of the International Radio Consulting Committee, Lisbon, September 22 to October 10, 1934. It has been published as Department of State Conference Series No. 21. The contents includes a list of the delegates and organization of the meeting, the reports of the committees on definitions and standardization, collaboration, operation, transmission, and organization; the opinions of C.C.I.R., the questions for the next meeting of C.C.I.R., and the opinions concerning radio issued by the International Consulting Committee on Telephony. Much valuable technical data on many different fields of radio communication are included. It is of particular interest in connection with the approaching 1937 meeting of C.C.I.R. in Bucharest.

†R. S. OULD

\* Hollis, L.I., N.Y.

† RCA Manufacturing Company, Inc., RCA Victor Division, Camden, N.J.

‡ Washington, D.C.

**BOOKLETS, CATALOGS, AND PAMPHLETS RECEIVED**

Copies of the publications listed on this page may be obtained without charge by addressing the publishers.

Production Instrument Company of 1325 S. Wabash Ave., Chicago, Ill., has issued Bulletin 14 on its pilot switch.

Carter Motor Company of 361 W. Superior St., Chicago, Ill., has issued a leaflet on its genemotor power plants.

The Western Electric 5-kilowatt radio transmitter is described in a booklet available from that organization which may be addressed at 195 Broadway, New York City.

"The Magic Magnet Speaker" is the title of a booklet issued by the Cinaudagraph Corporation of Stamford, Conn.

The Pacent Engineering Corporation of 79 Madison Ave., New York City, has issued Bulletin No. 102 on high fidelity sound equipment.

Electrostatic instruments are described in a leaflet issued by Sensitive Research Corporation of 4545 Bronx Blvd., New York City.

The Weston Electrical Instrument Corporation of Newark, N.J., has issued a leaflet on its checkmaster for broadcast receiver servicing.

The Westinghouse Lamp Company of Bloomfield, N.J., has issued information Bulletins No. 1 on Type WL-785 lenard-ray tube; No. 2 on an ultraviolet meter, and No. 3 on Type WL-787 demonstration triode tube. A booklet on their electronic tubes is also available.

Catalog No. 11 of the Roller-Smith Company, 233 Broadway, New York City, covers its "Hipot" potential indicator. Its Catalog No. 6 covers "Turblator" oil circuit breakers.

The Leeds and Northrup Company of 4902 Stenton Ave., Philadelphia, Pa., has issued Catalog N-33A covering its micromax thermocouple pyrometers.

International Resistance Company of 401 N. Broad St., Philadelphia, Pa., has issued Catalog V-50 covering various types of resistor units available from that organization.

Jefferson Electric Company, Belwood, Ill., has issued Bulletin PA-11 covering a twenty-watt audio-frequency amplifier.

Police radiotelephone equipment is described in a booklet issued recently by the Western Electric Company of 195 Broadway, New York City.

Models AVR-7B and AVR-7C aircraft receivers are described in a leaflet issued by the RCA Manufacturing Company of Camden, N.J.

Bulletin 60A and 60B of the Ward Leonard Electric Company of Mt. Vernon, N.Y., describe field rheostats for rotating machinery.



## CONTRIBUTORS TO THIS ISSUE

**Carter, Philip S.:** See PROCEEDINGS for April, 1936.

**Cunningham, F. W.:** Born November 22, 1885, at Hamilton Square, New Jersey. Received B.S. degree, Princeton University, 1907; E.E. degree, 1911; Ph.D. degree, University of Wisconsin, 1911. Edison Lamp Works of General Electric Company, 1912-1916; Winchester Repeating Arms Company, 1917-1919; Edison Storage Battery Company, 1919-1921; engineering department, Western Electric Company, 1922-1923; radio development department, Bell Telephone Laboratories, Inc., 1925 to date. Associate member, Institute of Radio Engineers, 1926; Member, 1928.

**Epstein, D. W.:** Born January 11, 1908, in Russia. Received B.S. degree in engineering physics, Lehigh University, 1930; M.S. degree in electrical engineering, University of Pennsylvania, 1934. Research division, engineering department, RCA Victor Company, Inc., 1930-1935; RCA Victor Division, RCA Manufacturing Company, Inc., 1935 to date. Member, American Physical Society. Associate member, Institute of Radio Engineers, 1934.

**Kilgore, G. Ross:** Born January 31, 1907, at Fremont, Nebraska. Received B.S. degree in electrical engineering, University of Nebraska, 1928; M.S. degree in electrical engineering, University of Pittsburgh, 1931. Student course, Westinghouse Electric and Manufacturing Company, 1928; Westinghouse Research Laboratories, 1929-1934; RCA Radiotron Division, Inc., 1934-1935; Radiotron Division, RCA Manufacturing Company, Inc., 1935 to date. Associate member, Institute of Radio Engineers, 1930.

**Kishpaugh, A. W.:** Born November 5, 1891, at Newberry, Michigan. Received E.E. degree, University of North Dakota, 1912. General Electric Company, 1912-1914; Utah Power and Light Company, 1914-1916; engineering department, Western Electric Company, 1916-1925; radio development department, Bell Telephone Laboratories, Inc., 1925 to date. Associate member, Institute of Radio Engineers, 1920; Member, 1930.

**Poppele, J. R.:** Born February 4, 1898, at Newark, New Jersey. Post Graduate course, Penn State. Radio marine operator, 1915-1917; Army transport service radio operator, 1917-1919; RCA Communication Service, 1919-1920; chief engineer, Bamberger Broadcasting Service, 1922 to date. Associate member, Institute of Radio Engineers, 1930.

**Wickizer, Gilbert S.:** Born August 20, 1904, at Warren, Pennsylvania. Received B.S. degree in electrical engineering, Pennsylvania State College, 1926. Operating division, Radio Corporation of America, 1926-1927; communication receiver research and development, RCA Communications, Inc., 1927 to date. Associate member, Institute of Radio Engineers, 1928.